DETERMINATION OF CAPSAICIN USING CARBON NANOTUBE BASED ELECTROCHEMICAL BIOSENSORS

By

Thabani Eugene Mpanza

Student Number: 19001540

Submitted in fulfilment of the requirements for the Degree of Master of Applied Science in Chemistry in the Faculty of Applied Sciences at the Durban University of Technology

July 2016

Declaration

I, Thabani Eugene Mpanza, hereby declare that this thesis has not been submitted to any University or any other Institution. I therefore declare that this is my own work, where others work was used, that has been duly acknowledged in the text and references.

_____ _____/____/_____

Signature of Student Date

_____ ____/_____/_____

Signature of the Promoter Date

_____ _____/_____/_____

Signature of Co- Supervisor

_____ ____/_____/_____

Signature of the HOD Date

Dedication

This work is dedicated to my late son, Mnotho Siwela Mmangaliso Mpanza, who passed away on the 11th November 2014, aged 14 years. He will be sorely missed and may his soul rest in peace.

Acknowledgements

To God be the Glory, Special thanks to my Lord and Saviour, Jesus Christ for giving me strength throughout my period of study and during difficult times.

I wish to express my sincere gratitude to my promoter, Professor K. Bisetty for his help and direction throughout my research. A special thanks to Dr Parvesh Singh (co- supervisor) for helping with identification of Enzymes to be used in this project. I would also like to extend my heartfelt gratitude to my fellow research partner and doctoral student, Myalo Sabela for his invaluable knowledge of research he shared with me, which helped in successful completion of this work.

I wish to thank Dr Kanchi (post-doctoral fellow) at DUT for his support and for sharing his experience with me. I would also like to thank Dr Michael Shapi my HOD at Mangosuthu University of Technology for allowing me time off from work to engage in this project.

Finally, my special thanks to my wife, Cordy and children (Thabisa and Aphiwe) for their support and understanding throughout this project.

Abstract

This study involves the development of a sensitive electrochemical biosensor for the determination of capsaicin extracted from chilli pepper fruit, based on a novel signal amplification strategy. The study therefore, seeks to provide a sensitive electro-analytical technique to be used for the determination of capsaicin in food and spicy products. Electrochemical measurements using cyclic voltammetry (CV) and differential pulse voltammetry (DPV) modes were utilized in order to understand the redox mechanism of capsaicin and to test the performance of the developed biosensor supported with computational techniques. In this work two different enzymes, Phenylalanine ammonia lyase (PAL) and Glucose oxidase (GOx) were used for electrode modifications respectively.

For this purpose three different types of working electrodes namely: glassy carbon electrode (GCE), platinum electrode (Pt-E) and gold electrode (Au-E) were used and their performances were compared.

For the first time, the three electrodes were modified with PAL and GOx enzymes on multiwalled carbon nanotubes used in this study and characterized by attenuated total reflectance infrared spectroscopy, transmittance electron microscopy and thermo-gravimetric analysis supported by computational methods. The comparison of the results obtained from the bare and modified platinum electrodes revealed the sensitivity of the developed biosensor with modified electrode having high sensitivity of 0.1863 $\mu g.L^{-1}$ and electron transfer rate constant (*ks*) of 3.02 s^{-1}. To understand the redox mechanism completely, adsorption and ligand-enzyme docking simulations were carried out. Docking studies revealed that capsaicin formed hydrogen bonds with Glutamates (GLU355, GLU541, GLU586), Arginine (ARG) and other amino acids of the hydrophobic channel of the binding sites which facilitated the redox reaction for detection of capsaicin. These results confirm that the PAL enzyme facilitated the electron transfer from the capsaicin ligand, hence improving the biosensing response. Our results suggest potential applications of this methodology for the determination of capsaicin in the food industry.

Table of Contents

List of Tables

List of Figures

Definitions

Capsaicinoids: is a class of compounds found present in members of the capsicum family of plants.

Capsaicin: is the major and active component of chilli peppers, which belong to genus capsicum.

Voltammetry:is a category of electro-analytical methods used in analytical chemistry, where information about an analyte is obtained by measuring current (I) as the potential (V) is varied.

Biosensor: is an analytical device used for detection of an analyte that combines a biological component with physicochemical detector.

Enzymes: are biological molecules (proteins) that act as catalysts and help complex reactions occur everywhere in life.

Phenylalanine ammonia lyase (PAL): is an enzyme that catalysis a reaction converting L- phenylalanine to ammonia and trans-cinnamon acid.

Glucose Oxidase (GOx): is an oxido-reductase enzyme that catalyses the oxidation of glucose to hydrogen peroxide and D-glucono lactone.

Nanotechnology: is the study about the manipulation of matter on an atomic and molecular scale.

Nafion: Is a sulfonated tetra-fluoroethylene based fluoropolymer which can be used as a membrane in biosensor development.

Acronyms and Symbols

AdsSV	Adsorptive stripping voltammetry
AMDTC	Ammonium morpholine dithiocarbamate
ATR-IR	Attenuated total reflectance- infrared spectroscopy
Au-E	Gold electrode
AuNPs	Gold nanoparticles
BPPGE	Basal plane pyrolytic graphite electrode
CNTs	Carbon nanotubes
CV	Cyclic voltammetry
Da	Dalton
DMF	Dimethyl formamide
DPV	Differential pulse voltammetry
ECS	Electrochemical sensors
FAD	Flavin adenine dinucleotide
GCE	Glassy carbon electrode
GOx	Glucose oxidase
HAL	Histidine ammonia lyase
HPCE	High performance capillary electrophoresis
HPLC	High performance liquid chromatography
HPLC-ED	High performance liquid chromatography with electrochemical detection
HRTEM	High resolution transmission electron microscopy
kDa	kilo Dalton

MWCNTs	Multi walled carbon nanotubes
PAL	Phenylalanine ammonia lyase
PDB	Protein data bank
Pt-E	Platinum electrode
R^2	Coefficient of determination
RDE	Rotating disk electrode
SEM	Scanning electron microscopy
SPE	Screen-printed electrode
SPME	Solid phase micro-extraction
SWCNTs	Single walled carbon nanotubes
TEM	Transmission electron microscopy
TGA	Thermogravimetric analysis
TLC	Thin layer chromatography
UPLC	Ultra performance liquid chromatography
UV-VIS	Ultraviolet visible spectroscopy
V	Voltage
$V.s^{-1}$	Volts per second

Research Outputs

Poster Presentations

41st National Convention of the South African Chemical Institute held at Walter Sisulu University, East London, South Africa, 1st to 6th December **2013**. "Gold Nanoparticles decorated carbon nanotubes on glassy carbon electrodes: Capsaicin as test case"

MAM-14, **7th** International Symposium on Macro and Supra-molecular Architectures and Materials, Emperors Palace, Johannesburg, South Africa, 23 – 27 November **2014.** "Electro oxidation of Capsaicinoids by Glucose Oxidase enzyme on a multi walled carbon nanotube-based glassy carbon electrode"

World Congress and Expo on Materials Science and Polymer Engineering held at Dubai Deira Crowne Plaza, Dubai, UAE, 26 – 28 November **2015**. Determination of Capsaicin using carbon nanotubes based electrochemical biosensors.

Publications

Thabani Mpanza, Myalowenkosi I. Sabela, Sanele S. Mathenjwa, Suvardhan Kanchi and Krishna Bisetty, "Electrochemical determination of Capsaicin and Silymarin using a Glassy Carbon Electrode modified by Gold Nanoparticle decorated Multi Walled Carbon Nanotubes", *Analytical letters*, 47 (**2014):** 2813-2828**.**

Myalowenkosi I. Sabela, **Thabani Mpanza**, Suvardhan Kanchi, Deepali Sharma and Krishna Bisetty, " Electrochemical sensing platform amplified with a nanobiocomposite of L-phenylalanine ammonia-lyase enzyme for the detection of capsaicin", *Biosensors and Bioelectronics,* 83 (2016): 45-53

CHAPTER 1

INTRODUCTION

This chapter provides a brief overview of food additives with particular emphasis on the determination of capsaicin in chilli peppers according to the food industry standards. The aims and objectives of the thesis work are also presented here.

1.1 Food Additives

Food additives are substances added to food in order to enhance its taste and appearance or to preserve its flavour. Other food additives are used to provide nutrition and also for making food appealing to the consumer. Most human beings use these additives when preparing food, for example; spices are added for good flavour. Chilli pepper fruits are used in spices when preparing food or used to prepare other spices which are more or less pungent. Chilli pepper fruits are also used in the production of curry powder, chilli sauces and many other food stuffs of different pungency degree.

Chilli peppers have been widely used around the world for many centuries as food additives and spices. Its origin is believed to be as old as 7000 B.C, Mexicans are known for having grown and cultivated chillies as early as 3500 B.C (Bosland, 1996). Christopher Columbus was among the first Europeans to encounter chilli peppers and was instrumental in introducing it in Europe and other parts of the world (http://en.wikipedia.org/wiki/chili_pepper, 2012). Chilli peppers are mainly consumed because of their hotness or pungent flavour, and capsaicinoids are the main component for the pungency flavour of hot chilli peppers (Kachoosangi et al. 2008). Capsaicinoids are also known for their medicinal properties that they possess and also for pain relief properties; this compound has also been used in manufacturing of pepper sprays. Capsaicin was chosen as an analyte of interest in this study in order to help design and manufacture an electrochemical biosensor that will be used in the spice and food industry.

Literature studies revealed that different methods have been used to measure or determine the hotness or pungency of chilli peppers, the oldest method being the Scoville Organoleptic test (Kachoosangi et al. 2008). Other methods included sophisticated laboratory instruments such as "High performance liquid chromatography with electrochemical detection (HPLC-ED)," a reliable but costly method (Supalkova et al. 2007). Another analytical method worth mentioning involved solid phase microextraction-gas chromatography-mass spectrometry for the detection of capsaicin in peppers and chilli sauces (Peña-Alvarez et al. 2009). The Scoville method, along with other techniques for the determination of capsaicin are discussed in detail in Chapter 2.

1.2 Problem statement

Previous studies on the determination of capsaicin revealed that the Scoville organoleptic test is subjective, as it is based on human palate which differ from person to person. Other methods are expensive to use, hence the employment of an electro-analytical method using modified electrodes is used in this study. Modification of the bare electrodes (GCE, Pt-E or Au-E) with multi walled carbon nanotubes and later with an enzyme would enhance the electrode sensitivity.

1.3 Aims and Objectives

Aim:

This study was aimed at the determination of capsaicin in ripe chilli pepper fruit, using electrochemical methods supported by computational techniques.

Objectives:

- To develop an electrochemical biosensor from bare electrodes (Glassy carbon, Platinum and Gold) by immobilizing carbon nanotubes on the surface of the electrode disk immobilized with a biological component (enzyme) on the MWCNTs modified electrode to form biosensors.
- To test the performance and sensitivity of the developed sensors by electrochemical characterisation techniques using capsaicin extracted from chilli pepper as an analyte of interest for the quantification.

- To identify the best performing biosensor for the determination of capsaicin

- To evaluate the performance of (Glassy carbon, Platinum, and Gold) electrodes modified with MWCNTs decorated with PAL and GOx respectively.

- To compare the activities of the modified electrodes against unmodified electrodes in order to measure the contribution of MWCNTs and the enzymes for the improvement of electrochemical detection of capsaicin.

- To contribute towards the manufacturing of highly sensitive electrochemical biosensors, to be used in the spice manufacturing industries.

This study involved the determination of capsaicin, belonging to a group of capsaicinoids using electrochemical biosensing devices. In this work obsolete and expensive methods are replaced with a less expensive, but highly sensitive electro-analytical method using a normal bare rotating disk electrode modified with MWCNTs) and an enzyme in order to convert an electrochemical sensor into a biosensor.

1.4 Thesis Outline

After providing an overview of capsaicin and its role in the food industry in this chapter, the further chapters in this thesis are organized as follows:

Chapter 2 deals with the literature review discussing capsaicinoids applications and their properties, electrochemical biosensors, nanotechnology and electroanalytical techniques.

Chapter 3 outlines the experimental and computational methodology employed in this study including instrumentation, reagents and its preparation, electrode modification, computational and real sample preparation.

Chapter 4 covers experimental results obtained using different electrodes (GC-E, Pt-E and Au-E) modified with MWCNTs and enzymes, including molecular docking studies as part of the computational work.

Chapter 5 outlines the conclusions of this study.

Chapter 6 provides a list of References used in this dissertation.

CHAPTER 2

LITERATURE REVIEW

This chapter provides an overview of capsaicinoids mainly aimed at the determination of capsaicin using the various analytical techniques. A review on electrochemical biosensors in relation to applied nanotechnology is also presented.

2.1 Capsaicinoids

Capsaicinoids are a group of pungent chemical compounds found in hot peppers (*capsicum annum and capsicum frutescens*) (Reilly et al. 2001). The burning taste of pepper is induced by six chemically related compounds derived from phenylalkylamide alkaloid (capsaicinoids) group. Capsaicin and its derivative dihydrocapsaicin have the strongest burning effects and it is assumed that capsaicin was evolved as a plant protection against herbivores (Supalkova et al. 2007). Capsaicin and dihydrocapsaicin are the main components of capsaicinoids and are responsible for about 90% or more of the total capsaicinoids, the other 10% or less are nordihydrocapsaicin, homocapsaicin and homodihydrocapsaicin (Laskaridou-Monnerville, 1999).

There are five naturally occurring capsaicinoids, the most abundant and potent analogues in peppers (and consequently pepper extracts) are capsaicin and dihydrocapsaicin. The other three are also present, but generally contribute little to the total capsaicinoids concentration and pungency of pepper. The sixth capsaicinoid is nonivamide, which is a "synthetic" capsaicin and it exhibits the same pungency as capsaicin, but has not been conclusively identified as a natural product (Reilly et al. 2001). Capsaicinoids possess some biological properties that can be beneficial for human health, they have high antioxidant power (Henderson et al. 1999) in addition to anti-tumoral (Sanchez et al. 2006), anti-bacterial (Satya Narayana, 2006) and anti-carcinogenic properties (Huynh and Teel, 2005).

The level of heat in peppers and hot sauces has previously been measured by a classical method known as Scoville Organoleptic Test, which was created by an American chemist, Wilbur Scoville in 1912. In this method pungency was detected by tasting a solution of pepper extract diluted in a solution of sugar water until the heat or pungency is no longer detectable to the tongues of a panel of specially trained tasters. The level of dilution of the extract using sugar water solution then gives the Scoville unit which is a measure of the "hotness" of a chilli pepper. The greater the number of Scoville units, the higher the levels of hotness. But this method suffers from imprecision as it is subjective, hence the development of new methods (Kachoosangi et al. 2008). Table 2.1 shows different types of capsaicinoid compositions, their structures and properties.

Table 2.1: Chemical properties and structures of different capsaicinoids

Name	Relative Amount	Formula	Molar mass (Da)	Scoville heat units	Chemical Structure
Capsaicin	69 %	$C_{18}H_{27}NO_3$	305.41	$16x10^6$	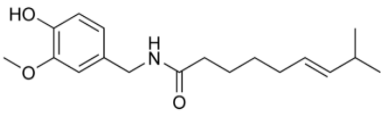
Dihydro-capsaicin	22 %	$C_{18}H_{29}NO_3$	307.43	$15x10^6$	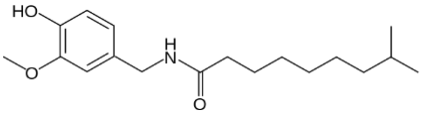
Nordihydro-capsaicin	7 %	$C_{17}H_{27}NO_3$	293.41	$9.1x10^6$	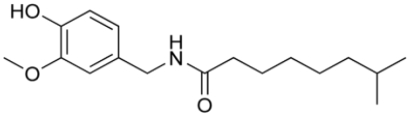
Homodihydro-capsaicin	1 %	$C_{19}H_{31}NO_3$	321.46	$8.6x10^6$	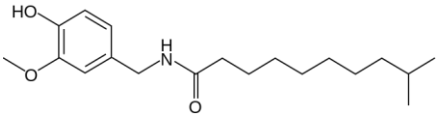
Homo-capsaicin	1 %	$C_{19}H_{29}NO_3$	319.43	$8.6x10^6$	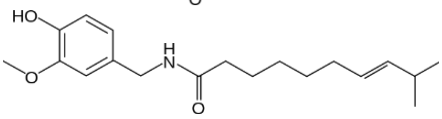
Nonivamide		$C_{17}H_{27}NO_3$	293.41	$9.2x10^6$	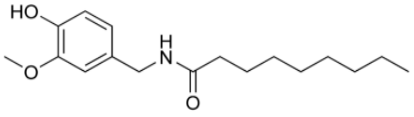

2.1.1 Capsaicin

Capsaicin (*8-methyl-N-vanillyl-6-nonenamide*) shown in Figure 2.1 is the major alkaloid responsible for the mucosal irritant properties of plant species from the

Genus capsicum (Buck and Burks, 1985). Capsaicin has a molecular weight of 305.41 Da, and its molecular formula is $C_{18}H_{27}NO_3$. Capsaicin is soluble in ethanol, acetone and fatty oils, but is insoluble in cold water (Barceloux, 2009). It is an irritant for mammals including humans and produces a sensation of burning in any tissue with which it comes into contact.

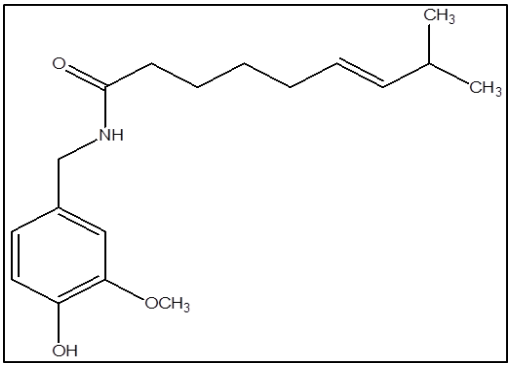

Figure 2.1: Chemical structure of Capsaicin (8-methyl-N-vanillyl-6-nonenamide)

Capsaicin has been used for different applications in the past. It is used in spices and chilli sauces. It has also been used as pain-inducing defensive pepper sprays (Pershing et al. 2006). Exposure to pepper sprays elicits an intense physiological response that includes nociception, temporary blindness, lacrimation, disorientation, shortness of breath, and choking (Hyder, 1996). Capsaicin-containing creams are mainly used for the treatment of painful conditions, such as psoriasis, rheumatoid arthritis, diabetic neuropathy, cluster headache and reflex sympathetic dystrophy (Hautkappe et al. 1998).

Capsaicin content increases with the maturity of the pepper fruit (Balbaa et al. 1968), the medical effects of capsaicin results from the initial period of intense excitation of the primary afferent sensory nerves followed by a prolonged period of relative resistance to nociceptive chemical stimuli. Physiologically, capsaicin reduces vasodilation and heat pain thresholds, leading to increased pain sensitivity (Barceloux, 2009). Repeated exposure to capsaicin causes desensitization of the stimulatory effects on the sensory nerves (Carpenter and Lynn, 1981).

Over the years, different methods for the detection of capsaicinoids have been used including the Scoville organoleptic test as described in Section 2.1. In the next page, Table 2.2 shows the comparison of previous studies for the determination of capsaicin followed by a brief discussion of each analytical technique.

Table 2.2: *Comparison of previous studies for the determination of capsaicin*

Experimental			Analytical Parameters				
Methods	**Sample**	**Analyte**	**Linear dynamic range [Equation]**	**R^2**	**Limit of detection**	**Limit of quantification**	**Reference**
SPME-GC-MS	Peppers and pepper sauces	capsaicin dihydrocapsaicin	0.109-1.323 µg/mL 0.107-1.713 µg/mL	>0.9970 >0.9970	0.014 µg/mL 0.022 µg/mL	0.069 µg/mL 0.108 µg/mL	Peña-Alvarez et al. 2009
AdsSV MWCNT-BPPGE	Chilli peppers	capsaicin	0.5 to 15 µM [$y=5.31x10^{-7}$ $x - 2.52 \times 10^{-7}$]	0.9900	0.31 µM	NR	Kachoosangi et al. 2008
AdsSV MWCNT – SPE	Chilli peppers	capsaicin	0.5 to 35 µM [$y=3.07 \times 10^{-7}$ x-1.52×10^{-7}]	0.9900	0.45 µM	NR	Kachoosangi et al. 2008
HPCE	Capsicum annum, pepper sauce and porous capsicum plaster	capsaicin dihydrocapsaicin	1 to 400 µg/mL 1 to 400 µg/mL	0.9994 0.9994	0.66 µg/mL 0.073 µg/mL	NR	Liu et al. 2010
HPLC- ED	Pepper fruit	capsaicin	31.3 to 125 µg/mL	0.9948	305 ng/mL	NR	Supalkova et al. 2007
HPLC fluorescence	Hot peppers	capsaicin dihydrocapsaicin	[$y=112.901x + 187$] [$y=151.770x +4589$]	0.9995 0.9995	0.008 mg/L 0.011 mg/L	0.028 mg/L 0.036 mg/L	Barbero et al. 2008
UPLC	gochujang	capsaicin dihydrocapsaicin	0.2 to 10.0 µg/mL 0.2 to 10.0 µg/mL	0.9995 0.9999	0.05 µg /g 0.05 µg /g	0.16 µg /g 0.16 µg /g	Ha et al. 2010
AdsSV	Chilli peppers	capsaicin	0.15 to 35.0 µM I_p(µA)=46.24C-12.21	0.9953	0.083 $\mu g.L^{-1}$	0.276 $\mu g.L^{-1}$	Mpanza et al. 2014

2.1.2 Liquid Chromatography with Electrochemical detection

In this method, high performance liquid chromatography with electrochemical detection (HPLC-ED) system which consists of a solvent delivery pump, a guard cell, a chromatographic column and an electrochemical detector was used. This method has a comparable detection limit and can be used for characterisation of pepper cultivars with respect to capsaicin content (Supalkova et al. 2007) as shown in Table 2.2. Other workers also used HPLC method for the purification of glucosides of capsaicin and dihydrocapsaicin, where these glucosides were detected in various pungent cultivars of *C. annuum*, *Capsicum frutescens*, and *Capsicum chinense* by liquid chromatography−mass spectrometry. However, they were not detected in nonpungent cultivars of *C. annuum* (Higashiguchi et al. 2006). Supalkova et al. concluded that HPLC-ED method has a comparable detection limit and can be used for the characterization of pepper cultivars with respect to capsaicin content.

2.1.3 UV-Vis spectrophotometry

According to Abdullah Al Othman and co-workers, for quantitative measurements, the UV detection wavelength is normally set at 222 nm, because this wavelength corresponds to the maximum absorbance for both capsaicin and dihydrocapsaicin (Othman et al. 2011). Therefore there is no differentiation between the two capsaicinoids when using UV, but the HPLC chromatograms show a complete separation between the two capsaicinoids, thus making it difficult to quantify different types of capsaicinoids using UV method.

2.1.4 Thin layer Chromatography (TLC)

Thin layer chromatography method involves the use of glass plates coated with thin layer absorbent material, with finely divided particles like silica gel as its stationary phase. Capsaicinoid sample is placed on the edge of the plate and placed into the mobile phase (developing solvent), where it is separated as the developing solvent transverses across the length of the plate. Spanyar and Blazovich wrote that the best capsaicin sample preparation was achieved using chloroform-ethanol (99+1) solvent system (Spanyar and Blazovich, 1969). This method gives an indication of sample migration, but is not as accurate as HPLC and voltammetry techniques. (Pankar and Magar, 1977) used a multi band thin layer chromatography for the determination of

capsaicin. Andre and Mile in 1975 developed a simple and sensitive TLC method for the determination of capsaicin at levels as low as 0.1 µg of capsaicin per spot, this method helped in distinguishing paprika variations according to their degree of pungency (De, 2004).

2.1.5 Adsorptive stripping voltammetry (AdsSV)

Capsaicin was determined using AdsSV at a multiwalled carbon nanotube modified basal plane pyrolytic graphite electrode (MWCNTs-BPPGE). The aim of this method is to determine the quantity of capsaicin where measuring the concentration of capsaicin is an indicator of how hot the chilli is. Kachoosangi and co-workers further developed this method by using a multiwalled carbon nanotube screen-printed electrode (MWCNTs-SPE) in order to demonstrate the proof that this approach can easily be incorporated into a sensing device. This method offers advantages such as precision and objectivity over potentially subjective Scoville method, and is facile and inexpensive compared to HPLC method (Kachoosangi et al. 2008). Kachoosangi and co-workers also found that when using MWCNTs-BPPGE capsaicin exhibited a linear dynamic range from 0.5 to 15 µM as shown in Table 2.2, whereas when using the disposable MWCNT-SPE the standard additions of capsaicin showed a linear range between 0.5 and 35 µM (Mpanza et al.2014).

2.2 Electrochemical biosensors

A biosensor is an analytical device used for the detection of an analyte, which combines a biological component with a physicochemical detector. According to Turner it can be defined as a "compact analytical device or unit incorporating a biological or biologically derived sensitive 'recognition' element integrated or associated with a physico-chemical transducer" (Turner, 2000).

An IUPAC definition of a biosensor states "It is an integrated receptor-transducer device, which is capable of providing selective quantitative or semi-quantitative analytical information using a biological recognition element" (Theavenot et al. 1999). The sensitive biological component/ element might include: microorganisms, biological tissues, enzymes, nucleic acids and many others. Some of the transducers used in conjunction with these biological elements in the fabrication of biosensors are: Electrochemical, amperometric, potentiometric, ion selective, conductometric and many others. In this study enzymes are used for the fabrication of biosensors. A biosensor consists mainly of three parts, which includes:

- Sensitive biological element (e.g. microorganisms, enzymes, antibodies, nucleic acids, cell receptors etc.)
- Transducer or detector element, that transforms signal resulting from the interaction of the analyte with the biological element into another signal that can be more easily measured or quantified.
- Associated electronics that are primarily responsible for the display of the results (Hierlemann et al. 2003).

Biosensor can be used in a variety of areas of interest. In the medical field, for example glucose biosensor are used for monitoring glucose in diabetic patients (Yoo and Lee, 2010). In environmental analysis biosensors are used to detect pesticides, heavy metals that can be found in river streams which are detrimental to humans, livestock and the environment (Haron and Ray, 2006). Biosensors are also used in food analysis; especially for the detection of allergenic components, pathogens and food toxins (Murugaboopathi et al. 2013).

2.2.1 Enzymes

Enzymes are large, proteinaceous biological molecules responsible for thousands of metabolic processes that sustain life (Smith, 1997); (Grisham and Garret, 1999). Enzymes are highly selective catalysts, greatly accelerating both the rate and specificity of metabolic reactions, from digestion of food to the synthesis of DNA (Sarmah and Mahanta, 2014). Like all catalysts, enzymes work by lowering the activation energy for a reaction, thus dramatically increasing the rate of reaction.

As much as they work as catalysts, their activity can be affected by other molecules (inhibitors) by decreasing enzyme activity. Enzymes used in this study were established by looking at enzymes that will interact with phenols and amides. Two enzymes were chosen based on their interaction with capsaicinoids. Other factors affecting enzyme activity are: temperature, pressure, chemical environment like pH and concentration of the substrate. The two enzymes used in this project were Phenylalanine ammonia lyase (PAL) and Glucose oxidase (GOx).

2.2.2 Phenylalanine ammonia lyase (PAL)

PAL is found widely in plants as well as some yeast and fungi, with isoenzymes existing within many different species. It has a molecular mass in the range of 270-330 kDa (Camm and Tower, 1973); (Watanabe et al. 1992). PAL is an enzyme that catalyses a reaction converting L-phenylalanine to ammonia and trans-cinnamic acid (Figure 2.3). Previously PAL was designated EC 4.3.1.5, but later redesignated as EC 4.3.1.24. Other names in common use include*: tyrase, phenylalanine deaminase, tyrosine ammonia-lyase, L-tyrosine ammonia-lyase, phenylalanine ammonium-lyase, PAL, and L-phenylalanine ammonia-lyase.*

PAL is the first step in the phenylpropanoid pathway and is therefore involved in the biosynthesis of the polyphenol compounds such as phenylpropanoids, flavonoids and lignin in plants. This enzyme is the member of the ammonia lyase family, which cleaves carbon-nitrogen bonds. Like other lyases, phenylalanine requires only one substrate for the forward reaction and two for the reverse reaction. It is thought to be mechanistically similar to the related enzymes, *histidine ammonia lyase* (EC: 4.3.1.3, HAL) (Schwede et al. 1999). Its activity is induced dramatically in response to

various stimuli such as tissue wounding, pathogenic attack, light, low temperatures, and hormones (Camm and Towers, 1973; Hahlbrock and Grisebach, 1979). A decade ago it was reported that PAL has possible therapeutic benefits in humans afflicted with phenylketonuria (Sarkissian and Gamez, 2005). 3D Image of Phenylalanine ammonia lyase enzyme is shown in Figure 2.2 below.

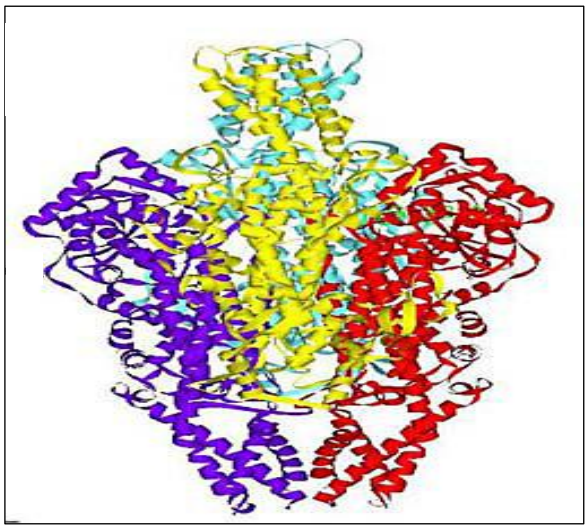

Figure 2.2: Image of Phenylalanine ammonia-lyase enzyme determined by high resolution X-ray crystallography (PDB, IDCODE: 1Y2M) (Gamez et al. 2007).

The first recorded observation of PAL and its catalysed reaction was reported by Koukol and Conn in 1961. In their work, PAL was isolated from *Hordeum vulgare* and initially given the name phenylalanine deaminase (Koukol and Conn, 1961). Phenylalanine ammonia lyase catalyses the nonoxidative deamination of L-phenylalanine to form trans-cinnamic acid and a free ammonium ion (Figure 2.3), (Koukol and Conn, 1961). The conversion of the amino acid phenylalanine to trans-cinnamic acid is the entry step for the channelling of carbon from primary metabolism into phenylpropanoid secondary metabolism in plants (Woo Hyun et al. 2011). PAL has been extensively studied because of its role in plant development and its response to a wide variety of environmental stimuli. The importance of PAL in plant metabolism is demonstrated by the huge diversity and large quantities of phenylpropanoid products found in plant materials (Jones, 1984). Protein sequence for PAL enzyme is shown in Appendix 1a.

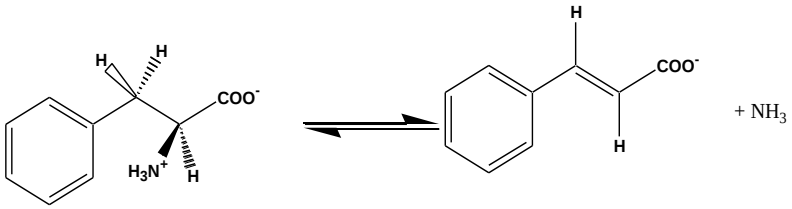

L- Phenylalanine Cinnamic acid Ammonia

Figure 2.3: Deamination of L-Phenylalanine by PAL (Woo Hyun et al. 2011)

2.2.3 Glucose Oxidase (GOx)

Glucose oxidase (GOx) (EC 1.1.3.4) is a large, dimeric protein consisting of two equal subunits with a formula weight of 160 kDa. It catalyses the oxidation of β-D-glucose to hydrogen peroxide and δ-D-gluconolactone, as shown in (Figure 2.4) below. Glucose oxidase contains one tightly-bound flavin adenine dinucleotide (FAD) unit per monomer. These redox-active groups are not covalently bound and may be released from the protein during denaturation (Lyons and Keeley, 2008; Bergmeyer, 1983).

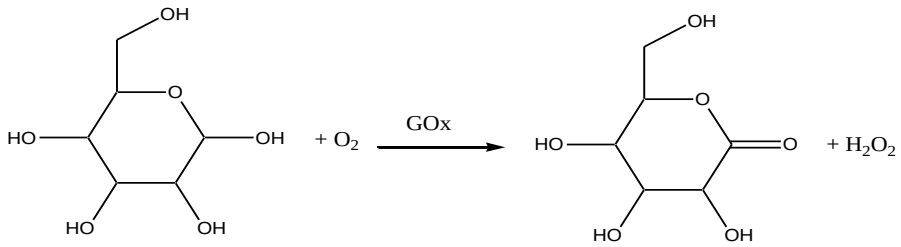

β-D-Glucose δ-D-Gluconolactone Hydrogen peroxide

Figure 2.4: Catalysis of the oxidation of D-glucose by Glucose oxidase enzyme (Wong et al. 2008)

There are different types of Glucose oxidase enzymes from *Aspergillus Niger*, namely: Type X-S, lyophilized powder 100 000 – 250 000 units.g^{-1} (solid); Type II, ≥ 15000 units.g^{-1} (solid); Type VII ≥100 000 units.g^{-1} lyophilized powder (Xu et al. 2012). The type of GOx used in this work is Glucose Oxidase Type VII extracted

from *Aspergillus niger*. GOx is extracted from *Aspergillus niger* by reversed micelles from mixtures of commercial enzymes and homogenates at 25°C, GOx recovery is then obtained by performing forward and backward extractions, for forward extraction isooctane is used as a solvent and hexanol and butanol as co-solvents at a ratio of 76/6/18 at pH 7.0, for backward extraction 0.2 M Cetyl trimethylammoniun bromide as a cationic surfactant was used, product will then be centrifuged and dried (Ferreira et al. 2005). Glucose oxidase can be utilised for the enzymatic determination of D-glucose in solution. This enzyme is a glycoprotein containing approximately 16% neutral sugar and 2% amino sugar (Tsuge et al, 1975). The enzyme also contains 3 cysteine residues and 8 potential sites for N-linked glycosylation (Frederick et al, 1990).

(a) (b)

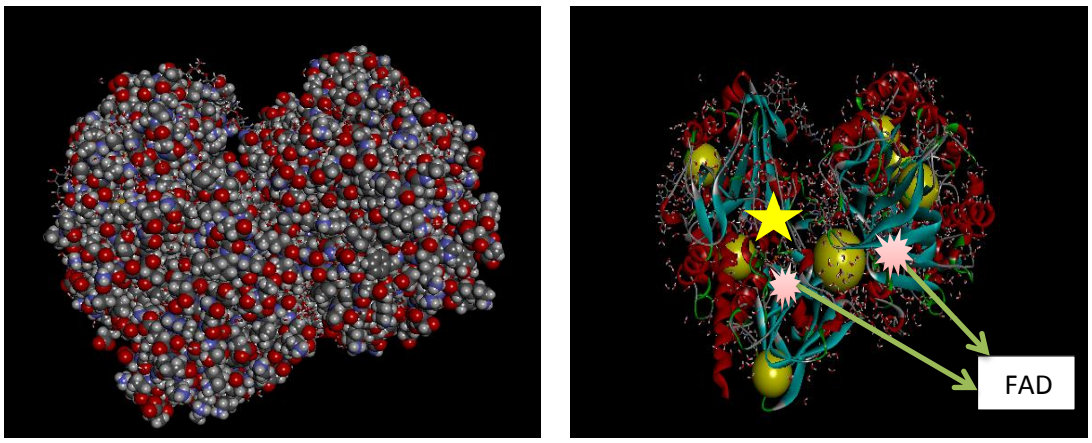

Figure 2.5: Images of Glucose Oxidase enzyme, (a) Image obtained from Protein data bank (PDB), and (b) Image created with RasMol (Goodsell, 2006)

A closer inspection of GOx structure on the right hand side, shows multiple binding sites represented by yellowish oval balls. Flavin adenine dinucleotide (FAD) cofactors which are bound deep inside the enzyme shown in pink; the oxidation reaction is performed by these FAD cofactors. The most active site where glucose binds is just above the FAD shown with a yellow star. GOx protein sequence and its protein properties are presented in Appendices 1b and 1c respectively.

2.3 Nanotechnology and Electroanalytical Techniques

Nanotechnology involves the manipulation of matter on an atomic and molecular scale. This concept earlier referred to the particular technological goal of precisely manipulating atoms and molecules for fabrication of macro-scale products (Drexler, 1986). Nanotechnology is naturally very broad, including fields of science as diverse as surface science, organic chemistry, molecular biology, semi-conductor physics, micro fabrication and many others. Research associated with nanotechnology extends to several approaches, like developing new materials with dimensions on the nanoscale. The evolution of technology and instrumentation, as well as its related scientific areas such as physics and chemistry are making the research on nanotechnology very attractive for many other areas (Lopez, 2009).

Taniguchi was the first to use the term "nanotechnology" when he presented his paper titled, "On the Basic Concept of 'nanotechnology" in 1974, where he described the manufacturing of products with tolerances of less than 1 μm (Taniguchi, 1974). Nanotechnology is considered the most advanced manufacturing technology because of the theoretical limit of accuracy which is the size of a molecule or an atom (King, 2007). The progress in nanotechnology has been enhanced by the discovery of atomically precise nanoscale materials such as fullerenes in 1980s and carbon nanotubes (CNTs) in 1991 (Meyyappan, 2005). The CNTs possesses outstanding properties which have over the years opened a new interesting research area in nanoscience and nanotechnology (Meyyappan, 2005); (Martin, 2006).

2.3.1 Nanomaterials

Nanomaterials are classified into two categories: Fullerenes and inorganic nanoparticles. Fullerenes are a class of allotropes of carbon, which conceptually are graphene sheets rolled into tubes or spheres; these include CNTs and are of interest because of their mechanical strength and electrical properties. Nanomaterials (gold, carbon, metals, meta oxides and alloys) as shown in Figure 2.6, have a variety of shapes like gold-nanoparticles, Buckminster fullerenes, titanium nanoflower and many others. Nanoparticles or nanocrystals have been used as quantum dots and as chemical catalysts such as nanomaterial-based catalysts (Ameta et al. 2014). Nanomaterials are usually considered to be materials with at least one external

dimension that measures 100 nanometres or less. They may be in the form of particles, tubes, rods, or fibres (Europa/health/scientific committees/nanomaterials, 2012).

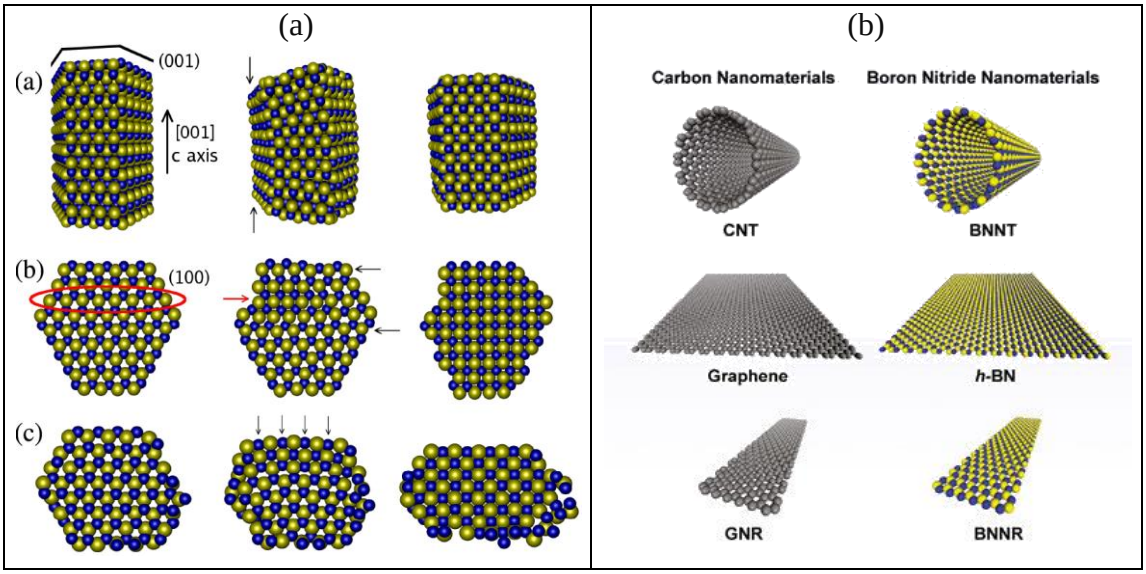

Figure 2.6: (a) and (b), Images of different structures of Nanomaterials (Grunwald et al. 2006; and http://nanotechweb.org/cws/article/tech/46378, 2011)

2.3.2 Carbon Nanotubes (CNTs)

Carbon nanotubes have received considerable attention in the field of electrochemical sensing, due to their unique structural, electronic and chemical properties. CNTs have unique tubular nanostructure, excellent conductivity, large surface area, good biocompatibility and many more (Chengguo and Shengshui, 2009). CNTs are widely used in electronic, biomedical, pharmaceutical, energy, catalytic, analytical and material fields. Special nanostructure properties make CNTs have some overwhelming advantages in fabricating electrochemical sensors. Carbon nanotube is one of many allotropes of carbon, others are: diamond, graphite, fullerenes and many others. There are two main types of CNTs: single-walled carbon nanotubes (SWCNTs) and multi-walled carbon nanotubes (MWCNTs). Structures of SWCNT and MWCNT are shown in Figures 2.7 (a) and (b) respectively (Pillay, 2012).

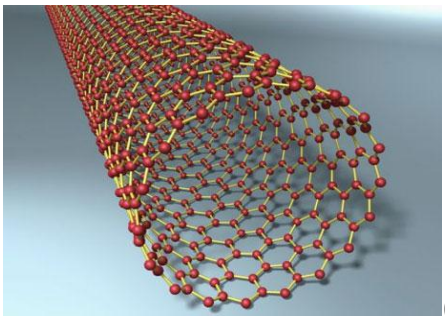
(a)

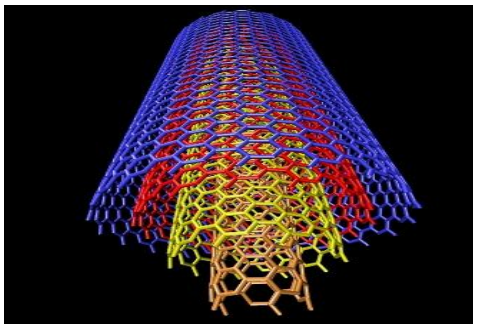
(b)

Figure. 2.7: (a) structure of SWCNT, (b) Structure of MWCNT (Pillay, 2012)

The name nanotubes are derived from their size, the diameter of a nanotube is about a few nanometers, (approximately 50 000 times smaller than the width of a human hair. CNTs possess a hollow core suitable for storing guest molecules and have the largest elastic modulus of any known material (Davis et al. 2003). The unique chemical and physical properties of CNT have paved the way to new and improved sensing devices, CNT-based electrochemical transducers offer substantial improvements in the performance of amperometric enzyme electrodes, immunosensors and biosensors (Wang, 2004), It is for this reason that they have become the subject of intense investigation for potential technological applications (Rao et al. 2001).

Properties of Carbon nanotubes

(a) Mechanical: The small diameter of CNTs has an important effect on the mechanical properties, compared with traditional micron-size graphitic fibres (Dresselhaus et al. 1988). One of the most important effect is the opportunity to associate high flexibility and high strength with high stiffness, a property which is absent in graphite fibres (Salvetat at al. 1999).

(b) Electrical: CNTs can be highly conductive and hence can be metallic. Their conductivity is shown as a function of their chirality, the degree of twist as well as their diameter (Lyons and Keeley, 2008). CNTs can be either metallic or semi-conducting in the electrical behaviour (Foley, 2006).

(c) Chemical: CNTs have high specific surface area and σ-π hybridization facilitate molecular adsorption, doping and charge transfer on nanotubes, which in turn

modulates electronic properties (Lopez, 2009). CNTs are polymers of pure carbon and possess all carbon versatility, including the ability to form countless combinations and derivatives. In addition the geometry of a nanotube allows for the formation of novel synthetic structures not possible with other carbon structures (http://www.cnanotech.com, 2013). CNT derivatives can be both covalently and non-covalently bonded. Sidewalls of CNT are electrically polarizable, polar molecules can easily adhere to their surfaces; CNTs can make sensitive chemical sensors (Snow et al. 2006).

(d) Thermal: A study by the University of Pennsylvania indicates that, CNTs may be the best heat conducting material man has ever known. They display very high thermal conductivity comparable to diamond crystal and in-plane graphite sheet (Che et al. 2000), it is therefore expected that nanotube reinforcements in polymeric materials may also improve significantly the thermal and thermo-mechanical properties of these composites (Foley, 2006).

Production of Carbon Nanotubes

There are numerous methods used for the production or synthesis of CNTs and fullerenes. The first method to be used was by applying an electric current across two carbonaceous materials, particularly graphite (Wilson et al. 2002). The most commonly used methods for the production of CNTs includes Carbon Arc discharge method, Laser method, Chemical Vapour deposition and Ball Milling method.

Carbon Arc Method

This method was initially used for the production of C60 fullerenes, and is the most common and perhaps the easiest way to produce CNTs. In general this method usually produces a crude complex mixture of components, which requires further purification to separate CNTs (Wilson et al. 2002). During the process carbon atoms are generated through an electric arc discharge at temperature >3000°C between two electrodes. Nanotubes are formed in the presence of suitable catalyst metal particles (Fe, Co or Ni), (Lopez, 2009). In Ando and Zhao's review of this method, they focused on the synthesis of multi-walled and single-walled carbon nanotubes respectively. They found out that MWCNTs were obtained in the cathode deposit of

the dc arc discharge of pure graphite rods, ambient gas played an important role but pure hydrogen gas was the best gas for obtaining high-crystallinity MWCNTs. In the case of SWCNTs by the same method, the incorporation of catalytic metal particles in a graphite anode was necessary, and SWCNTs were obtained as soot in an evaporation chamber (Ando and Zhao, 2006).

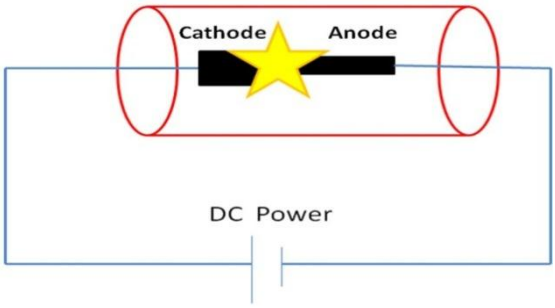

Figure 2.8: Schematic diagram of apparatus for Arc discharge method (Jahanshahi and Kiadehi, 2013)

Laser Method

This method was first discovered by Smalley and co-workers in 1995 (Rafique and Iqbal, 2011). Laser abrasion process synthesizes CNT by irradiating a pulsed laser on a graphite rod containing catalysts heated to 1000°C or higher (Lopez, 2009). Material produced by this method looks like a mat of ropes, 10-20nm in diameter and up to 100µm in length (Wilson et al. 2002). Further improvements in this method were done by (Thess et al. 1996 and Rao et al. 1997) where they used a double beam laser. Nanotubes produced by laser ablation method have higher purity of up to about 90% pure and their structure is better graphitized than those produced by the arc process (Rafique and Iqbal, 2011).

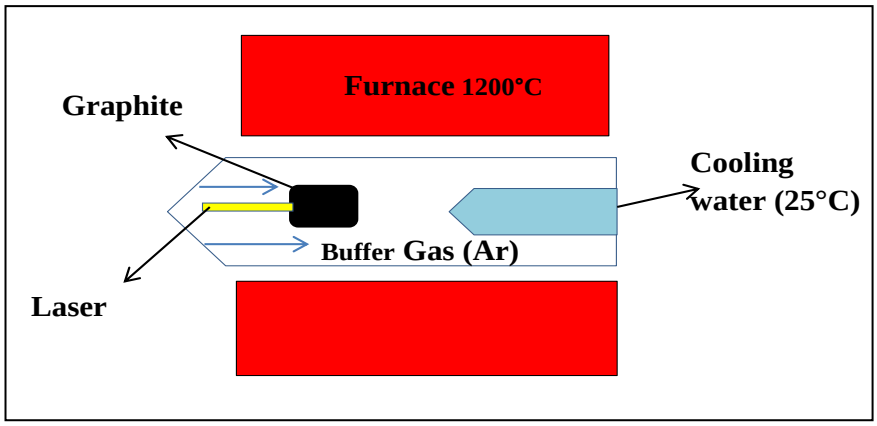

Figure 2.9: Schematic diagram of laser apparatus (Jahanshahi and Kiadehi, 2013)

Chemical Vapour Deposition (CVD) Method

In this method decomposition of a gaseous hydrocarbon source (ethylene or acetylene) is catalysed by metal nanoparticles (Co or Fe) at high temperatures (500 – 1000) °C. Carbon has a low solubility in these metals at high temperatures and thus the carbon will precipitate to form carbon nanotubes (Lopez, 2009). Chemical vapour deposition process seems to offer the best chance to obtain a controllable process for the selective production of nanotubes with predefined properties (Sinnott and Andrews, 2001). However there was no evidence that this technique could be used to synthesize carbon nanotubes until (Yacaman et al. 1993) succeeded.

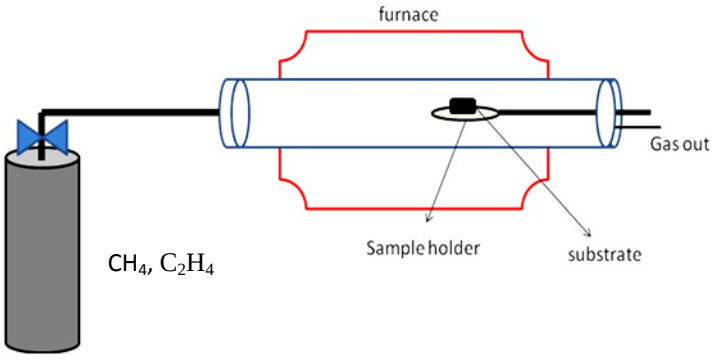

Figure 2.10: Schematic diagram of the setup used for CNT growth by CVD in its simplest form (Jahanshahi and Kiadehi, 2013).

Applications of Carbon Nanotubes

Carbon nanotubes have extraordinary electrical, thermal conductivity and mechanical properties. Therefore have a wide range of applications in materials, science, electronics, chemical processing, energy management, and many other fields have been reported in the literature (Lopez, 2009). CNTs have in recent years been widely used in modification of electrochemical and biosensors in order to enhance their electro-activity and sensitivity. CNTs are used in electronic devices and they have emerged as a promising class of electronic materials due to their nanoscale dimensions and outstanding properties, such as ballistic electronic conduction. CNTs are also used in energy applications as preferred alternative electrode material because of their unique electrical and electronic properties (Endo et al. 2008)

Mechanical and structural applications of CNTs have the ability to be the biggest large-scale application for the material. CNTs are considered to be the ideal form of fibres with superior mechanical properties compared to the best carbon fibres (Baughman et al. 2002). Carbon fibres have been used as reinforcements in high strength, light weight, high performance composites, like in spacecraft and aircraft body parts to expensive tennis rackets, and ideally, CNTs should perform far better than these fibres in mechanical applications (Endo et al. 2008). CNTs have been effective as sensing elements utilizing their electrical, electrochemical and optical properties. SWCNTs have been highlighted as promising gas-sensing elements, detecting low concentration of toxic gases which is important for environmental purposes and chemical safety. SWCNTs have advantages over conventional metal-oxide-based sensors in terms of power consumption, sensitivity, miniaturization and reliable mass production (Qi et al. 2003). They can also be used in field emission and lighting, field emitters due to their low threshold voltage, good emission stability and longer emitter lifetime (Saito and Uemura, 2000). These characteristics also make them useful in the fabrication of cathode-ray lighting elements and flat panel displays. The cathode ray tube lighting elements using arc derived MWCNTs as cold electron sources exhibit a stable electron emission, adequate luminance and long life of the emitters (Saito et al. 1998). DWCNTs and MWCNTs have been examined as the best field emitting materials because they show low threshold voltage compared

to SWCNTs and also a better structural stability compared to SWCNTs (Son et al. 2005; Jorio et al. 2007). CNTs are also important for biological applications; their optical properties impart promising advantages to their use in imaging applications within live cells and tissues (Heller et al. 2006).

Carbon nanotubes in electrochemical sensors and biosensors

Carbon nanotubes have been widely used in structure of different types of sensors. Various advantages of CNTs as sensor materials have been shown for the analysis of diversified chemicals of food quality, clinical and environmental interest. High thermal conductivity, remarkable mechanical properties, chemically stability and high surface to volume ratio of CNTs is very appealing for sensing applications. Electrochemical sensors (ECS) have been proven as an inexpensive and simple analytical method with remarkable detection sensitivity, reproducibility, and ease of miniaturization rather than other instrumental analysis methods. CNTs possess interesting electrochemical properties, which can be used for construction of electrochemical sensors. CNT-ECS exhibit low detection limit, high sensitivity and fast response due to the signal enhancement provided by high surface area, low overvoltage and rapid electrode kinetics (Mazloum-Ardakani and Sheikh-Mohseni, 2011).

Modification of Electrode surfaces

CNTs have been used to modify surfaces of bare electrodes, be it glassy carbon electrode (GCE), platinum or gold electrodes. Prior to modification the electrode is polished with alumina in water slurry using a polishing cloth and rinsed with deionised water. The immobilizing solution of MWCNTs is prepared by introducing 5 mg of MWCNTs into 5 ml of DMF. Since CNTs are insoluble in most solvents, ultra-sonication is required during preparation in order to effectively disperse the tubes (Balasubramanian and Burghard, 2006). In the report by Zare and co-workers, the modification was done by placing 10 µl of DMF-MWCNTs solution onto the bare electrode surface and dried at 50°C to form a MWCNTs film on the electrode surface as illustrated in Figure 2.11 below. After drying the surface was rinsed with deionised water (Zare and Nasirizadeh, 2011).

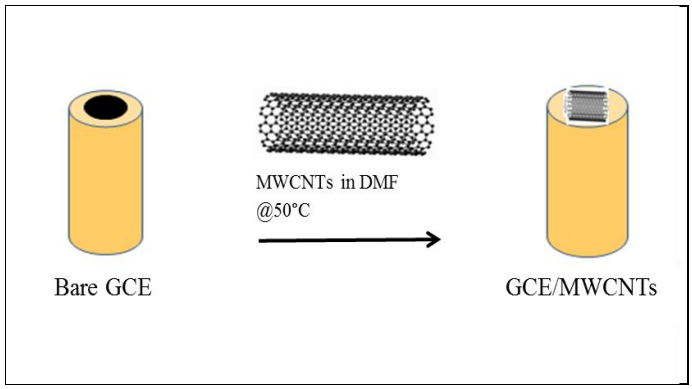

Figure 2.11: Schematic representation of Bare GCE modified with MWCNTs

Other methods use different solvents to disperse CNTs, Nafion (sulfonated tetra fluoro-ethylene) have been used extensively for the construction of amperometric biosensors owing to their unique ion-exchange, discriminative and biocompatibility properties. The ability of Nafion to solubilise CNTs provides a useful avenue for preparing CNTs-based electrode transducers for a wide range of sensing application (Wang at al. 2003).

The other method for modifying the electrode is the carbon paste method, (Figure 2.12) where a paste of (about 0.5 g) made of 70% graphite or CNTs powder and 30% mineral oil is housed in a Teflon body having a 2.5 mm-diameter disk surface. Prior to measurements, the electrode surface is renewed by polishing with a soft filter paper. Then, the surface is ready for measurement (Supalkova et al. 2007).

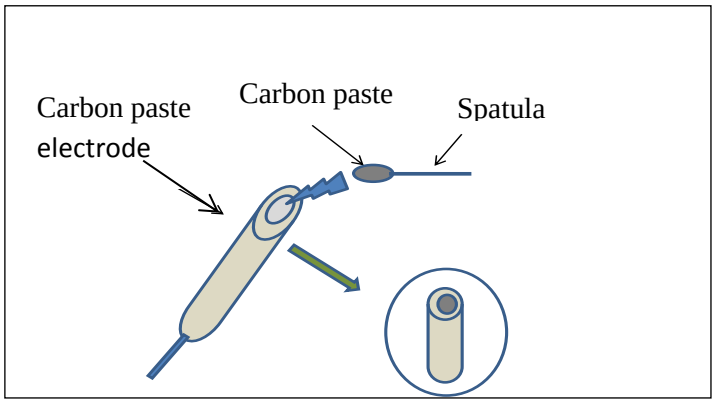

Figure 2.12: Schematic representation of preparation of carbon paste electrode

Electrochemical Sensors applications

Electrochemical sensors has become a very interesting and most attractive device for monitoring and measuring different types of substances, for quality control, and in medicinal and environmental chemistry. The importance of CNTs for sensors applications has led to wide research activities. One of the advantages of these sensors is that they can be used once and can be disposed-off after usage (Lopez, 2009). These electrochemical sensors can be used for detection of gases because of their potential applications in environmental pollution monitoring, flammable and toxic gas detection and food quality control. The most important problem in gas sensors is their selectivity, i.e. the capability to provide different responses when they are exposed to different gaseous species (Sayago et al. 2007).

Toxic metals are also detected by these sensitive electrochemical sensors especially when using sensitive electro-analytical techniques like voltammetry for trace metal analysis (Baldo et al. 2004). Most biomolecules are detected using CNTs modified electrodes; to it a biological element like (protein, enzyme, tissue etc.) is attached. Several analytes have been studied using biosensors, ranging from haemoglobin to glucose and many others. The remarkable properties of CNTs also suggest their use in developing (bio) sensing systems where nanoparticles have been involved. CNTs can be decorated with nanoparticles (Au, Ag, Ni, etc.) to enhance electrode's electro-activity and sensitivity. In recent years, several studies have aroused great interest in modifying electrode surfaces on the molecular scale with novel nanomaterials for the direct electron transfer of redox enzymes and retention of bioactivity (Liu et al. 2005).

2.3.3 Nanoparticles

A nanoparticle is the most fundamental component in the fabrication of a nanostructure; and is far smaller than everyday objects that are described by Newton's laws of motion, but bigger than an atom (Horikoshi and Serpone, 2013). In general, the size of a nanoparticle spans the range between 1 and 100 nm. It is interesting to note that metallic nanoparticles may exhibit size related properties that differ significantly from those observed in fine particles or bulk materials (Buzea et al. 2007). Nanoparticles often possess unexpected optical properties as they are small enough to confine their electrons and produce quantum effects (Hewakuruppu et al.

2013), for example, gold nanoparticles appear deep-red to black in solution. There are different types of metal nanoparticles for example, gold, silver, copper, zinc and many others, in this study gold nanoparticles were used. Gold nanoparticles melt at much lower temperature (approximately 300°C for a 2.5 nm size) than gold slabs which melt at 1064°C (Buffat and Borel, 1976). There are different types of techniques that can be used for characterization of nanoparticles, for example electron microscopy (TEM and SEM), XRD, NMR and many others.

2.3.4 Voltammetry

Voltammetry is a category of electro-analytical methods used in analytical chemistry and various industrial processes, according to Kounaves this technique's development is based on the discovery of polarography in 1922 by the Czech chemist Jaroslav Heyrovsky, for which he received the 1959 Nobel Prize in chemistry (Kounaves, 1997). In this electrochemical technique, information about an analyte is obtained by measuring the current as the potential is varied (Kissinger and Heineman, 1996; Zoski, 2001). Voltammetry setup with three electrode system is shown in Figure 2.13 below.

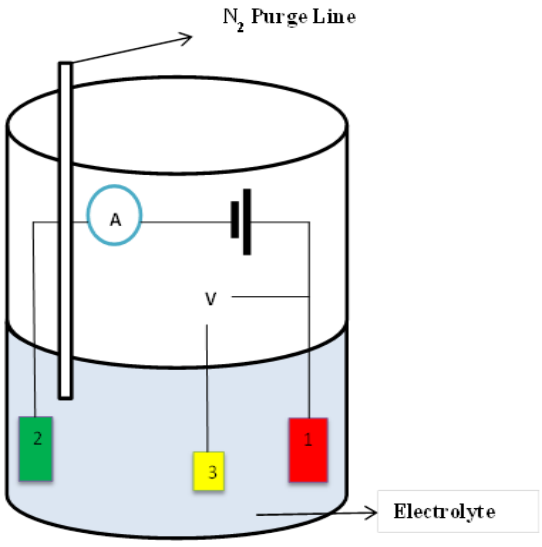

Figure 2.13: Voltammetric cell with three electrode setup: (1) Working electrode; (2) Auxiliary/counter electrode; (3) Reference electrode

The working electrode is the electrode in an electrochemical system on which the reaction of interest is occurring, types of working electrodes include, Rotating disk

electrode (RDE), hanging mercury drop electrode (HMDE) etc. Auxiliary electrode, also known as counter electrode, is an electrode used in a three electrode electrochemical cell for voltammetric analysis in which an electrical current is expected to flow. These electrodes are made out of electrochemically inert materials such as gold, platinum or carbon.

A reference electrode possesses a stable and well-known electrode potential, common types are: standard hydrogen electrode (SHE), saturated calomel electrode (SCE), silver chloride electrode and many others. Some of the analytical advantages of voltammetric techniques include excellent sensitivity with a wide linear concentration range for both organic and inorganic species (10^{-12} to 10^{-1} M). Figure 2.14 shows images of 797 VA computrace instrument used for electrochemical analyses in this study.

(a) (b)

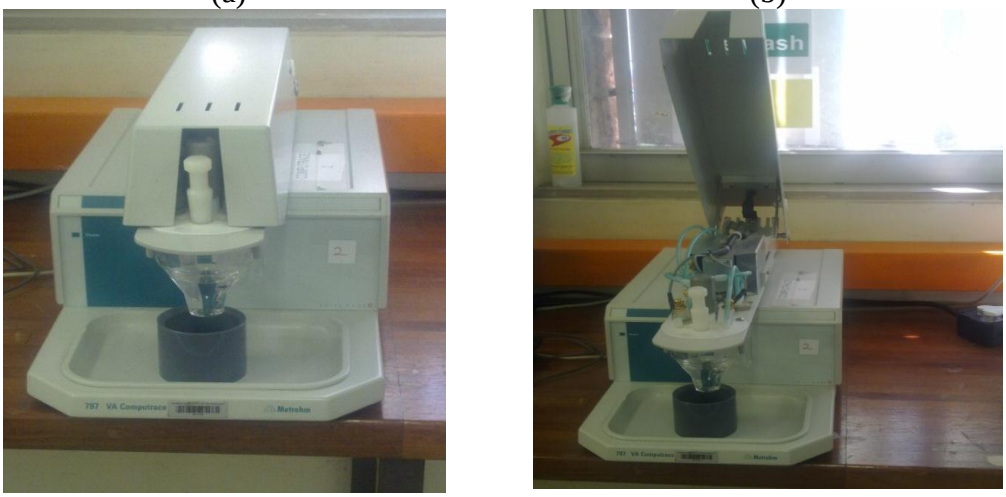

Figure 2.14: Images of 797 VA Computrace by Metrohm, (a) In a closed and rested state, (b) Open state ready to be used showing nitrogen pipes and electrodes connections.

2.3.4.1 Common applications

- Determination of metal ion concentration in water to parts-per-billion (ppb) levels
- Quantitative determination of pharmaceutical compounds
- Determination of redox potentials
- Detection of eluted analytes in HPLC and flow injection analysis

- Kinetic studies of reactions
- Determination of number of electrons in redox reactions.

Voltammetric techniques

There are different types of voltammetric techniques namely: Staircase voltammetry (SCV), Linear sweep voltammetry (LSV), Square wave voltammetry (SWV), Anodic stripping voltammetry (ASV), Cyclic voltammetry (CV), Cathodic stripping voltammetry (CSV), Adsorptive stripping voltammetry (AdSV), Normal pulse voltammetry (NPV) and Differential pulse voltammetry (DPV). Voltammetric techniques used in this study involve cyclic voltammetry (CV) and differential pulse voltammetry (DPV).

Cyclic voltammetry

Cyclic voltammetry is an important and widely used electro-analytical technique in many areas of chemistry. This technique is widely used for the study of redox processes. CV is mainly utilized for acquiring qualitative information about electrochemical reactions; it offers a rapid location of redox potentials of the electroactive species (Andrienko, 2008). In CV the voltage is swept between two values V_1 (E_{p1}) and V_2 (E_{p2}) at a fixed rate, when the voltage reaches V_2 the scan is reversed and the voltage is swept back to V_1, like in the voltammogram shown below in Figure 2.15 below.

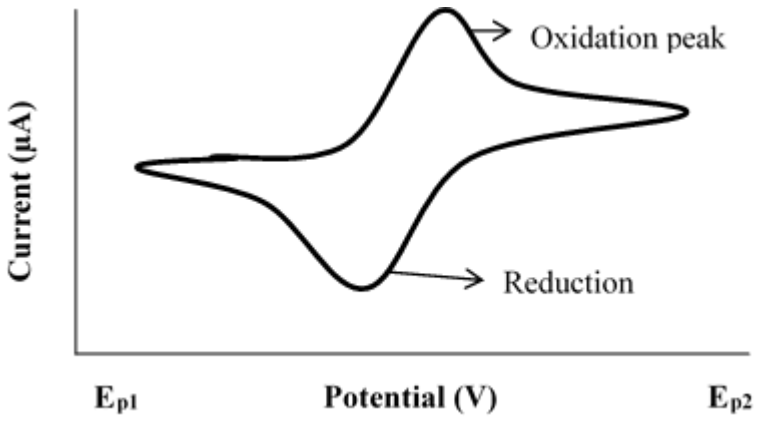

Figure 2.15: Schematic diagram of a cyclic voltammogram

The most important parameters in a cyclic voltammogram are the peaks potentials (E_{pc}, E_{pa}) and peak currents (i_{pc}, i_{pa}) of the cathodic and anodic peaks, respectively. CV is carried out in a quiescent solution to ensure diffusion control. CV operation is based on varying the applied potential at a working electrode in both forward and reverse directions while monitoring current (Kounaves, 1997). Cyclic voltammetry can be used to study qualitative information about electrochemical processes under various conditions, such as the presence of intermediates in oxidation-reduction reactions. CV can also be used for the determination of the electron stoichiometry of a system, the diffusion coefficient of an analyte, and the formal reduction potential of an analyte, which can be used as an identification tool (Carriedo, 1988).

From Nernst equation: $E = E_0 + RT/nF \ln [Ox] / [red.]$ where:

E is the potential of the cell (Volts)

T is the temperature in Kelvin (K)

E_0 is the standard potential

n is the number of electrons

F is the Faraday constant (96500 Coulombs/ mole)

R is the gas constant (8.31 $J.K^{-1}.mol^{-1}$)

For CV half-cell reactions the equation becomes $E^0 = E_{pa} + E_{pc} /2$ where E_{pa} and E_{pc} are anodic and cathodic peak potentials respectively.

Differential pulse voltammetry (DPV)

This technique can be compared to normal pulse voltammetry (NPV), in that the potential is also scanned with a series of pulses. However it differs from NPV because each potential pulse is fixed, of small amplitude (10 to 100 mV). Current is measured at two points for each pulse, the first point before the application of the pulse and the second at the end of the pulse as indicated in Figure 2.16. The difference between current measurements at these points for each pulse is determined and plotted against the base potential (Kounaves, 1997).

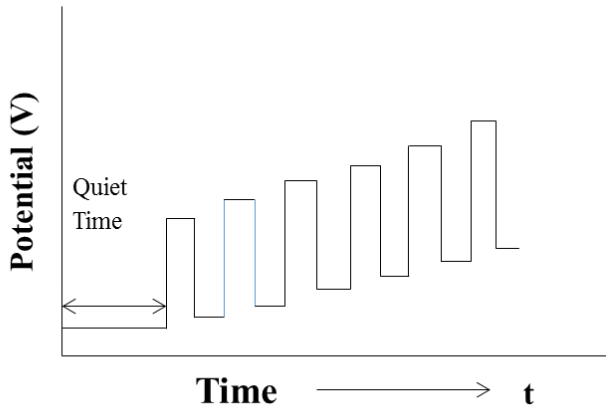

Figure 2.16: A typical DPV measurement process where current is measured before and after each pulse time.

In DPV, the occurrence of a signal peak at a particular potential gives an indication of the type of substance present, while the peak height (or peak area) gives a quantitative measure of the concentration of the analyte. The peak potential (E_p) occurs near the voltammetric half-wave potential and can be used to identify the species. The potential is applied as a ramped square wave, and the current is sampled just before and near the end of each pulse, and the data is recorded as a differential so that the concentration is represented by peak area or peak height.

Differential pulse voltammetry has the following characteristics:

- Reversible reactions show symmetrical peaks, and irreversible reactions show asymmetrical peaks.
- The peak potential is equal to $E_{1/2}{}^{r}$-ΔE in reversible reactions, and the peak current is proportional to the concentration.
- The detection limit as low as 10^{-8} M.

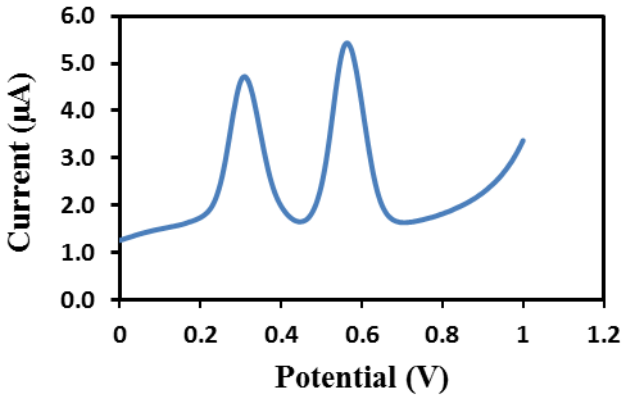

Figure 2.17: Typical current vs. potential curves for a capsaicin DPV measurement

The voltammogram in Figure 2.17 show two peaks at about 0.4V and 0.61V for capsaicin determination

CHAPTER 3

METHODOLOGY

The experimental techniques involving voltammetry and computational modelling are presented in this chapter. The computational methodology used in this study is outlined including optimization of the parameters.

3.1 Instrumentation

Voltammetric measurements were carried out using a 797 VA Computrace instrument from Metrohm (Herisau, Switzerland). Voltammograms were recorded at room temperature using a three electrode system in a polarographic cell, consisting of a 3mm diameter disc working electrode (GCE, Pt. and Au); Ag/AgCl (saturated AgCl, 3 M KCl) was used as a reference electrode, and the platinum wire as a counter electrode. A 781 pH/ion meter coupled with an 801 stirrer (Metrohm, Herisau, Switzerland) was used to adjust the pH of the buffer solutions. All working solutions including the buffer were prepared with deionized water from a water purification system, Aqua MaxTM Basic 360 (Trilab, SA). Buffer solutions, standard solutions and samples were refrigerated at 4 °C and all analytical measurements were performed at room temperature. Since carbon nanotubes are insoluble in most solvents, sonication during preparation of MWCNTs in DMF was employed in order to effectively disperse the tubes prior to immobilisation on electrode surface, this sonication was achieved using an Ultra-sonic 50194, Labcon, SA bath, and the Scientific oven Series 2000 was used to evaporate DMF.

3.2 Reagents and Chemicals

All chemicals were of analytical grade and were used as received without any further purification. Capsaicin-360376-IG (cas no. 404-86-4), PAL- Rhodotorula glutinis P1016-2UN enzyme and 20-30 % Carbon nanotubes MWCNTs basis, O.D. x L 7-12 nm x 0.5-10 µm (cas number 308068-56-6) were purchased from Sigma Aldrich (Durban, SA). *N, N*- dimethylformamide (cas no. 68-12-2), Glacial acetic acid (cas

no. 64-19-7) and Sodium Acetate anhydrous was supplied by Associated Chemical Enterprises (Johannesburg, SA). Nitrogen (99.9 % purity) was obtained from AFROX (Durban, SA). Ethanol (absolute, 99.9 %) used for extraction of samples and Nafion (cas no. 31175-20-9), 5 wt. % in lower aliphatic alcohols and water containing 15-20 % water were supplied by Capital Lab Supplies (Durban, SA). Glucose Oxidase Type VII from Aspergillus Niger EC 1.1.3.4, product number: G2133 and CAS# 9001-37-0 was purchased from Sigma, St Louis, Missouri 63103 USA.

3.3 Methods

3.3.1 Preparation of supporting electrolyte

Sodium acetate buffer solution was prepared by making 0.1 M sodium acetate solution and 0.1 M acetic acid solution; both solutions were mixed at a ratio of 85 % acetic acid to 15 % sodium acetate and adjusted to form 0.1M sodium acetate buffer solution of pH 4.01. This solution was then stored at 4 °C until used. To vary and increase the electrolyte pH values as presented in section 4.1.1, sodium acetate was quantitatively added.

3.3.2 Preparation of Capsaicin standard

Capsaicin standard solution was prepared by dissolving 10 mg capsaicin standard powder in 100 mL of absolute ethanol 99.9 % pure to produce 100 $mg.L^{-1}$ (ppm) standard solution. The capsaicin standard solution was also kept in the refrigerator at 4 °C until ready to use.

3.3.3 Electrode Modification

Working electrodes (GCE, Pt and Au) were mechanically polished for surface preparation prior to casting nanotube solution. A small portion of 0.05 µm alumina polish was placed on a polishing pad; a drop of deionised water was added to the powder to make a paste. The electrode was moved in a figure-of-eight motion when polishing to ensure uniform polishing. Once the polishing had been completed the electrode surface was thoroughly rinsed with deionised water to remove all traces of polishing material. After that the electrode was sonicated in deionised water for few minutes to ensure complete removal of alumina particles. Multiwalled carbon

nanotube was dispersed in *N*, *N*-Dimethylformamide (5 mg in 1 mL). This mixture was then sonicated in ultrasonic bath for 5 min (Wang et al. 2002), after which 10 µL aliquot was cast or immobilized onto the surface of the inverted electrode and oven-dried at 50 °C for about 15 min.

3.3.4 Preparation of PAL enzyme solution

Phenylalanine ammonia lyase (PAL) solution was prepared by adding 10 µL of PAL to 90 µL of 67 mM Phosphate buffer solution pH 7.4. About 10 µL of this solution was cast or immobilized on an electrode modified with MWCNTs allowed to dry at room temperature for a period of about 2 hours. After that a drop of Nafion solution (5 % nafion in ethanol) was cast on the electrode and allowed to dry at room temperature, this formed a film which covered the top of the electrode. The modified electrode (MWCNT/PAL/Nafion) was then rinsed with buffer solution before transferred to the electrochemical cell.

3.3.5 Preparation of Glucose Oxidase (GOx) enzyme solution

Solution of Glucose Oxidase was prepared by adding 3 mg of GOx into 1mL of 67 mM phosphate buffer solution (pH 7.4). The enzyme was physically adsorbed on the electrode surface modified with MWCNTs by dropping 10 µL of the enzyme solution on it; the solvent was allowed to dry at room temperature for a period of about 2 hours. Later 5 % Nafion solution was cast on electrode to form a film over the enzyme. The modified MWCNTs/GOx/Nafion electrode was then rinsed with the buffer solution prior to electrochemical determinations (Lyons and Keeley, 2008).

3.3.6 Real sample preparation

Capsaicin was extracted from ripe chilli pepper fruit as follows: Ripe chilli pepper fruit was crushed and blended, and 100 g was transferred into a 500 mL round bottom flask containing 350 mL of absolute ethanol. The mixture was refluxed for 2 hours, after refluxing solids were removed through filtration and discarded. Reddish-brown liquid containing chilli extract and ethanol was then transferred into another round bottom flask and the distillation system was set to distil off excess ethanol. The remaining chilli extract was then cooled and kept in an amber bottle at 4 °C in a refrigerator for subsequent electrochemical studies (Mpanza et al. 2014).

3.3.7 Computational Methods

Procedure for PAL with Capsaicin interaction using docking methods

The crystal structure of PAL enzyme was obtained from the Protein Data Bank ID: 1T6J (http://www.rcsb.org).The whole enzyme was selected and hydrogen atoms were added. Thereafter, it was cleaned by removing water molecules and seven alteration from the residues. Interestingly, there were no incomplete residues and alternate conformations in this structure, however the bonds and bond order were checked and corrected accordingly. The protein was energy minimized using the CHARMM based (Chemistry at HARvard Macromolecular Mechanics) force field described as the general purpose all atom force field in Discovery Studio 4.0 (Wu et al. 2003), at pH 7.4 corresponding to an ionic strength of 0.145. The protein ionization and residue pKa demonstrated that the protein possessed a zero charge at pH 7.7 and electrostatic energy of -36.00 kJ mol^{-1}.

Capsaicin ligand obtained from the Protein Data Bank (PDB) ID: 1548943 was optimized with Gaussian 9.0 (Frisch et al. 2009) and thereafter the conformation with the lowest energy was used for the docking simulation using Discovery Studio 4.0. Docking studies were performed using the CDOCKER module in Discovery studio, whereby the PAL enzyme was held rigid while the capsaicin ligands were flexible.

CDOCKER is a grid-based molecular docking method where the receptor is held rigid while the ligands are allowed to flex during the refinement. The CHARMm force field was used as an energy grid force field for docking and scoring function calculations. Random ligand conformations were generated from the initial structure through high temperature molecular dynamics, followed by random rotations which were further refined by grid-based (GRID 1) simulated annealing and a final grid-based minimization. Of the 10 best poses, one (conformation) having highest docking score (-CDOCKER energy) was used for the binding energy calculations and further analysis. The higher negative value of binding energy represents a more favourable binding of the complex.

CHAPTER 4

RESULTS AND DISCUSSION

This chapter deals with the optimization of parameters such as pH and scan rates followed by a methodological study to assess the sensitivity of the electrochemical biosensor for the determination of capsaicin extracted from chilli pepper fruits, using 3 different electrode modification approaches. The first, involved the modification of a glassy carbon electrode (GCE) immobilized with a glucose oxidase (GOx) enzyme onto a multiwalled carbon nanotubes (MWCNTs) modified electrode. The other determination step used MWCNTs modified electrode decorated with gold nanoparticles (AuNPs). The second approach involved replacing the GCE with the platinum electrode (Pt-E) and the glucose oxidase enzyme was replaced with phenylalanine ammonia lyase (PAL) enzyme. The third approach involved a comparative study of MWCNTs/GOx and MWCNTs/PAL biocomposite for the determination of capsaicin using gold electrode (Au-E).

4.1 Optimization of Parameters

4.1.1 Effect of electrolyte pH

Cyclic voltammetry analysis of 100 ppm capsaicin standards were performed using acetate buffer solution as an electrolyte at different pH levels, in order to determine the optimum pH value for the detection of capsaicin.

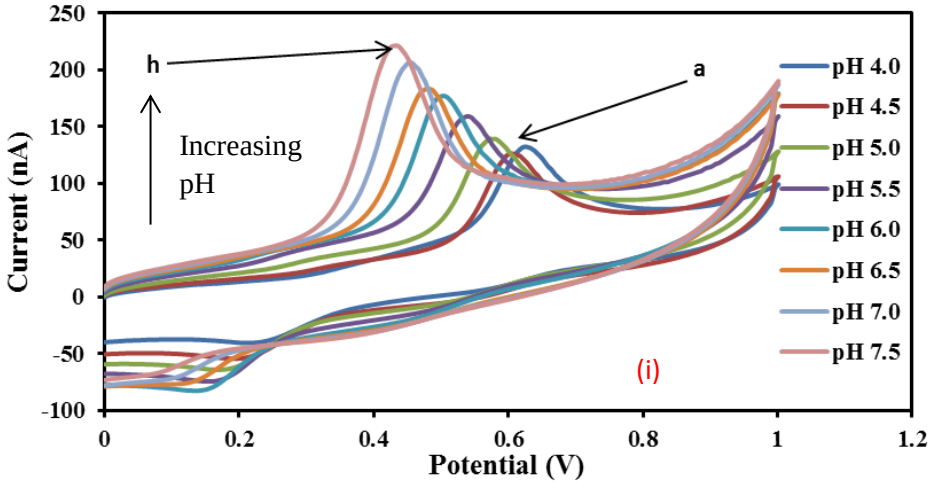

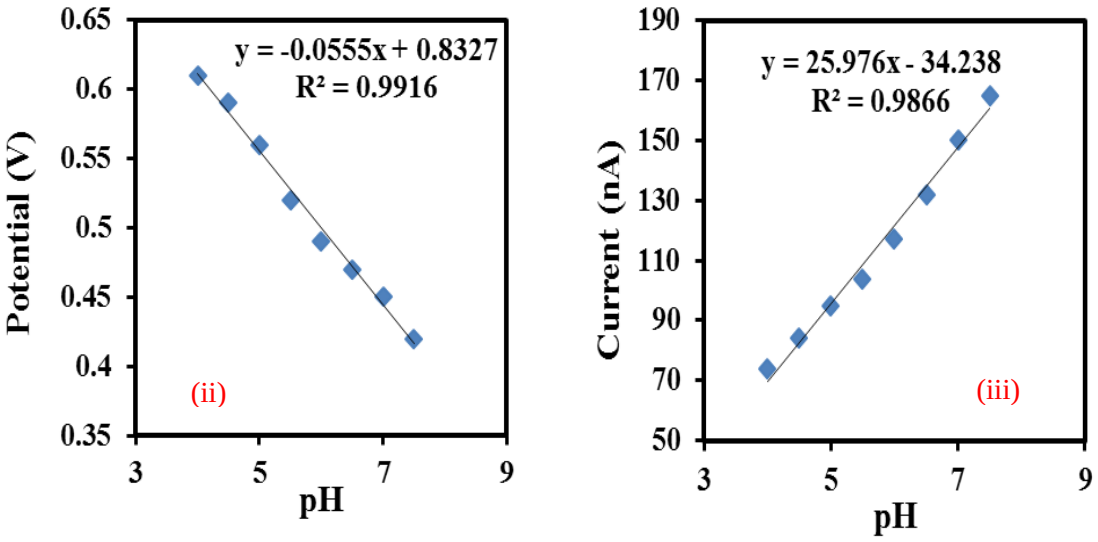

Figure 4.1: (i -iii) Effect of electrolyte pH on capsaicin using Bare GCE.

The scans along with data presented in Figure 4.1 shows that an increase in pH results in a decreased potential, with a shift in potential from **a** to **h** over a pH ranging from 4.0 to 7.5. The linearity of the pH versus the oxidation peak potential in (ii) above is confirmed by the regression equation y = -0.0555x + 0.8327 with a coefficient of R^2 = 0.9916. This relationship shows a gradual decrease in peak potential (potential shifting to the left) with an increase in pH value on the graph which seems to be consistent, and also confirmed by the coefficient of determination (R^2) of 0.9916. The shift in peak potential to a more negative potential by 55 mV per unit increase in pH, is close to the ideal potential shift of -59 mV per unit increase in pH, as predicted by the Nernst equation (Kachoosangi et al. 2008).

A similar analysis of the oxidation peak currents presented in Figure 4.1(iii) reveals that an increase in pH of the acetate buffer solution results in an increase in the peak currents. The linearity of the pH versus the oxidation peak current is confirmed by the regression equation y = 25.976x -34.238 with a coefficient of R^2 = 0.9866. Peak currents in general are proportional to pH, as the pH of the buffer is increased so does the peak current, here this indicates that the rate of oxidation of capsaicin is increased with an increasing pH. For comparative evaluation and characterization at

all pHs studied the anodic peak in Figure 4.1 is broad and well defined than the cathodic peak. The optimum pH was found to be 4.0.

4.1.2 Effect of Scan rates

The effect of scan rates on the oxidation and reduction peak currents of the cyclic voltammetric signals of capsaicin using a bare GCE in a 0.1M acetate buffer at pH 4.01 was studied.

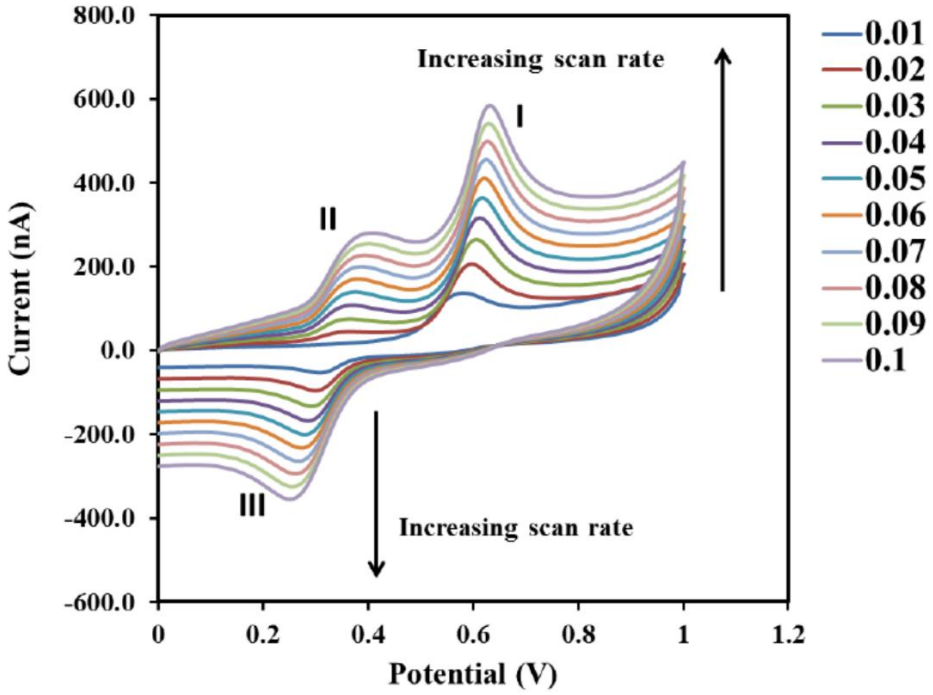

Figure 4.2: Scan rate effect from 0.01 to 0.1 $V.s^{-1}$ on capsaicin

Figure 4.2 reveals three distinct capsaicin peaks obtained by cyclic voltammetry, two of which are oxidation peaks and one reduction peak. A broader oxidation peak I observed at about 0.6 V, and a smaller oxidation peak II observed at about 0.4 V, while a reduction peak III at about 0.3 V. It is also evident that as the scan rate increases from 0.01 $V.s^{-1}$ to 0.1 $V.s^{-1}$, the oxidation peaks currents also increased and shifted towards the right, whereas the reduction peak currents also increased but shifted towards the left. Table 4.1 shows scan rates of (0.01 to 0.1) $V.s^{-1}$ and the peak

currents for all three peaks as depicted in Figure 4.2. A linear relationship of the scan rates against the peak currents (I-III) are graphically represented in Figure 4.3.

Table 4.1: Scan rates and peak currents of oxidation and reduction peaks of Figure 4.2

scan rate ($V.s^{-1}$)	Peak 1 Current (nA)	Peak II current (nA)	Peak III current (nA)
0.01	138	17	-53
0.02	206	43	-96
0.03	265	75	-134
0.04	315	106	-167
0.05	362	140	-200
0.06	411	170	-233
0.07	455	200	-263
0.08	499	227	-294
0.09	542	255	-324
0.1	583	281	-354

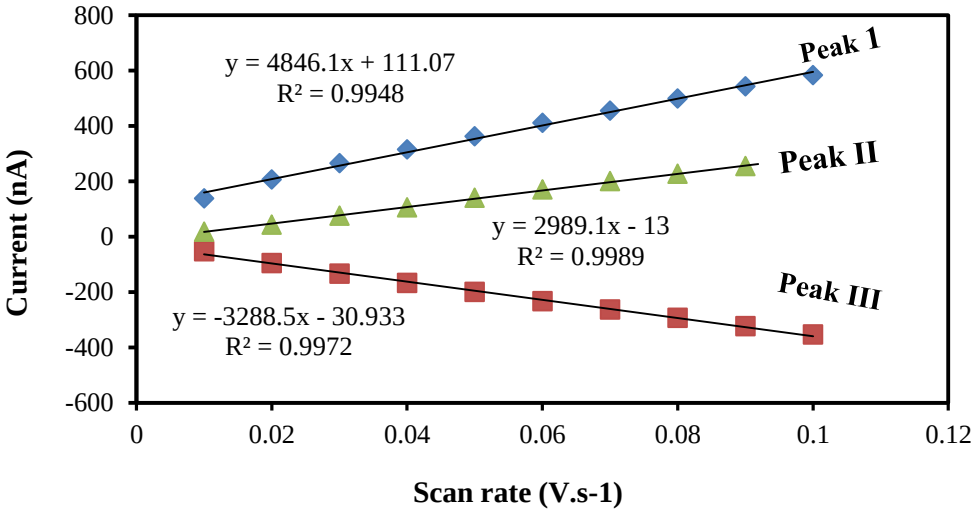

Figure 4.3: Graphical representation of capsaicin peak currents against Scan rates from Table 4.1.

With increasing scan rates from 0.01 to 0.1 $V.s^{-1}$ the oxidative and reductive peak currents of capsaicin shows a linear relationship which indicates the adsorption of capsaicin onto the electrode surface, rather than diffusion as a preferred mechanism of detection. The linear relationship between redox peak currents and the scan rates depicted in the calibration curve in Figure 4.3, were correlated with R^2 values at peak

I = 0.9948, peak II = 0.9989 and peak III = 0.9972. Moreover, the mechanism of the conversion of capsaicin structure (Scheme 1) by losing H^+ ions (guaiacol to benzophenone) is a forward reaction and this is attributed to peak I, the reaction between benzoquinone and catechol is reversible represented by peak II and III respectively.

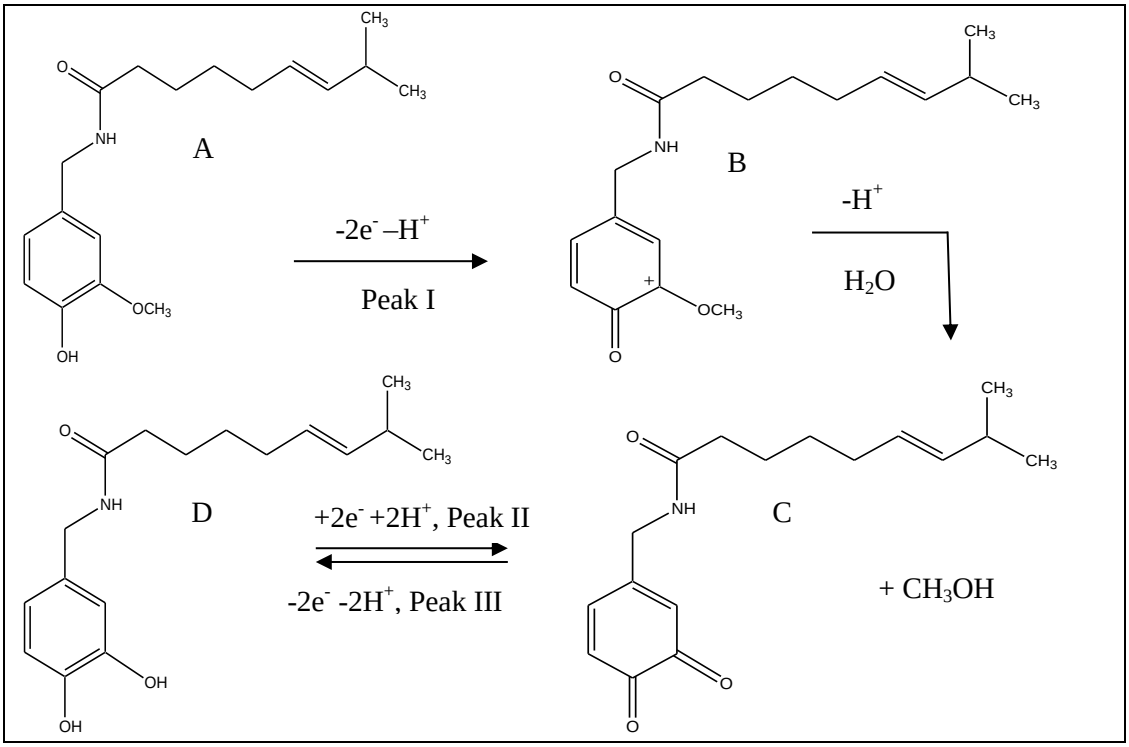

Scheme 4.1: Mechanism for the electrochemical oxidation/ reduction of capsaicin that occurs at the electrode surface (Kachoosangi et al. 2008).

The chemical structure of capsaicin [A] shows that the benzene ring and the (–OH and OCH_3) are attached and referred to as Guaiacol. The loss of H^+ produces an intermediate structure [B] and with a further loss of H^+ and hydrolysis of the 2-methoxy group forms structure [C] converting the guaiacol to benzoquinone (two double bond oxygen atoms replacing -OH and OCH_3) respectively. The gain of $2e^-$ and $2H^+$ ions converts benzoquinone to catechol, structure [D].

4.2 Determination of Capsaicin using Glassy Carbon Electrode (GCE)

In this study, electrochemical analysis of capsaicin were first carried out using bare GCE, cyclic voltammetry (CV) and differential pulse voltammetry (DPV) scans shown in Figures 4.4 (a)-(b) followed by the modification of the bare GCE.

4.2.1 Bare GCE

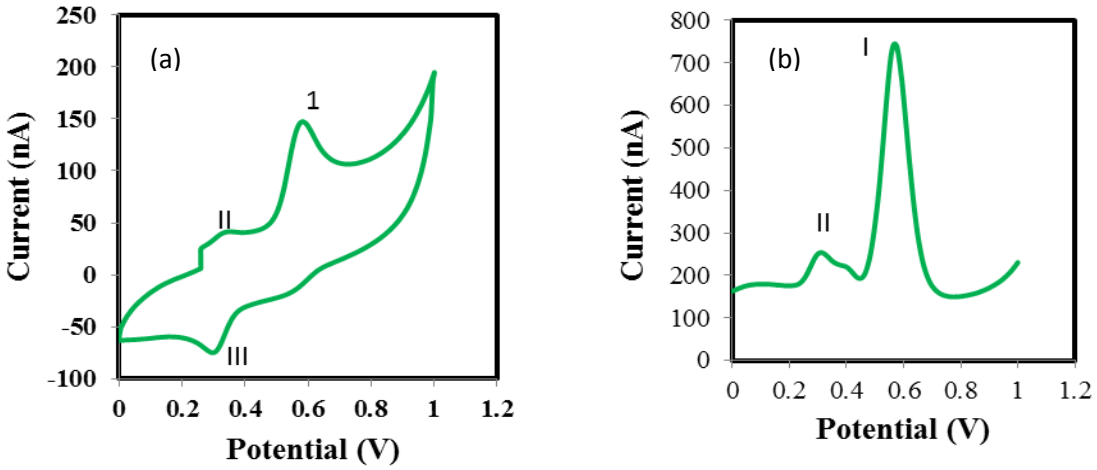

Figure 4.4: (a) CV and (b) DPV voltammograms of capsaicin sample (0.2 mL) from chilli extract in 0.1 M acetate buffer solution of pH 4.01 and scan rate of 0.01 $V.s^{-1}$ using bare GCE.

Figure 4.4 (a) shows three capsaicin peaks, two of which are oxidation peaks with the major peak labelled "I" at 0.59 V and the smaller peak II at about 0.4 V, with a reduction peak III at 0.26 V. The differential pulse voltammogram in Figure 4.4 (b) shows two capsaicin peaks I and II, at 0.57 V and 0.30 V respectively. It is noticed from the results above that the peak current on the bare GCE is recorded in nano-amperes (nA). Accordingly, the optimization and sensitivity of the bare glassy carbon electrode were established according to the protocols described in the Methods section.

4.2.2 Glassy carbon electrode modified with multi-walled carbon nanotubes (GCE-MWCNTs)

Results obtained from the cyclic and differential pulse voltammograms for GCE-MWCNTs are shown in Figures 4.5 (a)-(b).

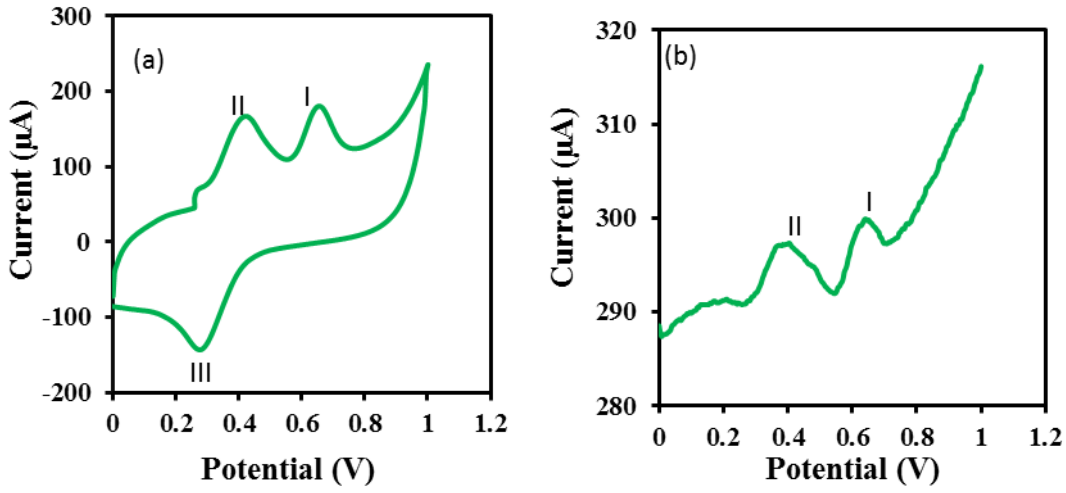

Figure 4.5:(a) CV and (b) DP voltammograms of capsaicin sample (0.2 mL) from chilli extract in 0.1 M Acetate buffer solution of pH 4.01; scan rate of 0.01 $V.s^{-1}$ using GCE modified MWCNTs

In contrast to the bare GC electrode, Figure 4.5 (a) shows a clear and distinct oxidation and reduction peaks for capsaicin. In the case of the bare GCE, the peak currents are measured in nA, whereas for GCE-MWCNTs the peak current are in µA, suggesting that the introduction of MWCNTs enhanced the sensitivity of the electrode. Similar responses were observed in the case of the DPV scan shown in Figure 4.5 (b). The enhancement of the peak currents confirms the sensitivity, probably due to the stronger adsorptive properties of the MWCNTs, in contrast to the bare electrode. Clearly, the inclusion of the MWCNTs onto the electrode surface showed a significant difference on the electrochemical behaviour of capsaicin when compared to a normal bare electrode. Additionally, there is also an increase in peak current readings, (Mpanza et al. 2014) and this significant increase in peak heights can also be attributed to a better surface area and electrical conductivity provided by MWCNTs.

4.2.3 GCE-MWCNTs decorated with Gold Nanoparticles (AuNPs)

Multi walled carbon nanotubes were decorated with AuNPs; this was done by involving the functionalization of the thiol groups with ammonium morphiline dithiocarbamate as per preparation method in (Mpanza et al. 2014).

The MWCNTs and AuNPs-MWCNTs were characterized using High resolution transmission electron microscopy (HR-TEM) and Attenuated total reflectance infra-red (ATR-IR) spectroscopy, shown in Figures 4.6 (a)-(b).

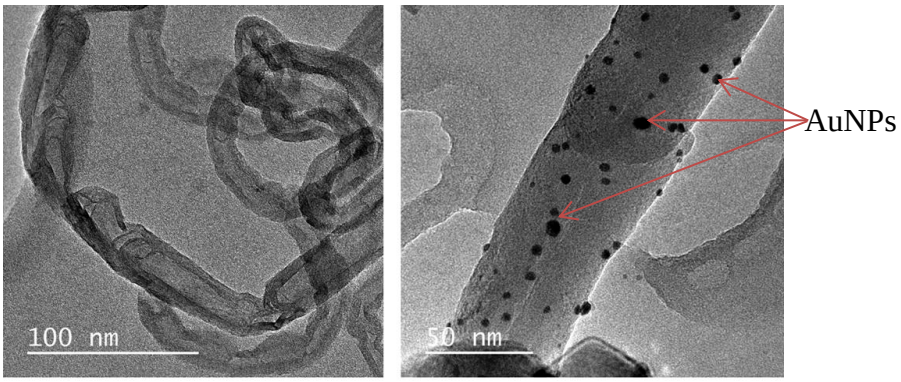

(a) (b)

Figure 4.6: High-resolution transmission electron micrograph of (a) multi-walled carbon nanotubes and (b) multi-walled carbon nanotubes decorated with gold nanoparticles obtained at 100 nm and 50 nm magnification respectively.

The HR-TEM morphology of the undecorated MWCNTs (Figure 4.6 (a)) illustrated hollow cylindrically shaped MWCNTs conjugate formation depicted by the presence of AuNPs shown in Figure 4.6 (b). The covalent bonding of the ammonium morpholine dithiocarbamate on the surface of MWCNTs prior to decoration with AuNPs also reduced the nanoparticle aggregation, thus enhancing a uniform attachment around the surface of the functionalized MWCNTs. The conjugation mechanism is also dependent on the chelation of the gold nanoparticles with the sulphur atoms of the ammonium morpholine dithiocarbamate complex. Further characterization involving infrared analysis revealed that the MWCNTs exhibited a stronger absorbance shown in Figure 4.7.

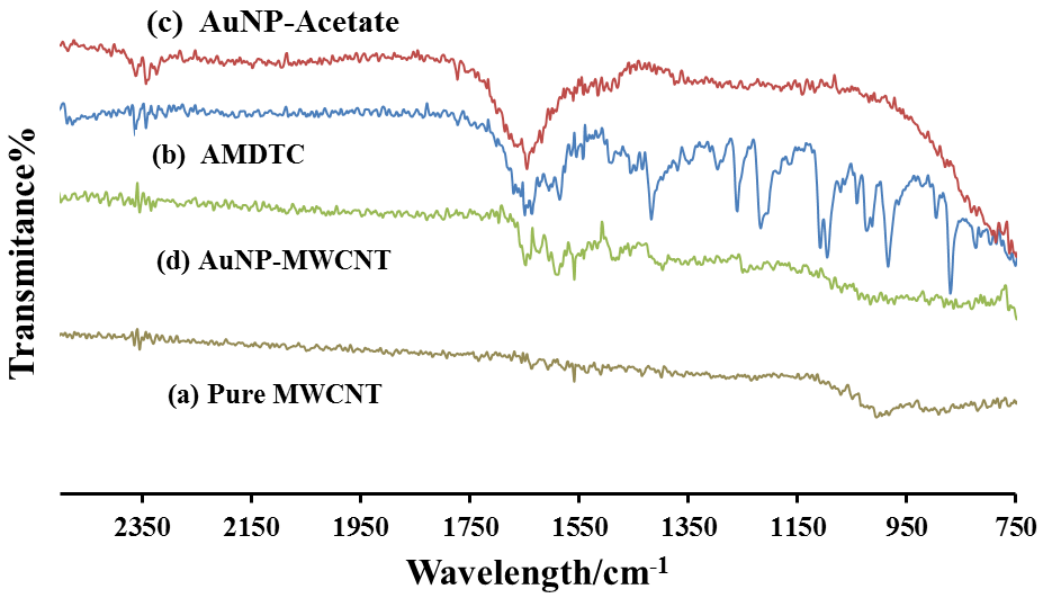

Figure 4.7: Infrared spectra of (a) pure multi-walled carbon nanotubes, (b) ammonium morpholine dithiocarbamate, (c) gold nanoparticles-acetate, and (d) gold nanoparticles-multiwalled carbon nanotubes

The spectra shown in Figure 4.7 were recorded and collected over the range 4,000–550 cm^{-1} at 3 cm^{-1} resolution, and hence peaks corresponding to ammonium morpholine dithiocarbamate on the surface of MWCNTs were elucidated. As expected, MWCNTs did not produce any spectral absorption while from the gold nanoparticles-acetate, a C=O stretching vibration at 1640 cm^{-1} was observed after conjugation of the AuNPs with the MWCNTs. However, this band was relatively small, probably due to the lower concentration of the prepared AuNPs. Primary amine bands were observed in the 1580 cm^{-1} region, due to the presence of ammonium morpholine dithiocarbamate retained in the final conjugation. This was confirmed by the participation of the sulphur atoms rather than nitrogens and oxygens in the complexation of AuNPs-MWCNTs, resulting in linkage of oxygen atoms of the ammonium morpholine dithiocarbamate complex to the GCE.

Electrochemical studies were performed using capsaicin as an electro-active species. Earlier optimization studies carried out using cyclic voltammograms shown in Figure

4.2, showed a well-defined electroactivity with redox reversibility and charge transfer controlled process with higher stability. This electrochemical reaction involved a charge transfer that was enhanced by the surface of the AuNPs-MWCNTs attached to the GCE. It is noticed that the oxidation and reduction peak heights increased significantly when AuNPs-MWCNTs-GCE was used, which indicates a much better surface area and electrical conductivity compared to the bare GCE. The decoration of MWCNTs with AuNPs facilitates electron transfer between the analyte and modified electrode surface.

However, quantification studies involving differential pulse voltammogram (DPV) of capsaicin showed a better adsorption on the MWCNTs-GCE and the AuNPs-MWCNTs-GCE shown in Figure 4.8, due to the stronger adsorptive properties of the AuNPs and MWCNTs. Overlays of the differential pulse voltammograms were prepared to relate potential against current for three types of electrodes.

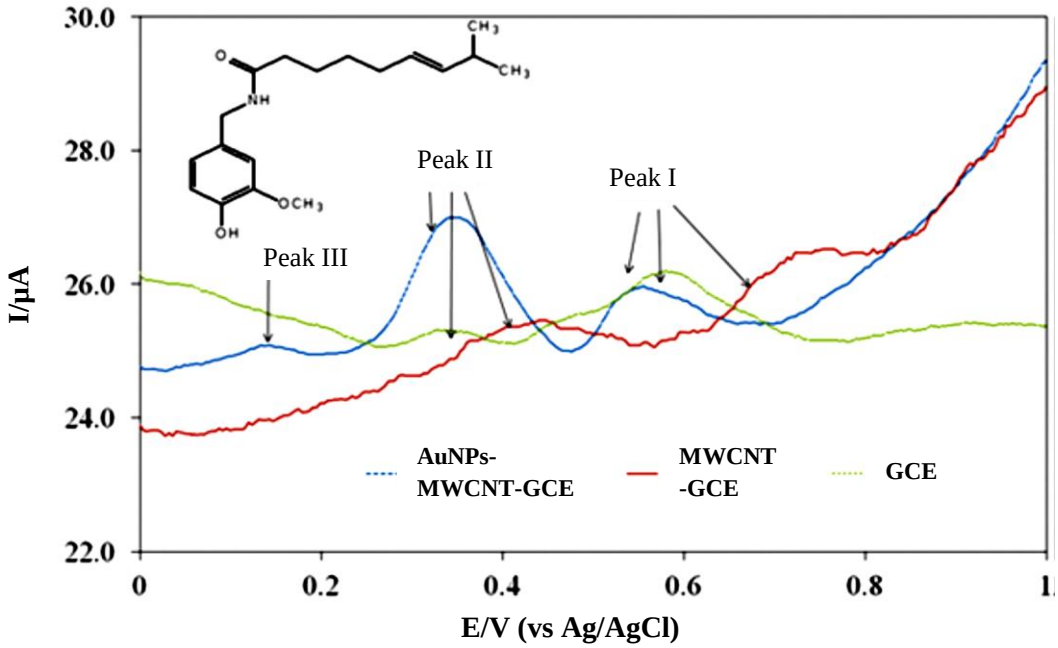

Figure 4.8: Differential pulse voltammogram of Capsaicin using bare GCE; multi-walled carbon nanotubes on a GCE (MWCNT-GCE, and gold nanoparticles on a MWCNTs-GCE (AuNP-MWCNTs-GCE) with a pulse time of 0.04 s, a sweep rate of 0.01 $V.s^{-1}$ and a step of 0.003 V.

4.2.4 Enzyme immobilization on MWCNTs modified GCE

In order to develop the biosensor, enzyme immobilization on modified glassy carbon electrode: GCE-MWCNTs-Enzyme using Glucose oxidase (GOx) were used in this study. Preparation of the GOx enzyme solution are described in the Methods section. Electrochemical determination of capsaicin were performed similar to those of the bare and MWCNTs modified GCE. Cyclic and Differential pulse voltammograms for GCE-MWCNTs-GOx are shown in Figures 4.9 (a)-(b) below.

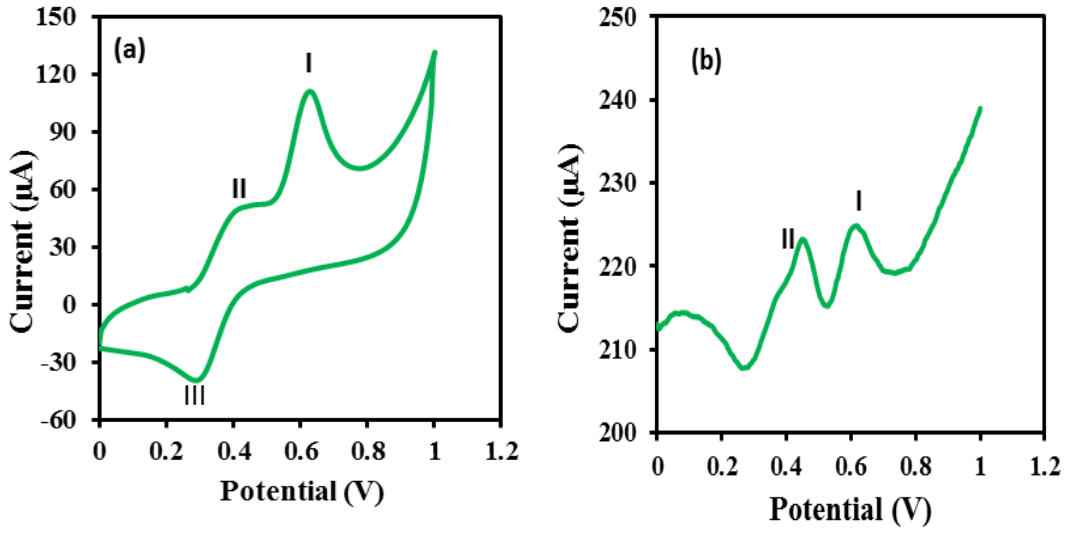

Figure 4.9 (a) CV scan and (b) DPV scan for Capsaicin sample (0.2 mL) from chilli extract in 0.1M Acetate buffer solution of pH 4.01; scan rate of 0.01 $V.s^{-1}$ using GCE-MWCNTs-GOx modified electrode

All capsaicin peaks are easily identifiable on both CV and DPV voltammograms depicted in Figures 4.9 (a)-(b) respectively. The catalytic activity of glucose enzyme is evident and thus confirms the sensitivity of the GCE-MWCNTs-GOx electrode.

Table 4.2 shows the summary of electrochemical results obtained while running capsaicin analysis using bare GC electrode, GCE modified with MWCNTs and immobilising glucose oxidase (GOx) enzyme on the MWCNTs modified GCE.

Table 4.2: Comparison for determination of Capsaicin using a bare GCE, multi-walled carbon nanotubes on GCE (GCE-MWCNT), and glucose oxidase enzyme (GOx) on GCE modified with multi walled carbon nanotubes (GCE-MWCNT-GOx)

Technique	Peak	Parameters	GCE	GCE-MWCNTs	GCE-MWCNTs- GOx
	1	$E_{pa\ (V)}$	0.59	0.62	0.61
		$i_{pa\ (\mu A)}$	7.53	15.29	42.13
CV	2	$E_{pa\ (V)}$	0.41	0.39	0.39
		$i_{pa\ (\mu A)}$	0.13	17.96	16.54
	3	$E_{pc\ (V)}$	0.32	0.29	0.30
		$i_{pc\ (\mu A)}$	0.63	20.88	21.46
DPV	1	$E_{p\ (V)}$	0.54	0.62	0.60
		$i_{p\ (\mu A)}$	1.85	3.87	6.51
	2	$E_{p\ (V)}$	0.29	0.38	0.43
		$i_{p\ (\mu A)}$	0.37	5.47	9.72

Further analyses were performed to assess the impact on the sensitivity on the electrode modification by glucose oxidase enzyme on the electrode surface of bare glassy carbon electrode. Overlaid scans were for both CV and DPV are illustrated on Figures 4.10 (a)-(b) respectively.

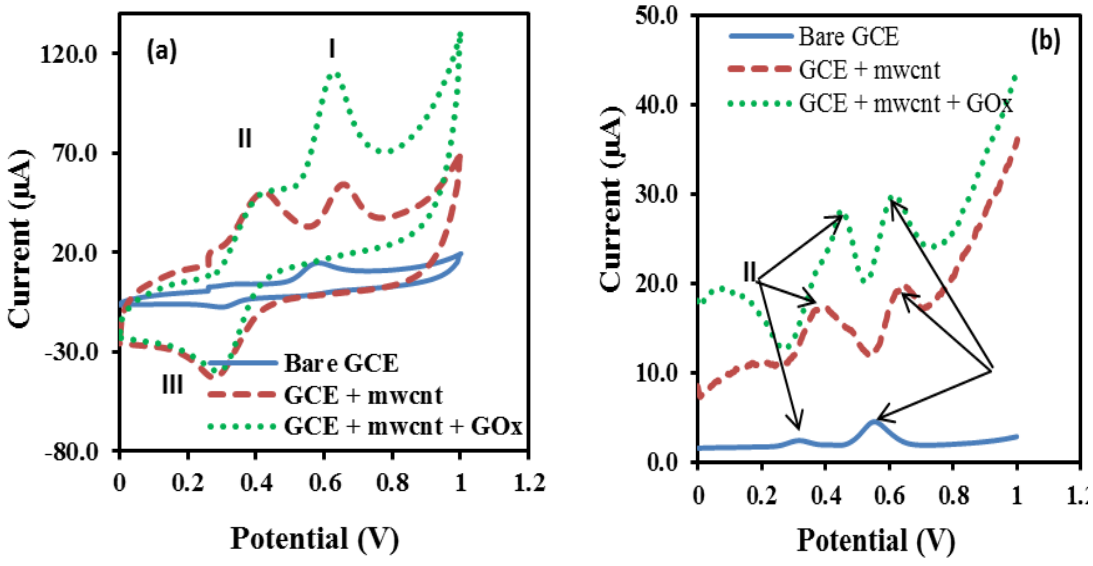

Figure 4.10 (a) CV and (b) DPV scans of capsaicin using bare GCE, GCE- MWCNTs and GCE-MWCNTs-GOx modified electrodes

Cyclic voltammograms for GOx modified electrodes show the highest peak heights of all electrodes used, followed by multi walled carbon nanotubes modified electrode and the bare GCE show the lowest peak height, suggesting an increased sensitivity. The CV scan of capsaicin in Figure 4.10 (a) show two oxidation peaks, one at about 0.4 V (peak II) and the other at about 0.6 V (peak I). The scans for the bare GCE show peak I, but peak II is not clearly visible, however the situation changes when MWCNTs-GCE and GOx-MWCNTs-GCE are introduced, where peak II is clearly visible and magnified. Clearly, a significant difference between the magnitudes of the voltammetric signals on the MWCNTs-GCE compared to the bare GCE, with a signal difference also evident when comparing the scans of MWCNTs-GCE with those of GOx-MWCNTs-GCE. The CV scans of capsaicin also show a reduction peak at about 0.3 V. Interestingly, the oxidation and reduction peak heights are significantly increased in the order of bare GCE to MWCNTs-GCE to GOx-MWCNTs-GCE, thus confirming the impact MWCNTs and GOx enzyme has on capsaicin detection.

Similar relationship observed in CV scans is also evident in DPV voltammograms as shown in Figure 4.10 (b) above. One can deduce that this is probably due to larger surface area of the MWCNTs-GCE and its electrical conductivity in comparison to the bare GCE, and also due to catalytic activity of GOx enzyme when introduced to the MWCNTs modified electrode. Furthermore we can say that, looking at the voltammograms above, the higher the peak current on GOx-MWCNTs-GCE and MWCNTs-GCE signals compared to bare GCE, the stronger the adsorption effect on modified electrodes than on the bare GCE.

The GCE modified with a mixture of multi-walled carbon nanotubes and glucose oxidase enzyme was characterised by Attenuated Total Reflectance Infrared (ATR-IR) spectroscopy and Thermo-gravimetric Analysis (TGA) depicted in Figures 4.11 and 4.12 respectively.

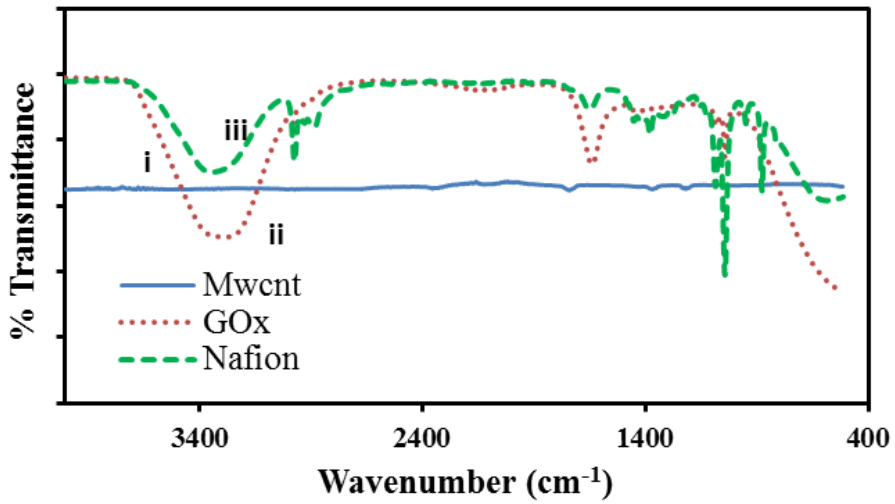

Figure 4.11 IR spectra for (i) MWCNT, (ii) GOx enzyme and (iii) Nafion

The IR spectra shown in Figure 4.11 were recorded over the range 4000 to 515 cm^{-1} at 4 cm^{-1} resolution. The spectrum of pure MWCNTs show a peak at 1740 cm^{-1} which is assigned to the stretching mode of C=C bonds that form the framework of carbon nanotubes side walls. At 2900 cm^{-1} there is a peak band which corresponds to C-H asymmetric and symmetric stretching, at 3300 cm^{-1} O-H peaks due to carboxylic acid show broad and less intense peak. On MWCNTs/GOx/Nafion spectra, there is a broad O-H stretching peak at 3395 cm^{-1}, C-H stretching is found at 2982 cm^{-1}, there is also an evident peak at 1650 cm^{-1} assigned to C=C bond stretch and at 1044 cm^{-1} is an aromatic in place C-H bend. Nafion spectrum show C-O-C stretching vibrations at 879 cm^{-1}, S-O stretching symmetric at 1045 cm^{-1}, CF_2 symmetric stretching at 1087 cm^{-1}; since nafion was a 5% solution in ethanol the spectrum show broad O-H stretching at 3350 cm^{-1} and C-H alkyl group stretching at 2974 cm^{-1} from ethanol. GOx spectrum has a broad O-H stretching peak at 3277 cm^{-1}, at 1639 cm^{-1} is an amide bond peak and enzyme interaction with C-O bond peak is realised at 1045 cm^{-1}.

In order to assess the thermal stability of the electrode surface Thermal analysis studies were carried out and the TGA scan depicted in Figure 4.12.

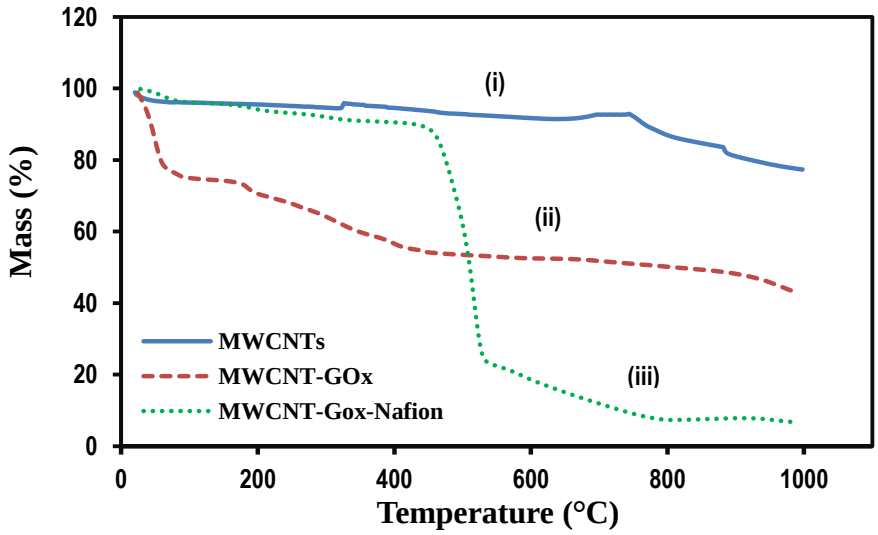

Figure 4.12 TGA curves of (i) MWCNTs, (ii) MWCNTs-GOx and (iii) MWCNTs-GOx-Nafion

This approach was very informative for a better understanding of the thickness of the surface as the layer by layer modification was performed. MWCNTs curve show a change in temperature (decomposition temperature) at 710 °C, another drop in temperature is noticed at about 850 °C, this might be due to carbon oxidation. MWCNTs modified with glucose oxidase enzyme (GOx) show a TGA profile with three drop downs at 56 °C, 148 °C and 422 °C. The mass percentage loss of GOx on MWCNTs at first drop between 26 and 56°C is about 17.10 %, at second drop between 56 and 148 °C mass percentage loss is at 7.76%, and at the third drop between 148 and 422 °C, it is about 17.98 %. The first mass loss phase in MWCNTs-GOx curve can be attributed to irreversible thermal denaturation of glucose oxidase enzyme. The phase between 56-148 °C can be recognised as the normal dehydration process of GOx, and above 148°C we can attribute the further drop in mass percentage to melting and decomposition processes of GOx at temperatures higher than 300 °C. MWCNTs-GOx-Nafion curve show a small mass percentage loss of about 3.24 % between 26 -80 °C, this can be attributed to dehydration of nafion membrane. The major mass loss in this curve was noticed when the temperature reached about 422 °C which suggested total decomposition stage of the nafion

membrane, this curve also show that GOx enzyme was concealed beneath the nafion membrane.

4.2.5 Computational Section

Enzyme Preparation and Analysis

A Crystal structure of Glucose oxidase from *Aspergillus niger* with a pdb code **1GPE** was downloaded from the Protein data Bank (http://www.rcsb.org/pdb/explore/explore.do?structureId=1GPE) accessed on 04/09/2014

The molecule contained water molecules which were removed prior to protein cleaning, where seven alteration from the residue were deleted. Interestingly, there was no complete residues that were found, however the bonds and bond orders were checked and corrected where deemed necessary.

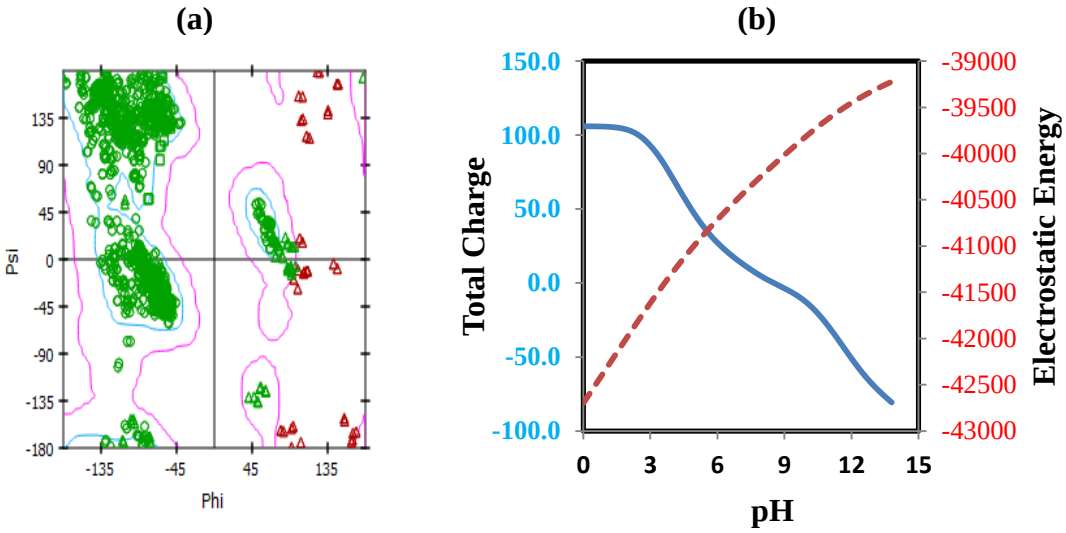

Figure 4.13: Ramachandran plot of the glucose oxidase showing the distribution of the protein groups. (a) acidic (b) total charge and electrostatic energy versus pH

The pH and ionic strength was critical in this study, as demonstrated by previous experimental studies (Mpanza et al. 2014) confirming that such variations could alter the analytical response of the analyte. The calculation of protein ionization and residue pKa demonstrated that the protein possesses a total charge approximately zero at pH 5 to 10 whilst it electrostatic energy ranges from to -41000 and -40105.

Molecular Docking

In order to ensure that the prepared ligand mimic or the experimental conditions used, it was allowed to ionise with pH 6.5 to 8.5 whilst the tautomers we enumerate. Thereafter full minimization was performed using a smart minimizer algorithm coupled with the CHARMM Force field. In the total of ten poses generated, none of them failed the simulation. After CDocker calculations, the output was subjected to scoring function. The binding site on the GOx protein with the co-ordinate -13.45, 0.18, -31.35 and 11.89 was selected using the default ligand.

Table 4.3.1: Energetics of the system

Ligand Name	Binding Energy (kcal/mol)	Ligand Energy (kcal/mol)	Protein Energy (kcal/mol)	Complex Energy (kcal/mol)	Entropic Energy (kcal/mol)
1548943	-145.40	25.24	-55 587.30	-55 707.40	19.90

Further analysis of interaction revealed, four conventional Hydrogen bond with bond distance ranging from 1.78 to 2.61 Angstrom (Å) as can be seen in Table 4.3.2, three C-H bonds are also evident with bond distances between 2.47 and 2.98 angstroms. There is one Pi-alkyl interaction with a bond length of 4.61 Å and a Pi-donor H-bond interaction with a distance of 2.36 angstrom. Interestingly the Pi bond interaction appeared to occur within the catechol ring of capsaicin as can be seen in Figure 4.14 below.

Table 4.3.2: Bond properties of Capsaicin / Gox interaction

Bond Type	Donor	H-Acceptor	Distance (Å)
Conv. H-bond	B:LYS473:HZ3	1548943:O1	1.7884
Conv. H-bond	1548943:H48	B:THR361:O	2.1844
Conv. H-bond	1548943:H48	B:ALA470:O	2.6161
Conv. H-bond	1548943:H49	B:ASP364:OD2	2.1707
C-H bond	B:LYS473:HE1	1548943:O1	2.9854
C-H bond	1548943:H35	B:ASP364:OD2	2.9026
C-H bond	1548943:H46	B:PHE362:O	2.4715
Pi- Donor H- bond	B:LYS473:HZ2	1548943	2.3616
Pi-Alkyl bond	1548943	B:LYS473	4.6182

***** 1548943 is the code of capsaicin structure

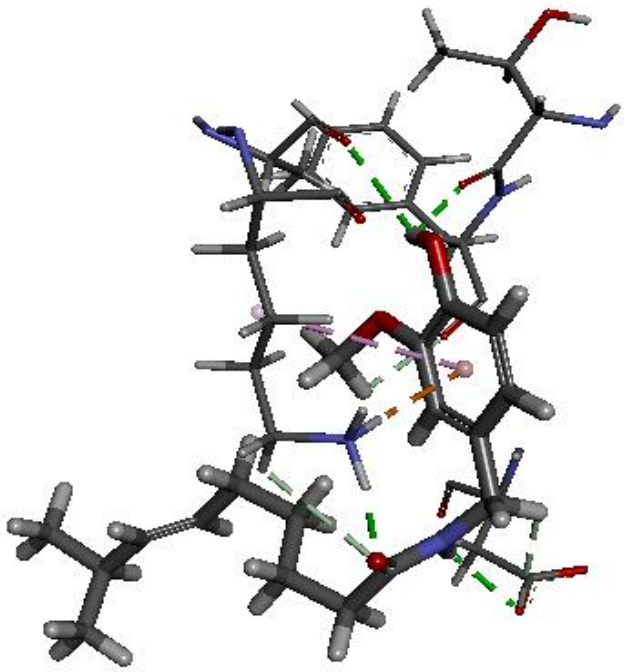

Figure 4.14: Docking complex of the protein (GOx) and ligand (Capsaicin)

The carbonyl of the amide group appeared to be the focal point of interaction showing four hydrogen bonds of 2. These results confirm the glucose oxidase facilitate the electron transfer from the capsaicin ligand, hence improving the response towards the biosensor.

4.2.6 Quantitative analysis of Real sample

Quantitative analysis was performed using a modified electrode or a biosensor, in order to quantify the concentration of real sample of capsaicin extracted from chilli pepper fruit. Table 4.4 shows a set of capsaicin standards concentrations against capsaicin peak currents and also real sample peak current.

Table 4.4: Concentration of capsaicin standards against capsaicin peak current

conc ($\mu g.mL^{-1}$)	I (μA)
20	1.80
40	2.66
60	3.33
80	4.00
100	4.81
sample	4.32

Developed biosensor was characterized using differential pulse voltammetry because of its ability to produce well resolved peaks at lower concentrations. A set of 5 standards was run in order to construct a calibration curve, a chilli sample extract of unknown concentration was also run and current obtained was computed according to linear graph equation in order to obtain the concentration of the real sample as illustrated in Figure 4.15.

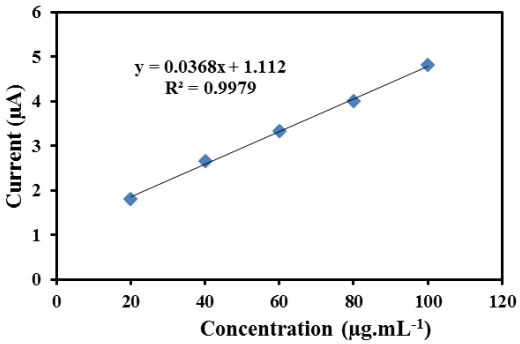

Figure 4.15: Calibration curve for capsaicin standards (peak current versus concentration)

The linear equation used for the quantification of real chilli extract sample was i_p (µA) = 0.0368 C + 1.112, with a correlation coefficient of R^2 = 0.9979. The concentration of real sample corresponding to a current of 4.32 µA, was calculated and found to be 87.17 µg.mL^{-1}.

4.3 Determination of Capsaicin using Platinum Electrode (Pt-E)

The second electrochemical analyses of capsaicin were conducted using the bare platinum electrode, Pt-E modified with multi-walled carbon nanotubes and enzyme immobilised on modified Pt-E. Platinum has been used as an electrode material for several decades, because of its excellent corrosion resistance (Schuettler, 2007). The analysis involved using bare Pt-E; cyclic voltammetry (CV) and differential pulse voltammetry (DPV) scans are shown in Figures 4.16 (a)-(b). The following parameters were used for all electrochemical determinations: 10 mL of 0.1 M Acetate buffer solution pH 4.01 was used as an electrolyte, 0.2 mL chilli extract, and the scan rate used was 0.01 $V.s^{-1}$

4.3.1 Bare Pt-E

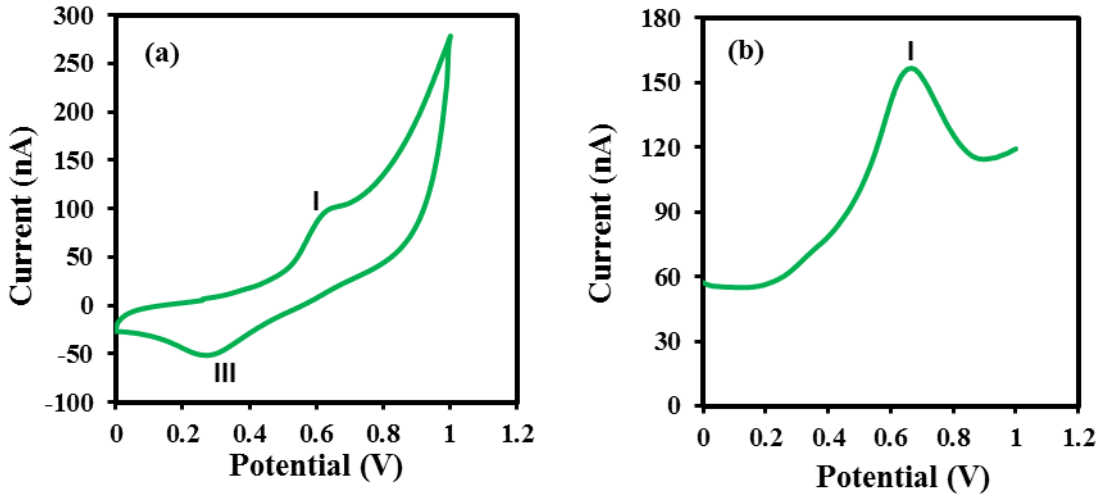

Figure 4.16: (a) CV voltammogram and (b) DPV voltammogram of capsaicin sample from chilli extract in 0.1 M acetate buffer solution of pH 4.01 and scan rate of 0.01 $V.s^{-1}$using bare Pt-E.

The CV scan shows only two peaks (oxidation and reduction), the oxidation peak I appear around 0.62 V, the second oxidation peak II was not detected as was the case with the bare GCE, and that might be due to bare platinum electrode sensitivity. It is also noticed that the intensity of these peaks are not that high as it was in the case of bare GCE. DPV scan also show one capsaicin peak at about 0.63 V, the non-existence of the second peak around 0.4 V is noticed which raises concern about the sensitiveness of the bare Pt-E when compared with bare GCE.

Accordingly, the optimization and sensitivity of the Pt-E electrode were established according to the protocols described in the Methods section, and the results are discussed below:

4.3.2 Platinum electrode modified with multi-walled carbon nanotubes (Pt-E-MWCNTs)

Bare platinum electrode was modified by dropping a solution of multi-walled carbon nanotubes on an inverted electrode, MWCNTs was firstly dispersed in DMF, this layer of MWCNTs was allowed to dry at 50 °C for 15 min, electrode was then cooled and washed with deionised water before it was used for electrochemical determinations. Similar procedure was followed for this modified electrode as for the bare Pt-E. Cyclic and Differential pulse voltammograms for Pt-E-MWCNTs are shown in Figures 4.17 (a)-(b).

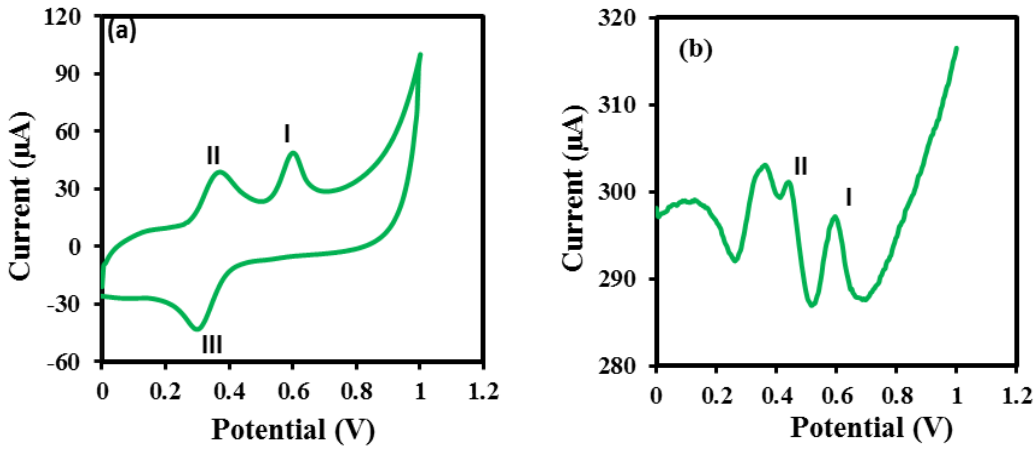

Figure 4.17: (a) CV voltammogram and (b) DPV voltammogram of capsaicin sample (0.2mL from chilli extract in 0.1M acetate buffer solution of pH 4.01; scan rate of 0.01 V.s-1 using Pt-E modified with multi walled carbon nanotubes (MWCNTs).

A comparison of the CV scans of Figure 4.16 (a) and Figure 4.17 (a) reveals significant differences. Firstly, the introduction of MWCNTs to the bare platinum electrode changed the detection capacity of an electrode completely. Secondly, the modified electrode's sensitivity was enormously enhanced; this is attributed to better surface area and electrical conductivity provided by the MWCNTs. The above DPV voltammogram depicted in Figure 4.17 (b) also followed the same pattern as the CV

scan, where the introduction of MWCNTs drastically increased the sensitivity of the Pt-E. The peak currents are also high when using Pt-E modified with MWCNTs as they are measuring in micro-amperes compared to nano-amperes when the bare electrode was used. Additionally, the CV and DPV scans show a vast difference in the peak height magnitude when compared to those obtained using a bare electrode. These peaks are clearly defined and much smoother, which can be attributed to the carbon nanotubes surface area and electrical conductivity of nanotubes which in turn enhances the sensitivity of the modified electrode.

4.3.3 Enzyme immobilization on MWCNTs modified platinum electrode

In order to develop the biosensor, enzyme immobilization on modified platinum electrode: Pt-E-MWCNTs-Enzyme, using Phenylalanine ammonia lyase (PAL) as an enzyme of choice in this study. Preparation of the PAL enzyme solution is described in the Methods section in Chapter 3. Electrochemical determinations of capsaicin were performed similar to those of bare and MWCNTs modified Pt-E. Cyclic and Differential pulse voltammograms for GCE-MWCNTs-Pt-E are shown in Figures 4.18 (a)-(b) below.

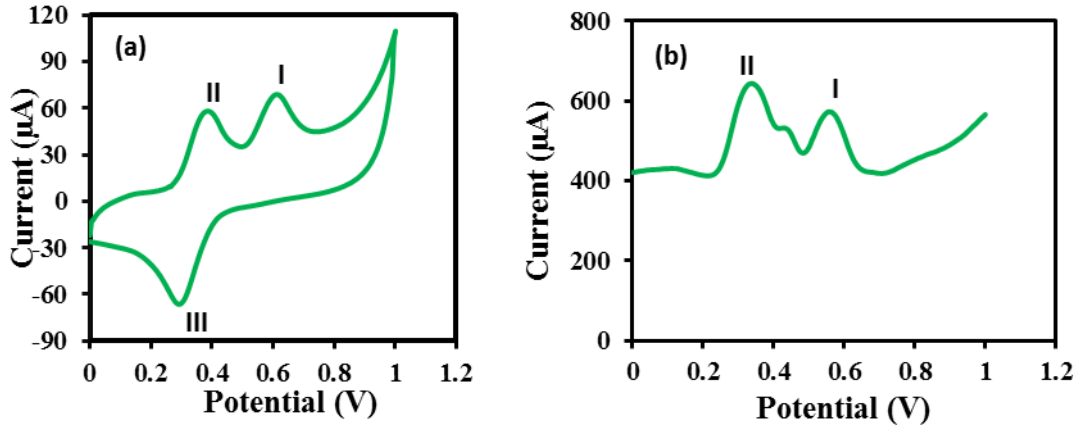

Figure 4.18: (a) CV scan and (b) DPV scan for capsaicin obtained using a Pt-E-MWCNTs-PAL enzyme modified electrode

Figures 4.18 (a)-(b) shows the impact of the enzyme on the sensitivity of the modified electrode, the increase in peak current can be attributed to catalytic activity

of the enzyme. Casting of PAL enzyme on a MWCNTs modified electrode contributed to the performance of the biosensor, sensitivity was enhanced further and the capsaicin peaks were clearly observed.

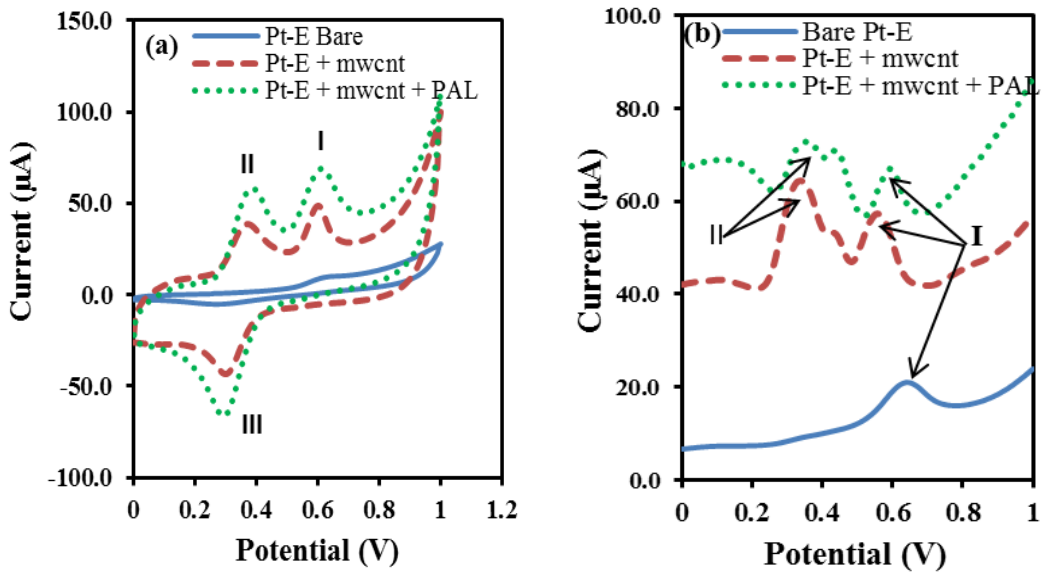

Figure 4.19(a) CV and (b) DPV of capsaicin using bare platinum electrode (Pt-E), multiwalled carbon nanotubes on Pt-E (Pt-E-MWCNTs) and PAL enzyme on a MWCNTs-Pt-E (Pt-E-MWCNTs-PAL)

All these scans (CV and DPV) for bare Pt-E, Pt-E-MWCNTs and Pt-E-MWCNTs-PAL are overlaid on the same graph in order to show the impact on electrode sensitivity shown by the involvement of MWCNTs and PAL enzyme.

Figures 4.19 (a)-(b) confirms that the biosensor exhibited higher capsaicin peak currents than the bare platinium electrode and Pt-E-MWCNTs, with the bare platinum electrode showing the least. The Pt-E-MWCNTs superiority over bare Pt-E is based on the electrical activity and surface area it possesses and greater adsorbance of capsaicin on a modified electrode. Introduction of an enzyme further increase the sensitivity due to enzyme catalytic activity.

4.3.4 Computational Section

HOMO-LUMO calculations

It is well understood that electron transfers from the highest occupied molecular orbitals (HOMO) in a molecule which is related to the ability of the molecule to undergo redox reaction. During the reduction process, the electrons will flow to the lowest unoccupied molecular orbital (LUMO). Therefore using the density functional theory we are able to locate the density of the electrons in the molecule thereby predict or confirm the active site of the ligand/molecule based on the electron density maps. Ideally the functional groups or atoms that are identified by the DFT calculation should be in agreement with the redox mechanism and the extent of HOMO-LUMO band gaps of the molecule thereby justify the ability of the molecule to undergo redox reaction. Initially, the structural geometry of the molecule has to be optimized using B3LYP basis set. With regards to Figure 4.20, the loosely bound electrons located in HOMO are located in the carbonyl functional group of the guaiacol ring contrary to those in the LOMO located in the functional groups.

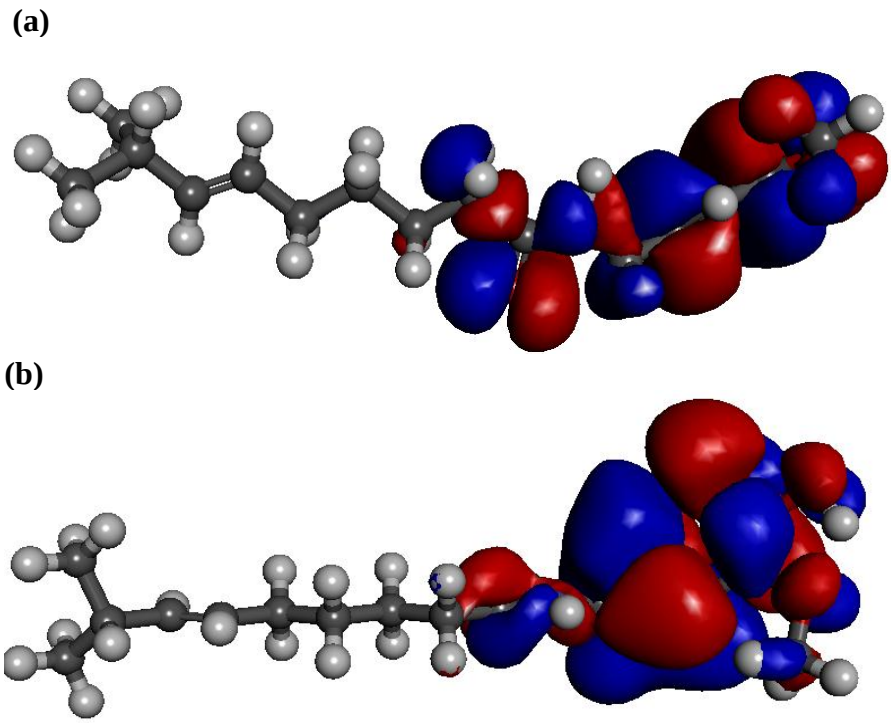

Figure 4.20: (a) Highest occupied molecular orbitals (HOMO) and (b) lowest occupied molecular orbitals (LUMO) of capsaicin obtained with DFT level 6-31+G (d) basis set

The redox mechanism (see Scheme 4.1) for capsaicin is a quasi-reversible reduction reaction between the OH and R-O-R groups of the guaiacol ring to the residues of the enzyme resulting in the reversible catechol ring. Therefore, the electron density is in agreement with redox mechanism in Scheme 4.1. Further details on the chemical interaction between the capsaicin and PAL protein were studied by docking approach.

Molecular Docking

In order to ensure that the prepared ligand mimic or the experimental conditions used, it was allowed to ionise with pH 6.5 to 8.5 whilst the tautomers we enumerate. Thereafter full minimization was performed using a smart minimizer algorithm coupled with the CHARMM Force field (Wu et al. 2003). From the same ligand, a total of ten poses were generated with Monte-Carlo ligand conformation generation, and docked using a LigandFit shape filter into an active site of the PAL protein with 573.15 Å that was derived based on the PDB site record (Venkatachalam et al. 2003). None of the 10 ligand confirmations failed the simulation so all of them were further explored with a set of scoring functions. This include calculation of binding energies during which the ligand flexible receptor atom properties were created by In Situ Ligand Minimization that enable ligand optimization in the binding pocket of the PAL enzyme (Tirado-Rives and Jorgensen 2006). Although the staring confirmations were not that poor but 1000 steps of Steepest Descent with a RMS gradient tolerance of 3, followed by Conjugate Gradient minimization were performed with a smart minimizer algorithm. Further analysis of interaction revealed thee Pi-alkyl interaction with an average distance of 4.75, 4.67, 5.03, and only one alkyl interaction with a distance of 4.51 Å. Interestingly these interaction appeared to occur on the hydrophobic end of capsaicin (Figure 4.21).

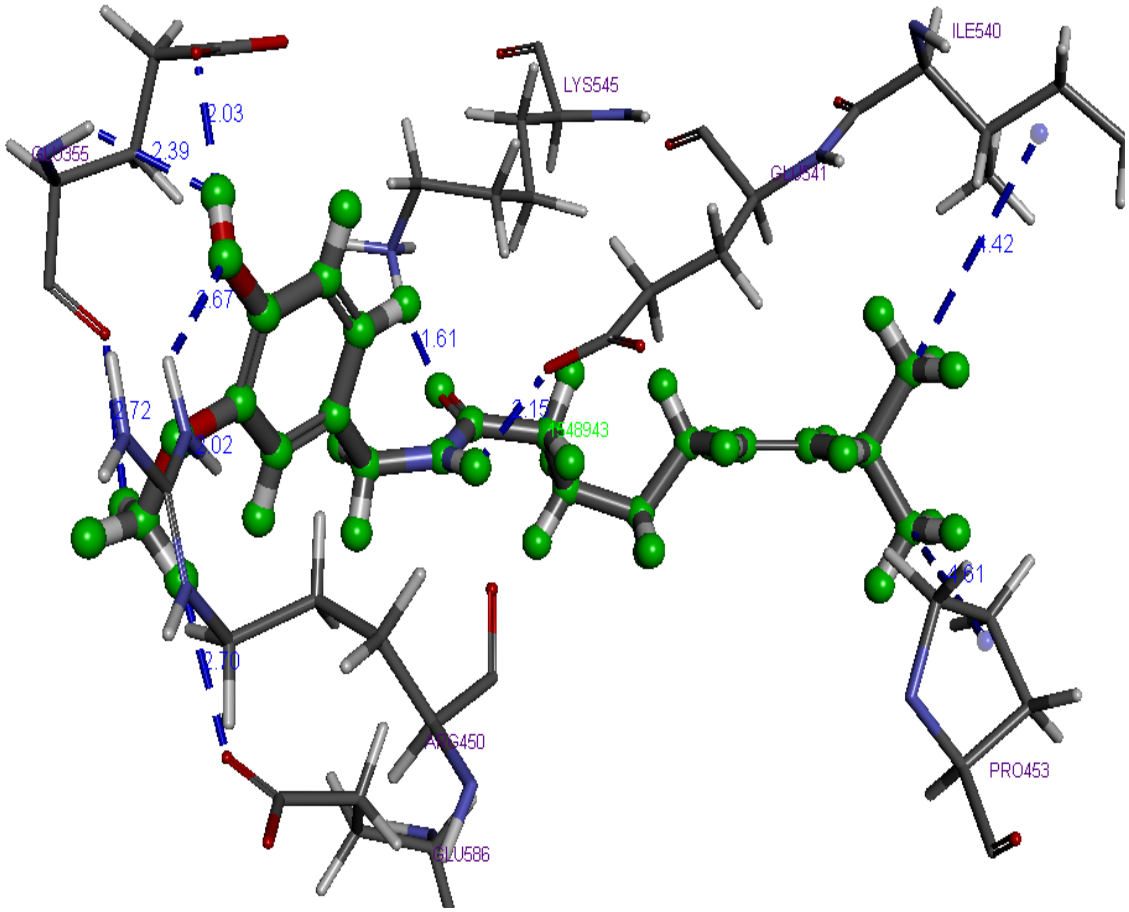

Figure 4.21: Docking complex of the capsaicin into PAL enzyme binding site.

The hydrophobic map of the PAL revealed that there is hydrophobicity in the site and therefore deemed responsible for the penetration with hydrogen bonds and hydrophilic interactions. The analysis of the ten ligand poses revealed that ARG 596 residue was most favourable because of large hydrogen bonding counts followed by ARG 450 with highest hydrophobic counts. However the conformation with the highest Dock Score had a total of seven hydrogen bonds (O---H) were observed with the shortest distance of 1.61 Å between LYS545 and O1 of the carbonyl. Among these bonds, four of them involved oxygen of the GLU residues as an acceptor for protons from the capsaicin molecule. Among the surrounding residues, GLU355 formed three hydrogen bonds, as the most interactive residue. Further analysis of interaction revealed only two hydrophobic-alkyl bonds for residues PRO 453 and

ILE 450 with 4.61 Å and 4.42 Å. The carbonyls of the capsaicin appeared to be the focal point of interaction participating in three hydrogen bonding. These results confirm the PAL facilitates the electron transfer from the capsaicin ligand, hence improving the response towards the biosensing.

4.3.5 Characterization of MWCNTs/PAL/Nafion

ATR-IR Spectroscopy

Platinum electrode modified with MWCNTs, PAL enzyme and Nafion was characterized by ATR-IR spectroscopy and TGA. The spectra in Figure 4.22 were recorded over the range 4000 to 500 cm^{-1} at 4 cm^{-1} resolution. The spectrum of pure MWCNTs show a peak at 1740 cm^{-1} which is assigned to the stretching mode of C=C bonds that form the framework of carbon nanotubes side walls.

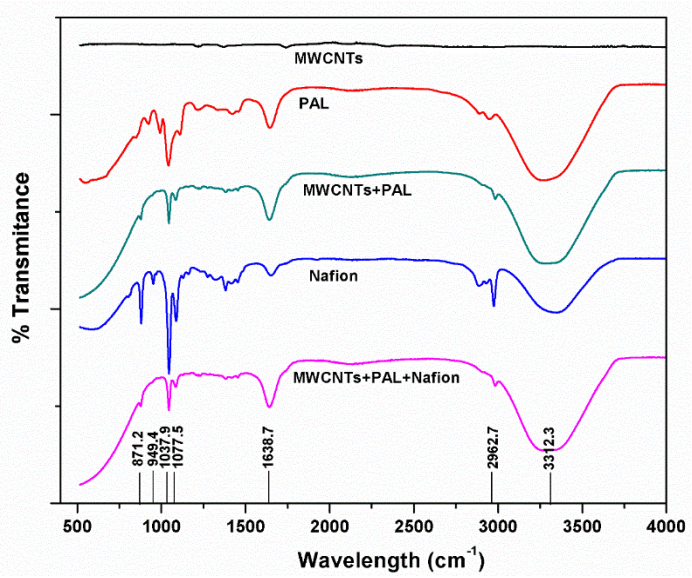

Figure 4.22: Infra-Red spectrum of MWCNTs, PAL enzyme and nafion in an order used for preparation of the biosensor with a layer by layer casting.

At 2962 cm^{-1} there is a peak band which corresponds to C-H asymmetric and symmetric stretching and at 3312 cm^{-1} O-H peaks due to carboxylic acid show broad and less intense peak. On Nafion/PAL/MWCNTs spectra, there is also a broad O-H stretching peak at 3312 cm^{-1}, C-H stretching is found at 2962 cm^{-1}, there is also an evident peak at 1638 cm^{-1} assigned to C=C bond stretch and at 1037 cm^{-1} is an

aromatic in place C-H bend. Nafion spectrum show C-O-C stretching vibrations at 871 cm^{-1}, S-O stretching symmetric at 1045 cm^{-1}, CF2 symmetric stretching at 1077 cm^{-1}; since nafion was a 5% solution in ethanol the spectrum show broad O-H stretching at 3312 cm^{-1} and C-H alkyl group stretching at 2963 cm^{-1} from ethanol. PAL spectrum has an amide bond peak at 1639 cm^{-1} which remains prominent on the final composite that is attached to the electrode.

Thermogravimmetric analysis of nanobiocomposite

The electrode composite was further studied for thermal stability and quantification for the composition by TGA in Figure 4.23. This approach was very informative for understanding the thickness of the surface as the layer by layer modification was performed.

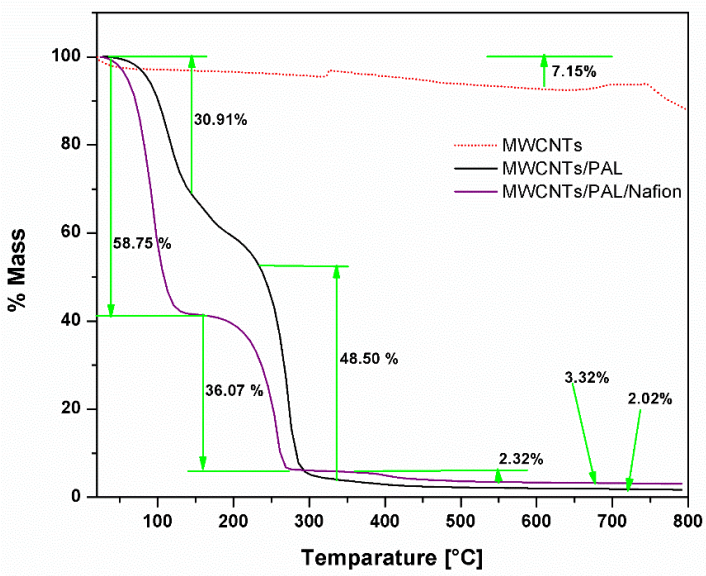

Figure 4.23: TGA curves of (i) MWCNTs, (ii) MWCNT/PAL and (iii) Nafion/ PAL/ MWCNTs. All the sample were studied at a linear heating rate of 10°C starting at 10 to 100°C.

MWCNTs curve show a change in mass (decomposition temperature) at 350 °C, another typical gradient drop in mass is noticed at about 750 °C, this might be due to carbon oxidation. MWCNTs modified with PAL enzyme show a TGA profile with two drop downs at 56 °C and 248 °C. The mass loss due to the first step is 30.91 %

while the second drop between at 248 °C has a mass loss of 48.50 %. The first mass loss phase in PAL/MWCNTs curve can be attributed to irreversible thermal denaturation of the enzyme, normal dehydration process of PAL and loss of DMF used as a dispersion medium. Beyond 248 °C we can observe the further drop in mass percentage to melting and decomposition processes of PAL as the temperature approaches 300 °C. The Nafion/PAL/MWCNTs curve shows a similar trend to that of PAL/MWCNTs however there is much higher loss of 58.75 % in the first step followed by a 36.07 % loss. Interesting, we observed an additional mass loss step of 2.32 % between 390 and 400 ^{o}C. Beyond that there is 3.32 % that is left behind and it is slighter that 2.02 % that is retained from PAL/MWCNTs conforming that the addition of PAL does improve the thermal stability of the bio-composite and most likely the ionic polymer, nafion improve the interfacial adhesion of PAL on the MWCNTs, as the last coating of the composite.

4.4 A comparative study of MWCNTs/GOx and MWCNTs/PAL biocomposites for the determination of Capsaicin with Gold electrode

A rotating disk electrode with a (3 mm diameter) gold tip was used in this study, similar procedures for its cleaning and modification were used as in the case of glassy carbon electrode and platinum electrode. Like platinum electrode, gold electrode offers a very favourable electron transfer kinetics and a wide anodic potential range, as noble metal electrodes they both have very stable chemical properties (Li and Miao, 2013).

4.4.1 Bare (Au-E)

Electrochemical analyses of capsaicin using a bare gold electrode are represented by the cyclic and differential pulse voltammograms shown in Figures 4.24 (a)-(b) respectively.

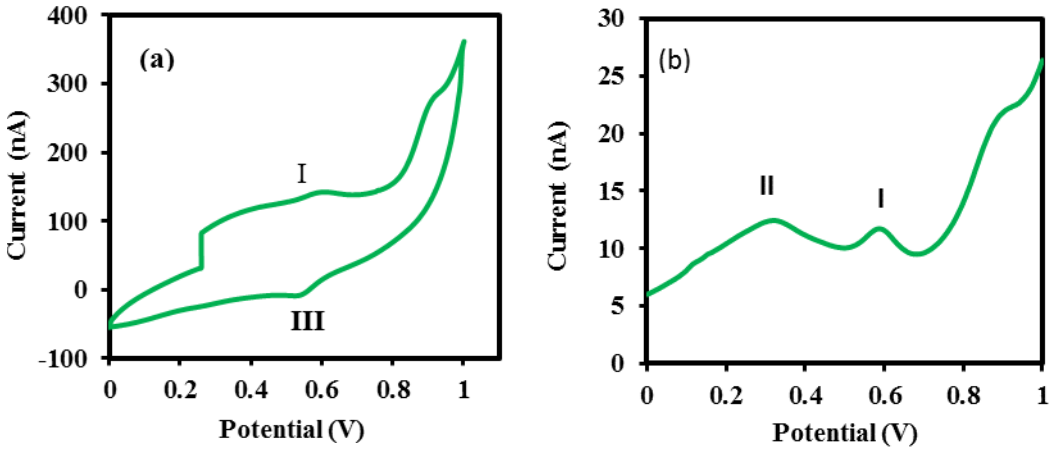

Figure 4.24: (a) CV and (b) DPV voltammograms of capsaicin sample (0.2 mL) from chilli extract in 0.1 M acetate buffer solution of pH 4.01 and scan rate of 0.01 $V.s^{-1}$ using bare Au-E

The CV scan in Figure 4.24 (a), show only one capsaicin oxidation peak that was detected, the reduction peak is detected but is found to have shifted to the right in the potential scale which shows poor electrode sensitivity. These capsaicin peaks are also very small and insignificant compared to those obtained with bare GCE. DPV voltammogram obtained by using bare AU-E shows two small but visible capsaicin peaks, and they appear within capsaicin detection range.

4.4.2 Gold electrode modified with Multi walled carbon nanotubes (Au-E-MWCNTs)

Coating of gold electrode with multi-walled carbon nanotubes was done in same way as in the case of glassy carbon electrode and platinum electrode. Below are CV and DPV voltammograms of capsaicin analysis using a modified gold electrode.

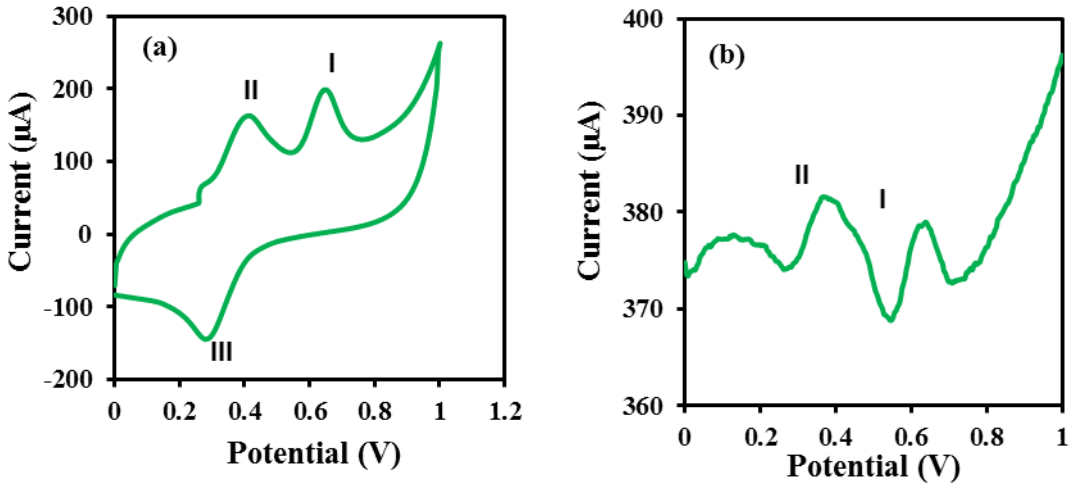

Figure 4.25: (a) CV and (b) DPV voltammograms of capsaicin sample (0.2mL) from chilli extract in 0.1M acetate buffer solution of pH 4.01; scan rate of 0.01 $V.s^{-1}$ using a gold electrode modified with MWCNTs.

Just like with the other electrode materials, introduction of MWCNTs drastically changed the performance of gold electrode, this significant change is noticed when comparing Figures 4.24 (a) and 4.25 (a). Au-E-MWCNTs voltammogram show all peaks clearly with higher peak currents. When comparing Figures 4.24 (b) and 4.25 (b), shapes and size of the peaks are more distinct when using an electrode that has been modified with nanotubes. Electrical properties of nanotubes prove the theory correct about enhancing the sensitivity of the electrochemical sensor; the enhancements of the peak current were expected due to stronger adsorptive properties of MWNCTs. These adsorptive properties of MWCNTs will increase the deprotonation of the phenolic moiety in capsaicin and the MWCNTs will increase the surface area of the modified electrode and current become stronger and easily adsorbed on the surface of an electrode.

4.4.3 Enzyme immobilization on carbon nanotubes modified gold electrode

Enzyme was immobilized on a MWCNTs modified gold electrode, but in this study two different enzymes were used, namely: Phenylalanine ammonia lyase (PAL) and Glucose oxidase (GOx).

PAL Enzyme

Clearly visible and distinct oxidation and reduction peaks were obtained when using gold electrode modified with MWCNTs and PAL enzyme as illustrated in Figure 4.26(a). The effect of PAL enzyme is noticed when all three electrode voltammograms are overlaid to show the difference in electrode sensitivity.

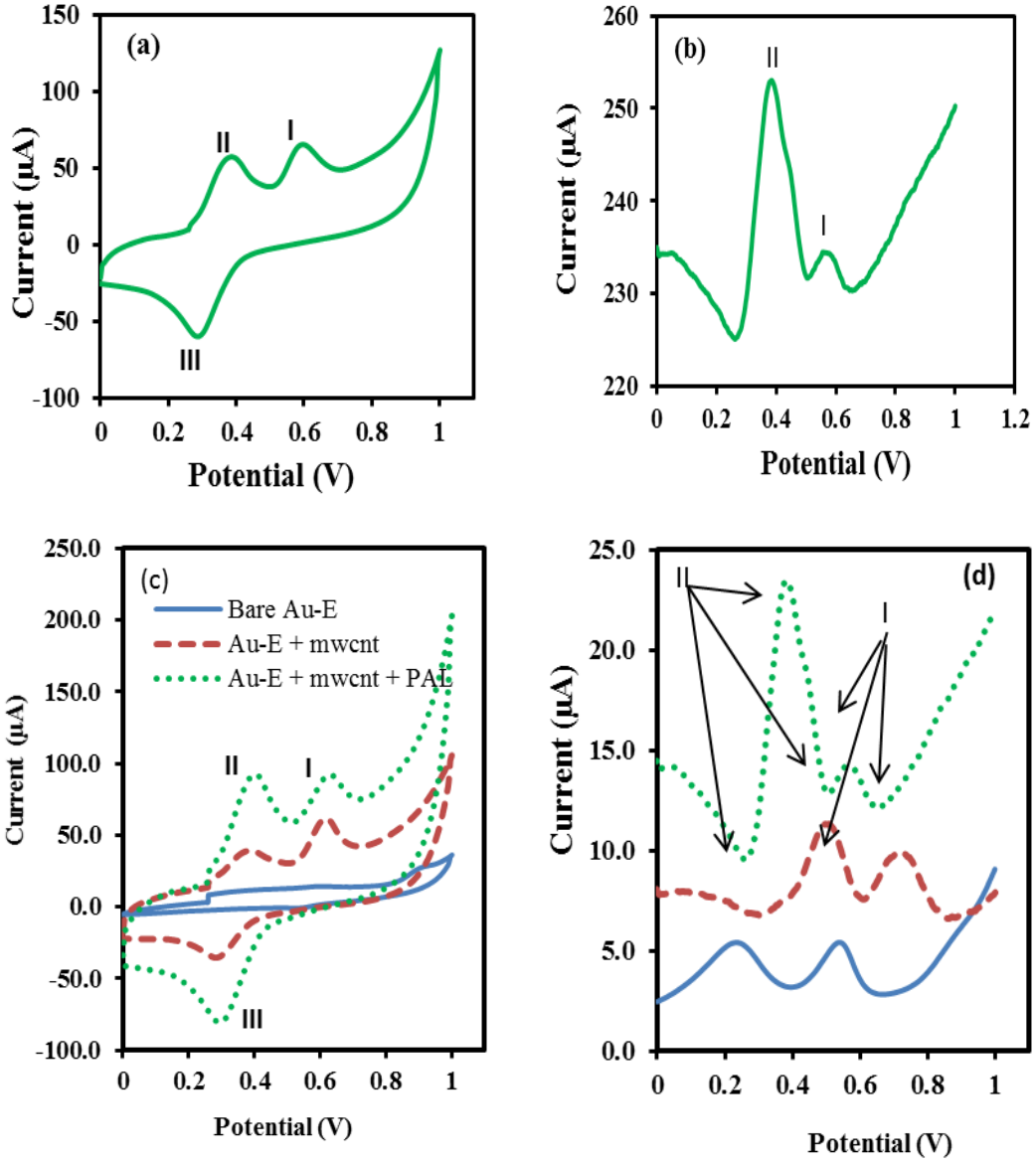

Figure 4.26: (a) CV scan and (b) DPV scan for capsaicin obtained using gold electrode modified with MWCNTs and PAL enzyme; (c): CV and (d) DPV scans for capsaicin using bare gold electrode (Au-E), multiwalled carbon nanotubes on Au-E (Au-E- MWCNTs) and PAL enzyme on a MWCNTs-Au-E (Au-E-MWCNTs-PAL)

DPV voltammogram shows that peak 2 has higher peak current than peak 1, this was not the case with Au-E-MWCNTs electrode, this might be due to the fact that catalytic activity of PAL enzyme is higher at potential scale around 0.4 V.

CV and DPV voltammograms for all three gold electrodes (bare, MWCNTs and MWCNTs-PAL) were overlaid in one graph which clearly shows the differences in analyte behaviour towards electrode modification. Higher peak currents were observed with modified electrodes, due to the adsorptive properties of both MWCNTs and the enzyme. Figures 4.26 (c)-(d) show that a biosensor has higher peak current than all other electrodes, it is also noticed that the peak potential for (Au-E-MWCNTs-PAL) slightly shifted towards the left, this can be attributed to better sensitivity compared to the bare electrode.

Glucose Oxidase Enzyme

Well defined peaks were observed when GOx enzyme was immobilized on a MWCNTs modified gold electrode. Enhanced peak currents can be attributed to catalytic properties of GOx enzyme possesses. Both CV and DPV scans behaved similarly, this is evident when looking at Figures 4.27 (a)-(b). CV and DPV voltammograms for different working electrodes (bare, MWCNTs modified and MWCNTs-GOx) were overlaid on one graph respectively, in order to show the difference in sensitivity and the impact of each electrode have on capsaicin detection. These differences are graphically represented in Figures 4.27 (c)-(d).

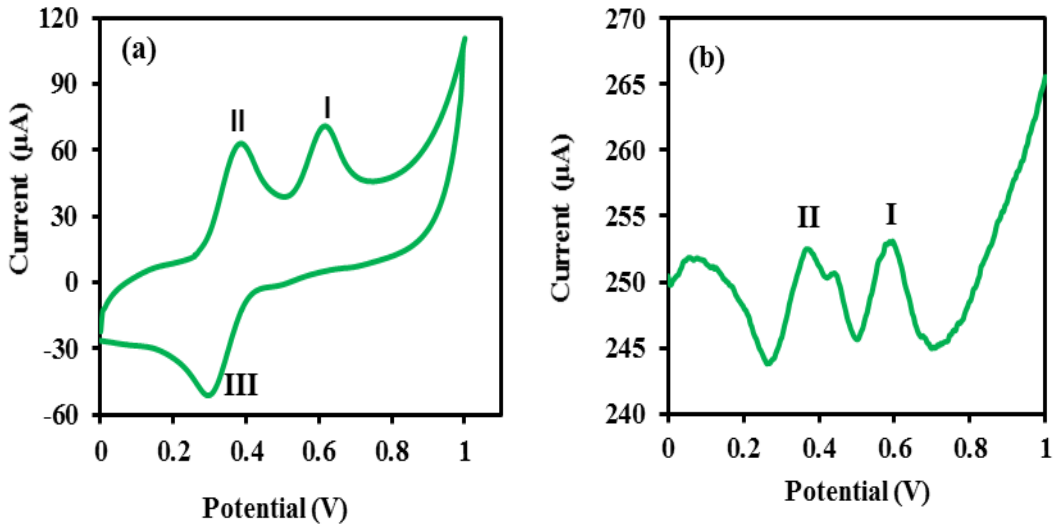

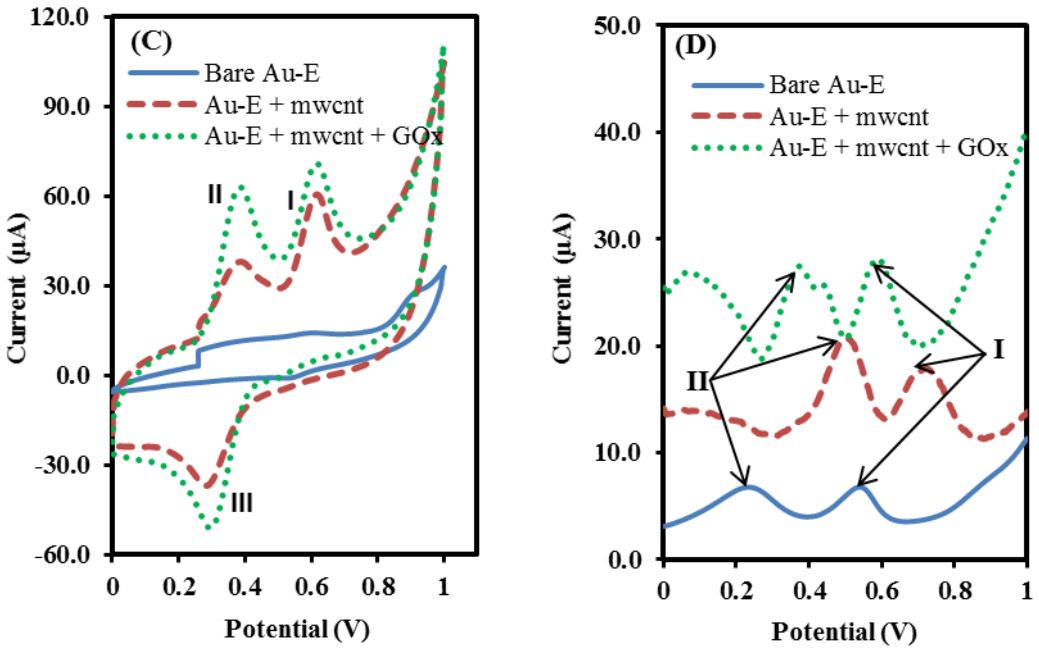

Figure 4.27: (a) CV scan and (b) DPV scan for capsaicin obtained using a gold electrode modified with MWCNTs and GOx enzyme. (c): CV and (d) DPV scans for capsaicin using bare gold electrode (Au-E), multiwalled carbon nanotubes on Au-E (Au-E- MWCNTs) and GOx enzyme on a MWCNTs-Au-E (Au-E-MWCNTs-GOx.)

In Figure 4.27 (c) we noticed that cyclic voltammetry curves for Au-E-MWNCTs and Au-E-MWCNTs-GOx are almost similar at higher potentials above 0.75V, but below this potential biosensor curve is clearly higher than that of Au-E-MWCNTs. In Figure 4.27 (d), we noticed that the biosensor curve shifted to the left of the potential scale when compared to that of MWCNTs electrode curve. These differences confirm the better sensitivity of the biosensor compared to MWCNTs-modified electrode and bare electrode. The enhancement of peak currents on coated electrodes was due to good conductivity, strong adsorptive properties of MWCNTs and good catalytic activity of GOx. Both biosensors produced when using PAL and GOx enzymes yielded good results, although GOx biosensor showed well defined peaks especially peak I.

CHAPTER 5

CONCLUSIONS AND RECOMMENDATIONS

5.1 Conclusions

The bare glassy carbon electrode produced better voltammograms for both CV and DPV scans when compared to bare platinum and bare gold electrodes. This can be attributed to better adsorption properties of capsaicin to glassy carbon surface than to platinum and gold surfaces. This picture changed completely when all these electrodes were modified with multiwalled carbon nanotubes, all three electrodes regardless of its material composition produced well distinct voltammograms with good looking peaks. This enhancement towards good CV and DPV voltammograms with significant high peak currents for capsaicin determination is attributed to a better surface area and good electrical conductivity provided by carbon nanotubes.

It was also observed that the introduction of enzymes onto the modified electrode increased the sensitivity of the biosensor even further compared to the bare and MWCNTs modified sensors across all types of electrode material used. This can be attributed to good catalytic activity of the enzymes used. However it was interesting to note that when comparing CV voltammograms for both PAL and GOx enzymes, GOx produced intense capsaicin peaks. This was also evident when the DPV scans were compared for both enzymes with GOx showing higher capsaicin peak currents than PAL. It can be concluded that glucose oxidase enzyme provided better sensitivity than PAL enzyme in the determination of capsaicin. The results showed that the combination of GCE, MWCNTs and GOx produced a better performing biosensor compared to other two combinations involving platinum and gold electrodes. The real capsaicin sample extracted from chilli pepper fruit was quantified at 87.17μg.mL^{-1}. The advantages of using MWCNTs and enzymes included, enhanced sensitivity, excellent reproducibility, steady coating and high exchange current density for capsaicin.

5.2 Recommendations for Further work

Future studies may involve manufacturing of highly sensitive electrochemical biosensors for the food industry. For future work the possibility of introducing an enzyme onto a gold nanoparticle modified electrode will be explored in order to see what impact it might bring towards electrode sensitivity.

REFERENCES:

Ameta, S.C., P.B. Punjabi, R. Ameta, C. Ameta, (**2014**), Microwave-Assisted Organic Synthesis: A Green Chemical Approach, *CRC Press.*

Ando, Y. and X. Zhao, (**2006**), Synthesis of Carbon Nanotubes by Arc Discharge Method, *New Diamond and Frontier Carbon Technology*, Vol. 16, No. 3

Andrienko, D., (**2008**). Cyclic voltammetry-mpip-mainz.mpg.de

Balasubramanian, K and M. Burghard, (**2006**): Biosensors based on carbon nanotubes, *Anal Bioanal Chem.* 385: 452-468

Balbaa, S.I., M.S. Karawya and A.N. Girgis, **(1968)**: The capsaicin content of capsicum fruits at different stages of maturity, *Lloydia*, 31: 272-274

Baldo, M.A., S. Daniele, I. Ciani, C. Bragato and J. Wang, (**2004**). *Electroanal.* 5, 6.

Barceloux, D.G., **(2009)**: Pepper and Capsaicin (Capsicum and Piper Species), *Vol.55, Issue 6,* 380-390.

Baughman, R.H., A.A. Zakhidov, W.A. Zakhidov, (**2002**): Carbon nanotubes- the route toward applications, *Science* **297**, 787-792.

Bergmeyer, H.U. (**1983**), Methods of Enzymatic Analysis, Volume 2, 3rd Edition, *Academic Press* (Deerfield Beach) pp. 201-202

Bosland, P.W., **(1996)**. Capsicums: Innovative uses of an ancient crop. In: *J. Janick (ed*), 479-487. Progress in new crops. *ASHS Press*, Arlington, VA.

Buck, S.H. and T.F. Burks, (**1985**) The neuropharmacology of capsaicin: review of some recent observations, *Pharmacol Rev*, 38: 179-226

Buffat Ph. and J.-P. Borel, (**1976**): "Size effect on the melting temperature of gold particles". *Physical Review* A 13 (6): 2287.

Buzea, C., I.I. Pacheo and K. Robbie. (**2007**), "Nanomaterials and Nanoparticles: Sources and Toxicity". *Biointerphases* 2 (4).

Camm, E.L. and G.H.N. Towers. (**1973**). Phenylalanine ammonia lyase. *Phytochemistry*, 12: 961-973. Doi: 10.1016/0031-9422(73) 85001-0

Carpenter, S.E. and B. Lynn. (**1981**): Vascular and sensory responses of human skin to mild injury after topical treatment with capsaicin, *Br. J. Pharmacol*, 73: 755-758.

References

Carriedo, G. A. (**1988**). "The use of cyclic voltammetry in the study of the chemistry of metal carbonyls". *J.Chem.Educ.* **65**: 1020.

Che, J., T. Cagin and W.A. Goddard III, (**2000**), Thermal conductivity of carbon Nanotubes, *Nanotechnology* 11, 65–69

Chengguo Hu and Shengshui Hu, **(2009**). Carbon nanotube-based electrochemical sensors: Principles and Applications in Biomedical systems, *Journal of sensors*, 1-41.

Davis, J.J., K. Coleman, B. Azamian, C. Bagshaw, M.L Green, (**2003**). *Chem. Eur. J.* 9, 3732

De, A.K. (**2004**), Capsicum: The Genus Capsicum, Medicinal and aromatic plants, *CRC Press*

Dresselhaus, M.S, G. Dresselhaus, K. Sugihara, I.L. Spain and H.A. Goldberg, (**1988**). Springer series in Material Science 5, *Springer-Verlag*, Berlin, Heidelberg.

Drexler, K. Eric (**1986**). Engines of Creation: The Coming Era of Nanotechnology. *Doubleday*. *ISBN 0-385-19973-2*.

Endo, M., M.S. Strano and P. M. Ajayan, **(2008)**, Potential Applications of Carbon Nanotubes, Shinshu University, 4-17-1 Wakasato, *Nagani-shi* 380-8553, Japan.

Ferreira, L.F.P., M.E. Taqueda, A. Converti, M. Vitolo and A. Pessoa Jr. (**2005**), Purification of Glucose Oxidase from Aspergillus Niger by Liquid-Liquid cationic reversed Micelles extraction. *Biotechnol. Prog*. 21 (3), 868-874

Foley, M. (**2006**), Cheap tubes Inc., http://www.nanotech-now.com/carbon-nanotubes-101.htm

Frederick, K.R., J. Tung, R.S. Emerick, F.R. Masiarz, S.H. Chamberlain, A. Vasavada, S. Rosenberg, S. Chakraborty and L.M. Schopter, (**1990**): Glucose Oxidase from Aspergillus niger. Cloning, gene sequence, secretion from Saccharomyces cerevisiae and kinetic analysis of a yeast-derived enzyme. *J. Biol. Chem*., 265: 3793-3802

Frisch, M.J., Trucks, G.W., Schlegel, H.B., Scuseria, G.E., Robb, M.A., Cheeseman, J.R., Scalmani, G., Barone, V., Mennucci, B., Petersson, G.A., Nakatsuji, H., Caricato, M., Li, X., Hratchian, H.P., Izmaylov, A.F., Bloino, J., Zheng, G., Sonnenberg, J.L., Hada, M., Ehara, M., Toyota, K., Fukuda, R., Hasegawa, J., Ishida, M., Nakajima, T., Honda, Y., Kitao, O., Nakai, H., Vreven, T., Montgomery Jr., J.A.,

Peralta, J.E., Ogliaro, F., Bearpark, M.J., Heyd, J., Brothers, E.N., Kudin, K.N., Staroverov, V.N., Kobayashi, R., Normand, J., Raghavachari, K., Rendell, A.P., Burant, J.C., Iyengar, S.S., Tomasi, J., Cossi, M., Rega, N., Millam, N.J., Klene, M., Knox, J.E., Cross, J.B., Bakken, V., Adamo, C., Jaramillo, J., Gomperts, R., Stratmann, R.E., Yazyev, O., Austin, A.J., Cammi, R., Pomelli, C., Ochterski, J.W., Martin, R.L., Morokuma, K., Zakrzewski, V.G., Voth, G.A., Salvador, P., Dannenberg, J.J., Dapprich, S., Daniels, A.D., Farkas, Ö., Foresman, J.B., Ortiz, J.V., Cioslowski, J., Fox, D.J., **2009**. Gaussian 09. *Gaussian, Inc.*, Wallingford, CT, USA.

Gamez, A., L. Wang, C.N. Sarkissian, D. Wendt, P. Fitzpatrick, J.F. Lemontt, C.R. Scriver and R.C. Stevens. (**2007**): Structure-based epitope and PE Gylation sites mapping of phenylalanine ammonia-lyase for enzyme substitution treatment of phenylketonuria. *Journal of Molecular Genetics and Metabolism*, 91 (4): 325-334

Goodsell, D. (**2006**), Molecule of the month, doi 10.2210/rcsb_pdb/mom_2006_5

Grisham, C. M. and R. H. Garrett (**1999)**. Biochemistry. Philadelphia: *Saunders College Pub* . pp. 426–7. ISBN 0-03-022318-0.

Grünwald, M., E. Rabani, and C. Dellago (**2006**), Mechanisms of the Wurtzite to Rocksalt Transformation in CdSe Nanocrystals, *Physical Review Letters*, PRL 96, 255701

Hahlbrock, K and H. Grisebach, (**1979**). "Enzymic Controls in the Biosynthesis of Lignin and Flavonoids". *Annual Review of Plant Physiology* **30** (1): 105–130.

Haron, S. and A.K. Ray, (**2006**), Optical biodetection of cadmium and lead ions in water. *Medical Engineering and Physics*, 28 (10). pp. 978-981. ISSN 1350-4533

Hautkappe, M., M.F. Roizen and A. Toledano. (**1998**): Review of the effectiveness of capsaicin for painful cutaneous disorders and neural dysfunction, *Clin. J. Pain*, 14: 97-106

Heller, D.A., E.S. Jeng, Tsun-Kwan Yeung, B.M. Martinez, A.E. Moll, J.B. Gastala, M.S. Strano, (**2006**): Optical detection of DNA conformational polymorphism on single-walled carbon nanotubes, *Science* 311, 505-511.

Henderson, D.E., A.M. Slickman and S.K.Henderson. (**1999**): *J. Agric. Food Chem.*, 47, 2563

Hewakuruppu, Y.L., L.A. Dombrovsky, C. Chen, V. Timchenko, X. Jiang, S. Baek and R.A. Taylor,(**2013**). Plasmonic “pump probe” method to study semi-transparent nanofluids, *Applied optics*, 52 (24): 6041-6050.

References

Hierlemann, A., O. Brand, C. Hagleitner, H. Baltes (**2003**). Microfabrication techniques for chemical/biosensors, Proceedings of the *IEEE*, 91 (6), 839-863. ISSN 0018-9219.

Higashiguchi, F., H. Nakamura, H. Hayashi and T. Kometani (**2006**). Purification and Structure Determination of Glucosides of Capsaicin and Dihydrocapsaicin from Various *Capsicum* Fruits, *J. Agric. Food Chem., 54* (16), 5948–5953

Horikoshi, S. and N. Serpone, (**2013**). Microwaves in Nanoparticle Synthesis: Fundamentals and Applications. Wiley Online Library, 1st Edition, *Wiley- VCH Verlag* GmbH & Co. KgaA.

http://ec.europa.eu/health/scientific_committees/opinions_layman/nanomaterials/en/l-2/1.htm, (Accessed **15 August 2012**)

http://en.wikipedia.org/wiki/chili_pepper, (Accessed **24 April 2012)**

http://en.wikipedia/wiki/enzyme, (Accessed **13 June 2013**)

http://nanotechweb.org/cws/article/tech/46378, 2011, (Accessed **9 October 2011)**

http://www.cnanotech.com, (Accessed **3 May 2013**)

http://www.rcsb.org/pdb/explore/explore.do?structureId=3RJ8 (accessed **04 September 2014)**

Huynh, H.T and R.W. Teel. (**2005**): *Anticancer Res*. : 25, 117

Hyder, K. (**1996**): Is CS the wrong solution? *New Sci.* 149: 12-13

Hyun, M.W., Y.H. Yun, J.Y. Kim, and S.H. Kim. (**2011**), Fungal and Plant Phenylalanine Ammonia-lyase, *mycobiology* 39(4): 257-265.

Jahanshahi, M. and A.D. Kiadehi, (**2013**). Fabrication, Purification and Characterization of Carbon Nanotubes: Arc-Discharge in Liquid Media (ADLM), *DOI: 10.5772/51116*

Jones, D.H. Phenylalanine ammonia-lyase. (**1984**): Regulation of its induction, and its role in plant development. *Phytochemistry*. 23: 1349-1359.

References

Jorio, A., G. Dresselhaus, M. S. Dresselhaus, (**2007**). Carbon Nanotubes: Advanced Topics in the Synthesis, Structure, Properties and Applications, *Springer Science & Business Media.*

Kachoosangi, R.T., G.R. Wildgoose and R.G. Compton. (**2008**): Carbon nanotube-based electrochemical sensors for quantifying the 'heat' of chilli peppers: the adsorptive stripping voltammetric determination of capsaicin. *Analyst* 133: 888-895

King, V.B. (**2007**). Nanotechnology Research Advances, *Nova Publishers*, ISBN 1600215254, 9781600215254, 187

Kissinger, P. and W.R. Heineman, (**1996)**. Laboratory Techniques in Electroanalytical Chemistry, Second Edition, *CRC*. ISBN 0-8247-9445-1.

Koukol, J. and E.E. Conn. (**1961**): Metabolism of aromatic compounds in higher plants. IV. Purification and properties of phenylalanine deaminase of Hordeum vulgare. *J. Biol. Chem*. 236: 2692-2698.

Kounaves, S.P., "Voltammetric Techniques", Handbook of Instrumental Techniques for Analytical chemistry, *Prentice Hall*, (**1997**), <www.prenhall.com/settle/chapters/ch37.pdf>.

Laskaridou-Monnerville, A. (**1999**): Determination of capsaicin and dihydrocapsaicin by micellar electrokinetic chromatography and its application to various species of Capsicum, Solanaceae, *J. Chromatogr*. 838: 293-302

Li, G. and P. Miao, (**2013**): Electrochemical Analysis of Proteins and Cells, *Springer Briefs in Molecular Science*, DOI: 10.1007/978-3-642-34252-3_2

Liu, J., A. Chou, W. Rahmat, M.N. Paddon-Row and J.J. Gooding, (**2005**). *Electrochim. Acta*, 51, 611-618.

Lopez, B.P. (**2009**). Carbon nanotube for electrochemical biosensing, PhD Thesis, Department de Quimica, Universitat Autonoma de Barcelona.

Lyons, M.E.G. and G.P. Keeley. (**2008**): Carbon Nanotube Based Modified Electrode Biosensors. Part 1. Electrochemical studies of the Flavin Group Redox Kinetics at SWCNT/Glucose Oxidase Composite Modified Electrodes, University of Dublin, Ireland, *Int. J. Electrochem.Sci*. 3: 819-853.

Martin, D.A., (**2006**), Focus on Nanotube research, *Nova Science Publishers, Inc.*

References

Mazloum-Ardakani, M. and M.A. Sheikh-Mohseni, (**2011**): Carbon Nanotubes in Electrochemical Sensors, Department of Chemistry, Faculty of Science, Yazd University, I.R, Iran.

Meyyappan, M. (**2005**). Carbon nanotubes: Science and Applications, *CRC Press* ISBN 0849321115, 9780849321115, 289

Mpanza, T.E., M.I. Sabela, S.S. Mathenjwa, S. Kanchi and K. Bisetty. (**2014**): Electrochemical Determination of Capsaicin and Silymarin using a Glassy Carbon Electrode modified by Gold Nanoparticle decorated Multi-walled Carbon Nanotubes, *Analytical letters*, 47: 2813-2828.

Murugaboopathi, G., V. Parthasarathy, C. Chellaram, T. Prem Anand **and** S. Vinurajkumar, (**2013**). Applications of Biosensors in Food Industry, *Biosci., Biotech. Res. Asia,* Vol. **10**(2), 711-714

Othman, Z.A.A, Y.B. Hadj Ahmed, M.A. Habila and A.A. Ghafar, **(2011)**: Determination of capsaicin and dihydrocapsaicin in capsicum fruit samples using high performance liquid chromatography. *Molecules* 16: 8919-8929

Oxford [Oxfordshire]: *Oxford University Press. ISBN 0-19-854768-4.*

Peña-Alvarez, A., E. Ramirez-Maya and L.A. Alvarado-Suarez. (**2009**), Analysis of capsaicin and dihydrocapsaicin in peppers and pepper sauces by solid phase microextraction-gas chromatography-mass spectrometry. *J. Chromatogr*. A 1216: 2843-2847

Pershing, L.K., C.A. Reilly, J.L. Corlett and D.J. Crouch. (**2006**). *J. Appl. Toxicol*., 26: 88

Pillay, K. (**2012**), Carbon Nanomaterials - A New Form of Ion Exchangers, *Ion Exchange Technologies*. DOI: 10.5772/54114.

Qi, P., O. Vermesh, M. Grecu, A. Javey, Q. Wang, H. Dai, S. Peng, and K.J. Cho, (**2003**): Toward large arrays of multiplex functionalized carbon nanotube sensors for highly sensitive and selective molecular detection, *Nano Lett.* 3, 347-351.

Rafique, M.M.A. and J. Iqbal, **(2011**), Production of Carbon Nanotubes by Different Routes – A Review, *J. Encapsulation Adsorpt. Sci.*1, 29-34

Rao, A.M.; E. Richter; S. Bandow; B. Chase; P.C. Eklund; K.A. Williams; S. Fang; K.R. Subbaswamy; M. Menon; A. Thess; R.E. Smalley; G. Dresselhaus; M.S.

Dresselhaus, (**1997)** Diameter-selective Raman scattering from vibrational modes in carbon nanotubes. *Science*, *275*, 187–191.

Rao, C.N., B.C. Satishkumar, A. Govindaraj, and M. Nath, (**200**1). *ChemPhysChem*. 79.

Reilly, C.A., D.J. Crouch and G.S. Yost. **(2001**): Quantitative analysis of capsaicinoids in fresh peppers, Oleoresin Capsicum and Pepper spray products, *J.Forensic Sci*. 46(3): 502-509.

Saito, Y. and S. Uemura, (**2000**): Field emission from carbon nanotubes and its applications to electron sources, *Carbon* 38, 169-182.

Saito, Y., S. Uemura, and K. Hamaguchi, (**1998**): Cathode ray tube lighting elements with carbon nanotube field emitters, Jpn. *J. Appl. Phys*. 37, L349-L348.

Salvetat, J.P., J.M. Bonard, N.H. Thomson, A.J. Kulik, L. Forró, W. Benoit, and L. Zuppiroli, (**1999**). Mechanical properties of Carbon nanotubes, Departement de Physique, Ecole Polytechnique de Lausanne, CH-1015, Lausanne, Switzerland.

Sanchez, A.M., M.G. Sanchez, S. Malagarie-Cazenave, N. Olea and I. Diaz-Laviada. (**2006**), *Aptosis*, 11, 89.

Sarkissian, C.N. and A. Gamez. (**2005**), Phenylalanine ammonia-lyase, enzyme substitution therapy for phenylketonuria, *Mol Genet Metab.* 86: 22-26.

Sarmah, P. and D. Mahanta (**2014**), Computational Methods for Enzyme Design and Its Biological Significance, *International Journal of Engineering and Advanced Technology (IJEAT)*, ISSN: 2249 – 8958, Volume-3, Issue-4

Satyanarayana, M.N. (**2006**): *Crit. Rev. Food Sci. Nutr*., 46, 275

Sayago, I., E. Terrado, M. Aleixandre, M.C. Horrillo, M.J. Fernandez, J. Lozano, E. Lafuente, W.K. Maser, A.M. Benito, M.T. Martinez, J. Gutierrez and E. Munoz, (**2007**). *Sens. Actuators* B, 122, 75

Schuettler, M. (**2007**), Electrochemical properties of platinum electrodes in vitro: Comparison of six different surface qualities, Conf. Proc IEEE, *Eng Med Biol Soc*., 186-189.

Schwede, T.F., J. Retey, G.E. Schulz. (**1999**): Crystal structure of histidine ammonia-lyase revealing a novel polypeptide modification as the catalytic electrophile. *Biochemistry* 38 (17): 5355-61.

Sinnott, S.B. and R. Andrews, (**2001**): Carbon Nanotubes: Synthesis, properties and applications. *Crit. Rev. Solid State Mater. Sci.*, *26*, 145–249.

Smith, AL (Ed) (**1997**). Oxford dictionary of biochemistry and molecular biology.

Snow, E.S., F. K. Perkins and J. A. Robinson, (**2006**), Chemical vapour detection using single-walled carbon nanotubes, *Chem. Soc. Rev*., 35, 790–798

Son, Y.W., S. Oh, J. Ihm and S. Han, (**2005**): Field emission properties of double-wall carbon nanotubes, *Nanotechnol.* 16, 125-128.

Spanyar, P. and M. Blazovich. (**1969**): A thin layer chromatographic method for the determination of capsaicin in ground paprika, *Analyst*. 144: 149-152

Supalkova, V., H. Stavelikova, S. Krizkova, V. Adam, A. Horna, L. Havel, P. Ryant, P. Babula and R. Kizek, (**2007**). Study of Capsaicin content in various parts of pepper fruit by Liquid Chromatography with Electrochemical detection, *Acta Chim. Slov.* 54:55-59.

Taniguchi, N. (**1974**). On the Basic Concept of Nanotechnology, *Proc. ICPB*, Tokyo, Japan

Theâvenot, D.R., K. Toth, R. A. Durst and G. S. Wilson, (**1999**). Electrochemical Biosensors: Recommended Definitions and Classification, *Pure Appl.Chem*. Vol. 71, No.12, pp. 2333-2348,

Thess, A.; R. Lee; P. Nikolaev,; H. Dai; P. Petit; J. Robert; Ch. Xu; Y.H. Lee; S.G. Kim; A.G. Rinzler; D.T. Colbert; G.E. Scuseria; D. Tománek; J.E. Fischer; R.E. Smalley, (**1996),** Crystalline ropes of metallic carbon nanotubes. *Science, 273*, 483–487.

Tirado-Rives, J., W.L Jorgensen, (**2006**). Contribution of Conformer Focusing to the Uncertainty in Predicting Free Energies for Protein−Ligand Binding. *J. Med. Chem.* 49(20), 5880-5884.

Tsuge, H.J., O. Natsuaki and K. Ohashi. (**1975**): Purification, Properties and Molecular features of Glucose Oxidase from Aspergillus niger. *J. Biochem*., 78: 835-843

Turner, A.P. (**2000)**. Biosensors – sense and sensitivity. *Science 290*, 1315–1317.

Venkatachalam, C.M., X. Jiang, T. Oldfield, M. Waldman, (**2003)**. LigandFit: a novel method for the shape-directed rapid docking of ligands to protein active sites. *J. Mol. Graphics Modell.* 21(4), 289-307.

Wang, J. (**2004**). Carbon nanotube based electrochemical biosensors: A Review, Department of Chemistry and Biochemistry, New York State University Las Cruces, NM 88003, USA.

Wang, J., M. Li, Z. Shi, N. Li, and Z. Gu. 2002. Investigation of the electrocatalytic behaviour of single-wall carbon nanotube films on an Au electrode. Microchem. J. 73: 325–333.

Wang, J., M. Musameh, Y. Lin, (**2003**), *J. Am. Chem. Soc*. 125, 2408

Watanabe, S.K., G. Hemandez-Velazco, F. Iturbe-Chinas, A. Lopez-Mungia. (**1992**). Phenylalanine ammonia lyase from Sporidiobolus pararoseus and Rhodosporidium toruloides: application for phenylalanine and tyrosine deamination. *World J. Microbiol. Biotechnol*. 8: 406-410.

Wilson, M., K. Kannangara, G. Smith, M. Simmons and B. Raguse, (**2002**). Nanotechnology: Basic science and Emerging Technologies. *Chapman & Hall, CRC Press*, London

Wong, C.M., K.H. Wong and X.D. Chen (2008), Glucose oxidase: natural occurrence, function, properties and industrial applications, *Appl. Microbiol and Biotechnol.* 78 (6): 927-938

Wu, G., Robertson, D.H., Brooks, C.L., Vieth, M., 2003. Detailed analysis of grid-based molecular docking: A case study of CDOCKER—A CHARMm-based MD docking algorithm. *J. Comput. Chem.* 24(13), 1549-1562.

Xu, G., S.B. Adeloju, Y. Wu, X. Zhang, (**2012**), Modification of polypyrrole nanowires array with platinum nanoparticles and glucose oxidase for fabrication of a novel glucose biosensor. *Anal. Chim. Acta, Elsevier,* 755: 100-107.

Yacamàn, M.J.; M.M. Yoshida; L. Rendon; J.G. Santiesteban, (**1993**), Catalytic growth of carbon microtubules with fullerene structure. *Appl. Phys. Lett.*, 62, 202–204.

Yoo, E.H., S.Y. Lee, (**2010**), Glucose Biosensors: An Overview of use in Clinical Practice, *Sensors (Basel),* 10 (5): 4558-4576

Zare, H.R., and N. Nasirizadeh, (**2011**). *J. Iran. Chem. Soc.,* Vol. 8, Suppl., pp.S55-S66

References

Zhang, L., Z. Shi, Q. Lang, J. Pan, (**2010**), Electrochemical synthesis of belt-like polyaniline network on p-phenylenediamine functionalized glassy carbon electrode and its use for the direct electrochemistry of horse heart cytochrome c, *Electrochim. Acta*, 55: 641-647

Zittel, H.R. and F.J. Miller, (**1965**), A Glassy Carbon Electrode for Voltammetry, *Anal. Chem*., 37 (2), pp. 200 – 203

Zoski, C.G., (**2001**). Handbook of Electrochemistry. *Elsevier Science.* ISBN 0-444-1958-0.

Appendix 1: Properties of Enzymes/Protein

Appendix 1a: Protein sequence of Phenylalanine Ammonia Lyase (PAL)

1W27:A|PDBID|CHAIN|SEQUENCE
MENGNGATTNGHVNGNGMDFCMKTEDPLYWGIAAEAMTGSHLDEVKKM
VAEYRKPVVKLGGETLTISQVAAISARDGSGV
AGVEGGFFELQPKEGLALVNGTAVGSGMASMVLFEANILAVLAEVMSAIFA
EVMQGKPEFTDHLTHKLKHHPGQIEAAAI
MEHILDGSAYVKAAQKLHEMDPLQKPKQDRYALRTSPQWLGPQIEVIRSST
KMIEREINSVNDNPLIDVSRNKAIHGGNF
QGTPIGVSMDNTRLAIAAIGKLMFAQFSELVNDFYNNGLPSNLSGGRNPSLD
YGFKGAEIAMASYCSELQFLANPVTNHV
QSAEQHNQDVNSLGLISSRKTSEAVEILKLMSTTFLVGLCQAIDLRHLEENLK
STVKNTVSSVAKRVLTMGVNGELHPSR
FCEKDLLRVVDREYIFAYIDDPCSATYPLMQKLRQTLVEHALKNGDNERNLS
TSIFQKIATFEDELKALLPKEVESARAA
LESGNPAIPNRIEECRSYPLYKFVRKELGTEYLTGEKVTSPGEEFEKVFIAMSK
GEIIDPLLECLESWNGAPLPIC

1W27:B|PDBID|CHAIN|SEQUENCE
MENGNGATTNGHVNGNGMDFCMKTEDPLYWGIAAEAMTGSHLDEVKKM
VAEYRKPVVKLGGETLTISQVAAISARDGSGV
TVELSEAARAGVKASSDWVMDSMNKGTDSYGVTTGFGATSHRRTKQGGAL
QKELIRFLNAGIFGNGSDNTLPHSATRAAM
LVRINTLLQGYSGIRFEILEAITKFLNQNITPCLPLRGTITASGDLVPLSYIAGLL
TGRPNSKAVGPTGVILSPEEAFKL
AGVEGGFFELQPKEGLALVNGTAVGSGMASMVLFEANILAVLAEVMSAIFA
EVMQGKPEFTDHLTHKLKHHPGQIEAAAI
MEHILDGSAYVKAAQKLHEMDPLQKPKQDRYALRTSPQWLGPQIEVIRSST
KMIEREINSVNDNPLIDVSRNKAIHGGNF
QGTPIGVSMDNTRLAIAAIGKLMFAQFSELVNDFYNNGLPSNLSGGRNPSLD
YGFKGAEIAMASYCSELQFLANPVTNHV
QSAEQHNQDVNSLGLISSRKTSEAVEILKLMSTTFLVGLCQAIDLRHLEENLK
STVKNTVSSVAKRVLTMGVNGELHPSR
FCEKDLLRVVDREYIFAYIDDPCSATYPLMQKLRQTLVEHALKNGDNERNLS
TSIFQKIATFEDELKALLPKEVESARAA
LESGNPAIPNRIEECRSYPLYKFVRKELGTEYLTGEKVTSPGEEFEKVFIAMSK
GEIIDPLLECLESWNGAPLPIC

Appendix 1b: Protein sequence of Glucose Oxidase (1GPE)

1GPE:A|PDBID|CHAIN|SEQUENCE
YLPAQQIDVQSSLLSDPSKVAGKTYDYIIAGGGLTGLTVAAKLTENPKIKVLV
IEKGFYESNDGAIIEDPNAYGQIFGTT
VDQNYLTVPLINNRTNNIKAGKGLGGSTLINGDSWTRPDKVQIDSWEKVFG
MEGWNWDNMFEYMKKAEAARTPTAAQLAA
GHSFNATCHGTNGTVQSGARDNGQPWSPIMKALMNTVSALGVPVQQDFLC
GHPRGVSMIMNNLDENQVRVDAARAWLLPN
YQRSNLEILTGQMVGKVLFKQTASGPQAVGVNFGTNKAVNFDVFAKHEVL
LAAGSAISPLILEYSGIGLKSVLDQANVTQ
LLDLPVGINMQDQTTTTVSSRASSAGAGQGQAVFFANFTETFGDYAPQARD
LLNTKLDQWAEETVARGGFHNVTALKVQY
ENYRNWLLDEDVAFAELFMDTEGKINFDLWDLIPFTRGSVHILSSDPYLWQF
ANDPKFFLNEFDLLGQAAASKLARDLTS
QGAMKEYFAGETLPGYNLVQNATLSQWSDYVLQNFRPNWHAVSSCSMMS
RELGGVVDATAKVYGTQGLRVIDGSIPPTQV
SSHVMTIFYGMALKVADAILDDYAKSA
>1GPE:B|PDBID|CHAIN|SEQUENCE
YLPAQQIDVQSSLLSDPSKVAGKTYDYIIAGGGLTGLTVAAKLTENPKIKVLV
IEKGFYESNDGAIIEDPNAYGQIFGTT
VDQNYLTVPLINNRTNNIKAGKGLGGSTLINGDSWTRPDKVQIDSWEKVFG
MEGWNWDNMFEYMKKAEAARTPTAAQLAA
GHSFNATCHGTNGTVQSGARDNGQPWSPIMKALMNTVSALGVPVQQDFLC
GHPRGVSMIMNNLDENQVRVDAARAWLLPN
YQRSNLEILTGQMVGKVLFKQTASGPQAVGVNFGTNKAVNFDVFAKHEVL
LAAGSAISPLILEYSGIGLKSVLDQANVTQ
LLDLPVGINMQDQTTTTVSSRASSAGAGQGQAVFFANFTETFGDYAPQARD
LLNTKLDQWAEETVARGGFHNVTALKVQY
ENYRNWLLDEDVAFAELFMDTEGKINFDLWDLIPFTRGSVHILSSDPYLWQF
ANDPKFFLNEFDLLGQAAASKLARDLTS
QGAMKEYFAGETLPGYNLVQNATLSQWSDYVLQNFRPNWHAVSSCSMMS
RELGGVVDATAKVYGTQGLRVIDGSIPPTQV
SSHVMTIFYGMALKVADAILDDYAKSA

Appendix 1c: Protein properties for 1GPE

Electrostatic Energy (KJ/mol	Relative Folding Energy	Electrostatic Energy (KJ/mol	Relative Folding Energy
-42 699.80	-1272.63	-40 419.80	-1058.66
-42 626.84	-1272.65	-40 372.85	-1047.89
-42 553.87	-1272.65	-40 326.46	-1037.37
-42 480.92	-1272.66	-40 280.62	-1027.13
-42 407.99	-1272.68	-40 235.29	-1017.14
-42 335.08	-1272.71	-40 190.44	-1007.36
-42 262.20	-1272.74	-40 146.05	-997.73
-42 189.39	-1272.81	-40 102.08	-988.15
-42 116.67	-1272.91	-40 058.54	-978.51
-42 044.08	-1273.04	-40 015.42	-968.64
-41 971.68	-1273.21	-39 972.73	-958.33
-41 899.56	-1273.43	-39 930.49	-947.29
-41 827.82	-1273.68	-39 888.75	-935.19
-41 756.58	-1273.88	-39 847.55	-921.67
-41 685.99	-1273.91	-39 807	-906.45
-41 616.19	-1273.54	-39 767.09	-889.36
-41 547.30	-1272.42	-39 728.00	-870.38
-41 479.45	-1270.13	-39 689.78	-849.67
-41 412.77	-1266.28	-39 652.52	-827.55
-41 347.38	-1260.56	-39 616.28	-804.39
-41 283.35	-1252.82	-39 581.13	-780.56
-41 220.72	-1243.16	-39 547.12	-756.35
-41 159.50	-1231.83	-39 514.27	-731.91
-41 099.66	-1219.23	-39 482.60	-707.3
-41 041.16	-1205.82	-39 452.09	-682.54
-40 983.98	-1192.09	-39 422.73	-657.68
-40 928.03	-1178.37	-39 394.47	-632.77
-40 873.23	-1164.91	-39 367.26	-607.97
-40 819.51	-1151.86	-39 341.04	-583.42
-40 766.78	-1139.26	-39 315.74	-559.24
-40 714.96	-1127.06	-39 291.30	-535.53
-40 663.98	-1115.2	-39 267.67	-512.38
-40 613.77	-1103.58	-39 244.81	-489.83
-40 564.29	-1092.14	-39222.69	-467.9
-40 515.50	-1080.83		
-40 467.34	-1069.65		

Appendix 1c. Protein properties for 1GPE continued…

1c (i): Graph of Electrostatic energy and Relative Folding energy against pH

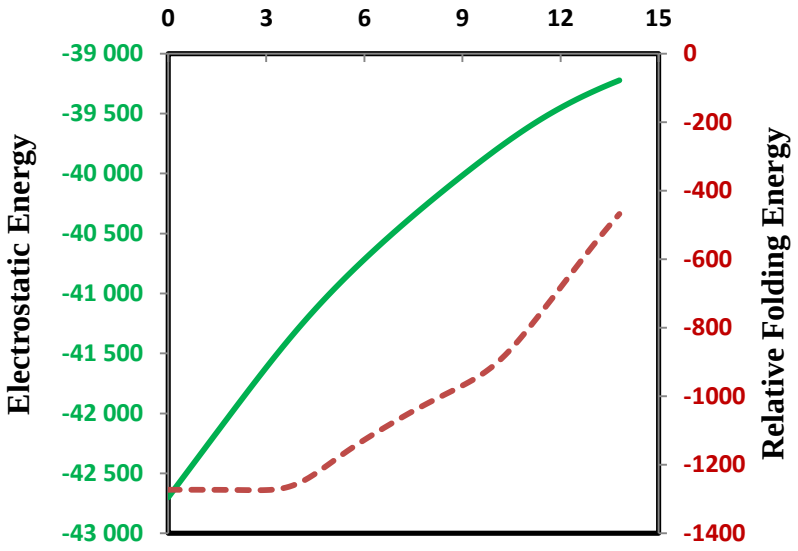

1c (ii): Graph of Total Charge and Relative Folding energy against pH

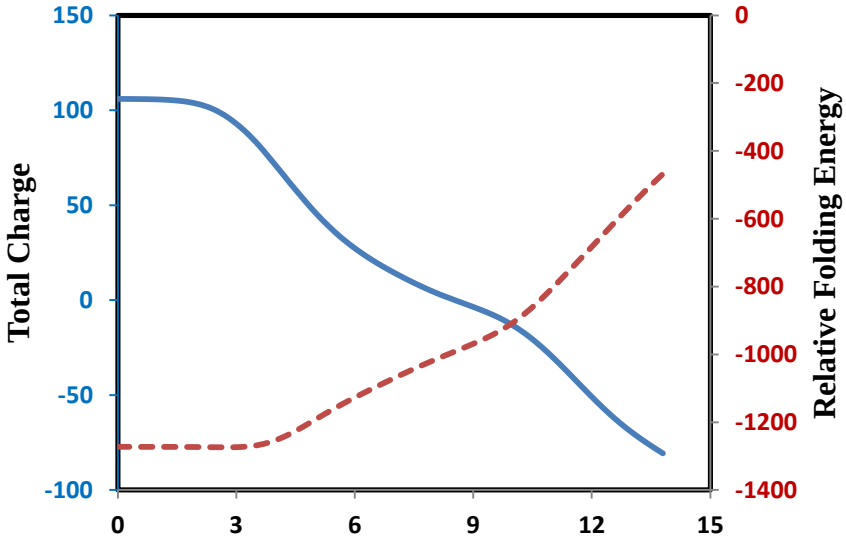

Appendix 1d. List of calculated pKa values of each residue in 1GPE protein

Number	Residues	pKa	Number	Residues	pKa
1	A:TYR1_NTR	9.591	35	A:ASP552	7.971
2	B:TYR1_NTR	10.05	36	A:ASP577	4.211
3	A:ASP8	4.414	37	A:ASP581	3.507
4	A:ASP16	4.9	38	A:ASP582	2.71
5	A:ASP26	3.315	39	B:ASP8	4.473
6	A:ASP63	8.811	40	B:ASP16	4.54
7	A:ASP69	4.665	41	B:ASP26	3.106
8	A:ASP82	8.029	42	B:ASP63	9.036
9	A:ASP113	11.159	43	B:ASP69	4.566
10	A:ASP119	6.623	44	B:ASP82	7.385
11	A:ASP124	4.201	45	B:ASP113	11.217
12	A:ASP138	3.115	46	B:ASP119	7.194
13	A:ASP181	4.865	47	B:ASP124	3.715
14	A:ASP207	6.436	48	B:ASP138	4.059
15	A:ASP224	3.674	49	B:ASP181	5.244
16	A:ASP231	7.571	50	B:ASP207	6.083
17	A:ASP282	3.959	51	B:ASP224	3.678
18	A:ASP314	3.409	52	B:ASP231	7.613
19	A:ASP323	3.811	53	B:ASP282	4.106
20	A:ASP332	9.247	54	B:ASP314	3.648
21	A:ASP364	3.157	55	B:ASP323	3.819
22	A:ASP371	3.885	56	B:ASP332	9.494
23	A:ASP378	2.922	57	B:ASP364	3.049
24	A:ASP409	4.05	58	B:ASP371	3.811
25	A:ASP411	3.492	59	B:ASP378	2.67
26	A:ASP420	6.409	60	B:ASP409	3.839
27	A:ASP428	5.023	61	B:ASP411	3.607
28	A:ASP431	12.107	62	B:ASP420	6.869
29	A:ASP446	6.726	63	B:ASP428	5.121
30	A:ASP455	6.083	64	B:ASP431	12.131
31	A:ASP464	9.901	65	B:ASP446	7.767
32	A:ASP477	4.329	66	B:ASP455	6.271
33	A:ASP509	3.492	67	B:ASP464	10.105
34	A:ASP537	4.692	68	B:ASP477	4.284

Number	Residues	pKa	Number	Residues	pKa
69	B:ASP509	3.612	105	B:GLU148	6.441
70	B:ASP537	4.559	106	B:GLU225	3.862
71	B:ASP552	8.049	107	B:GLU247	5.309
72	B:ASP577	4.423	108	B:GLU288	6.049
73	B:ASP581	3.662	109	B:GLU303	8.125
74	B:ASP582	2.535	110	B:GLU360	7.716
75	A:GLU45	3.887	111	B:GLU382	4.712
76	A:GLU55	10.882	112	B:GLU383	4.801
77	A:GLU60	13.657	113	B:GLU401	4.282
78	A:GLU68	6.064	114	B:GLU410	5.35
79	A:GLU127	3.973	115	B:GLU416	11.589
80	A:GLU133	3.685	116	B:GLU422	6.641
81	A:GLU142	3.739	117	B:GLU462	4.956
82	A:GLU148	6.313	118	B:GLU486	4.393
83	A:GLU225	4.021	119	B:GLU491	5.86
84	A:GLU247	5.16	120	B:GLU531	4.316
85	A:GLU288	5.62	121	A:TYR1	14.2
86	A:GLU303	8.053	122	A:TYR25	14.2
87	A:GLU360	5.357	123	A:TYR27	14.2
88	A:GLU382	4.839	124	A:TYR59	14.2
89	A:GLU383	5.037	125	A:TYR73	14.2
90	A:GLU401	4.573	126	A:TYR85	14.2
91	A:GLU410	5.136	127	A:TYR143	13.632
92	A:GLU416	11.281	128	A:TYR241	11.819
93	A:GLU422	5.983	129	A:TYR304	14.2
94	A:GLU462	4.525	130	A:TYR365	11.446
95	A:GLU486	4.629	131	A:TYR400	14.2
96	A:GLU491	5.575	132	A:TYR403	14.2
97	A:GLU531	4.473	133	A:TYR448	14.2
98	B:GLU45	3.609	134	A:TYR487	12.33
99	B:GLU55	10.931	135	A:TYR496	10.102
100	B:GLU60	13.629	136	A:TYR510	14.2
101	B:GLU68	6.697	137	A:TYR543	14.2
102	B:GLU127	4.47	138	A:TYR569	14.2
103	B:GLU133	3.78	139	A:TYR583	13.188
104	B:GLU142	3.895	140	B:TYR1	14.2

Number	Residues	pKa	Number	Residues	pKa
141	B:TYR25	14.2	177	A:LYS19	11.091
142	B:TYR27	14.2	178	A:LYS23	12.363
143	B:TYR59	14.2	179	A:LYS42	13.112
144	B:TYR73	14.2	180	A:LYS48	10.58
145	B:TYR85	14.2	181	A:LYS50	10.76
146	B:TYR143	13.849	182	A:LYS56	14.2
147	B:TYR241	13.631	183	A:LYS99	14.2
148	B:TYR304	14.2	184	A:LYS102	14.2
149	B:TYR365	11.63	185	A:LYS120	13.648
150	B:TYR400	14.2	186	A:LYS128	11.697
151	B:TYR403	14.2	187	A:LYS145	11.656
152	B:TYR448	14.2	188	A:LYS146	10.777
153	B:TYR487	12.579	189	A:LYS191	12.255
154	B:TYR496	10.69	190	A:LYS256	13.141
155	B:TYR510	14.2	191	A:LYS260	10.969
156	B:TYR543	14.2	192	A:LYS277	14.2
157	B:TYR569	14.2	193	A:LYS286	11.663
158	B:TYR583	13.872	194	A:LYS310	11.843
159	A:CYS525	14.2	195	A:LYS376	12.301
160	B:CYS525	14.2	196	A:LYS397	11.928
161	A:HIS162	12.263	197	A:LYS424	11.168
162	A:HIS169	12.014	198	A:LYS457	14.2
163	A:HIS212	9.641	199	A:LYS473	11.83
164	A:HIS287	8.604	200	A:LYS485	10.81
165	A:HIS391	7.425	201	A:LYS541	11.691
166	A:HIS441	9.898	202	A:LYS574	14.2
167	A:HIS520	13.083	203	A:LYS585	11.362
168	A:HIS563	14.2	204	B:LYS19	11.23
169	B:HIS162	11.978	205	B:LYS23	12.734
170	B:HIS169	11.287	206	B:LYS42	12.34
171	B:HIS212	10.302	207	B:LYS48	10.557
172	B:HIS287	8.659	208	B:LYS50	10.919
173	B:HIS391	7.571	209	B:LYS56	14.2
174	B:HIS441	10.291	210	B:LYS99	14.2
175	B:HIS520	14.2	211	B:LYS102	14.2
176	B:HIS563	14.2	212	B:LYS120	13.217

Number	Residues	pKa	Number	Residues	pKa
213	B:LYS128	11.406	249	B:ARG117	14.2
214	B:LYS145	11.595	250	B:ARG151	14.2
215	B:LYS146	12.039	251	B:ARG180	14.2
216	B:LYS191	12.186	252	B:ARG214	14.2
217	B:LYS256	13.358	253	B:ARG229	14.2
218	B:LYS260	12.459	254	B:ARG234	14.2
219	B:LYS277	14.2	255	B:ARG243	14.2
220	B:LYS286	10.783	256	B:ARG341	14.2
221	B:LYS310	12.523	257	B:ARG370	13.648
222	B:LYS376	12.123	258	B:ARG387	14.2
223	B:LYS397	11.953	259	B:ARG404	14.2
224	B:LYS424	11.194	260	B:ARG437	14.2
225	B:LYS457	14.2	261	B:ARG476	14.2
226	B:LYS473	12.378	262	B:ARG516	14.2
227	B:LYS485	10.74	263	B:ARG530	14.2
228	B:LYS541	11.84	264	B:ARG549	14.2
229	B:LYS574	14.2	265	A:ALA587_CTR	3.625
230	B:LYS585	11.27	266	B:ALA587_CTR	3.717
231	A:ARG94	14.2			
232	A:ARG117	14.2			
233	A:ARG151	14.2			
234	A:ARG180	14.2			
235	A:ARG214	14.2			
236	A:ARG229	14.2			
237	A:ARG234	14.2			
238	A:ARG243	14.2			
239	A:ARG341	14.2			
240	A:ARG370	14.2			
241	A:ARG387	14.2			
242	A:ARG404	14.2			
243	A:ARG437	14.2			
244	A:ARG476	14.2			
245	A:ARG516	14.2			
246	A:ARG530	14.2			
247	A:ARG549	14.2			
248	B:ARG94	14.2			

Appendix 2: Glassy Carbon Electrode Voltammograms

A1: Bare GCE, CV Voltammograms

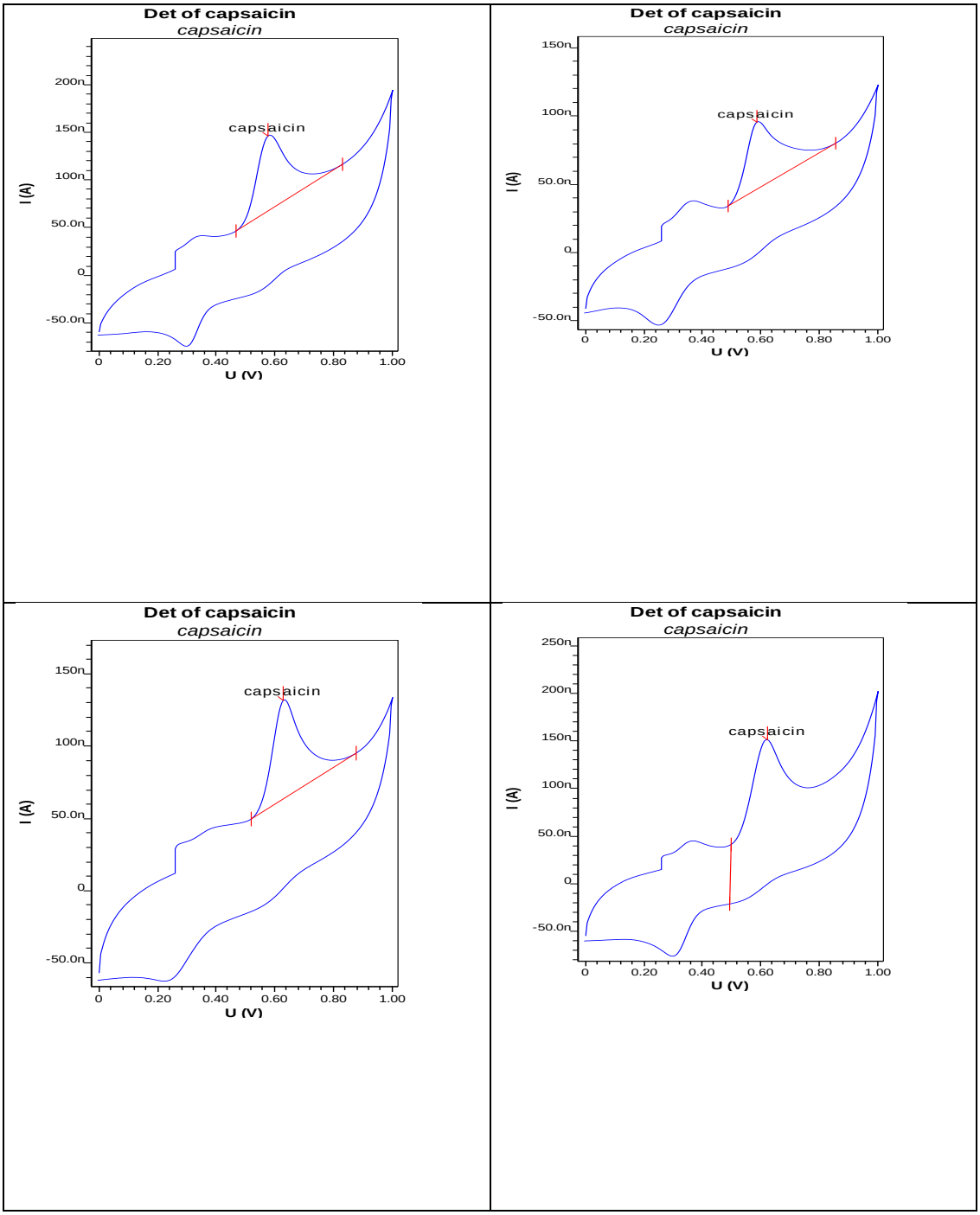

A2: Bare GCE, DPV Voltammograms

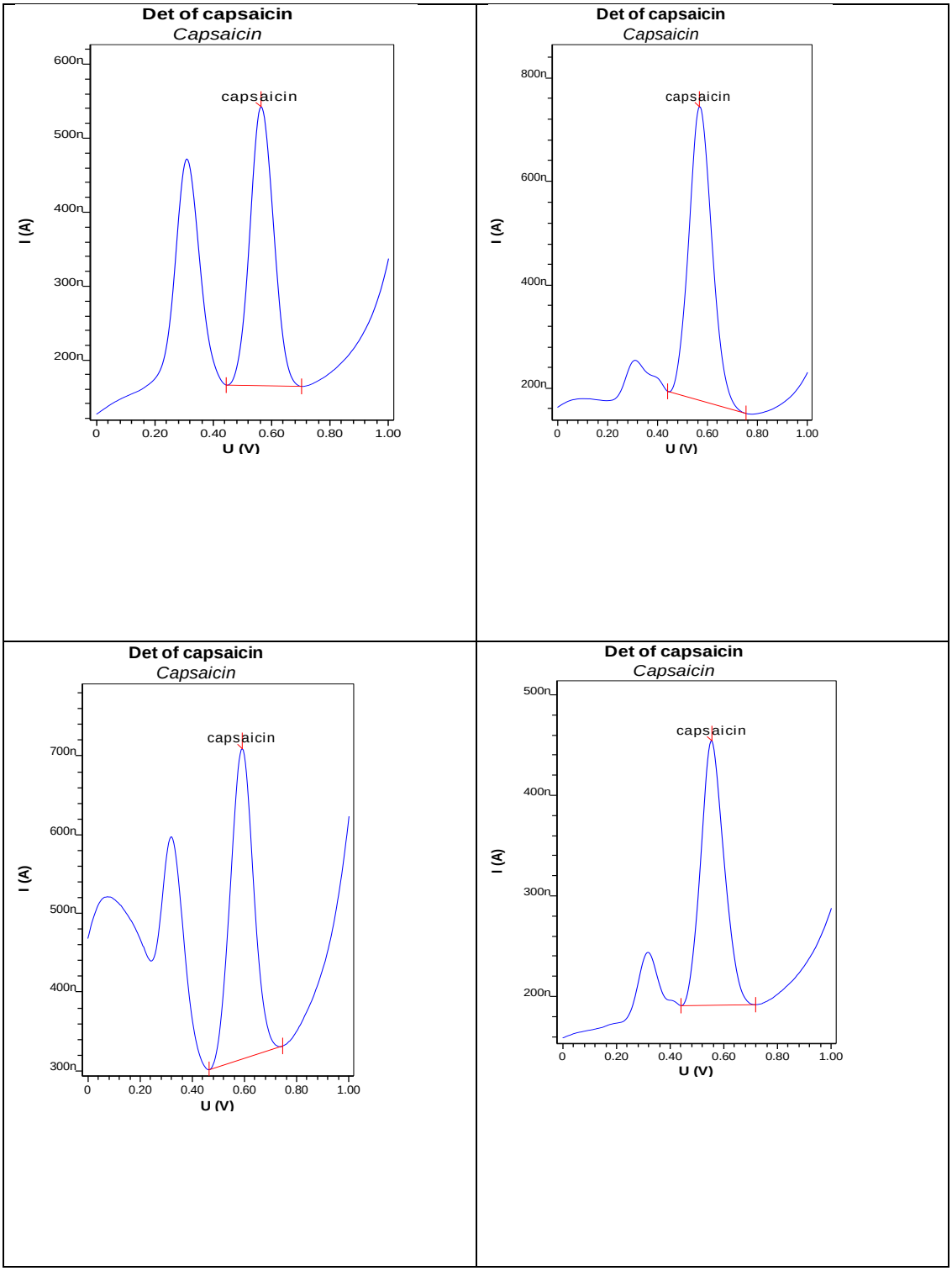

B1: GCE- MWCNT, CV Voltammograms

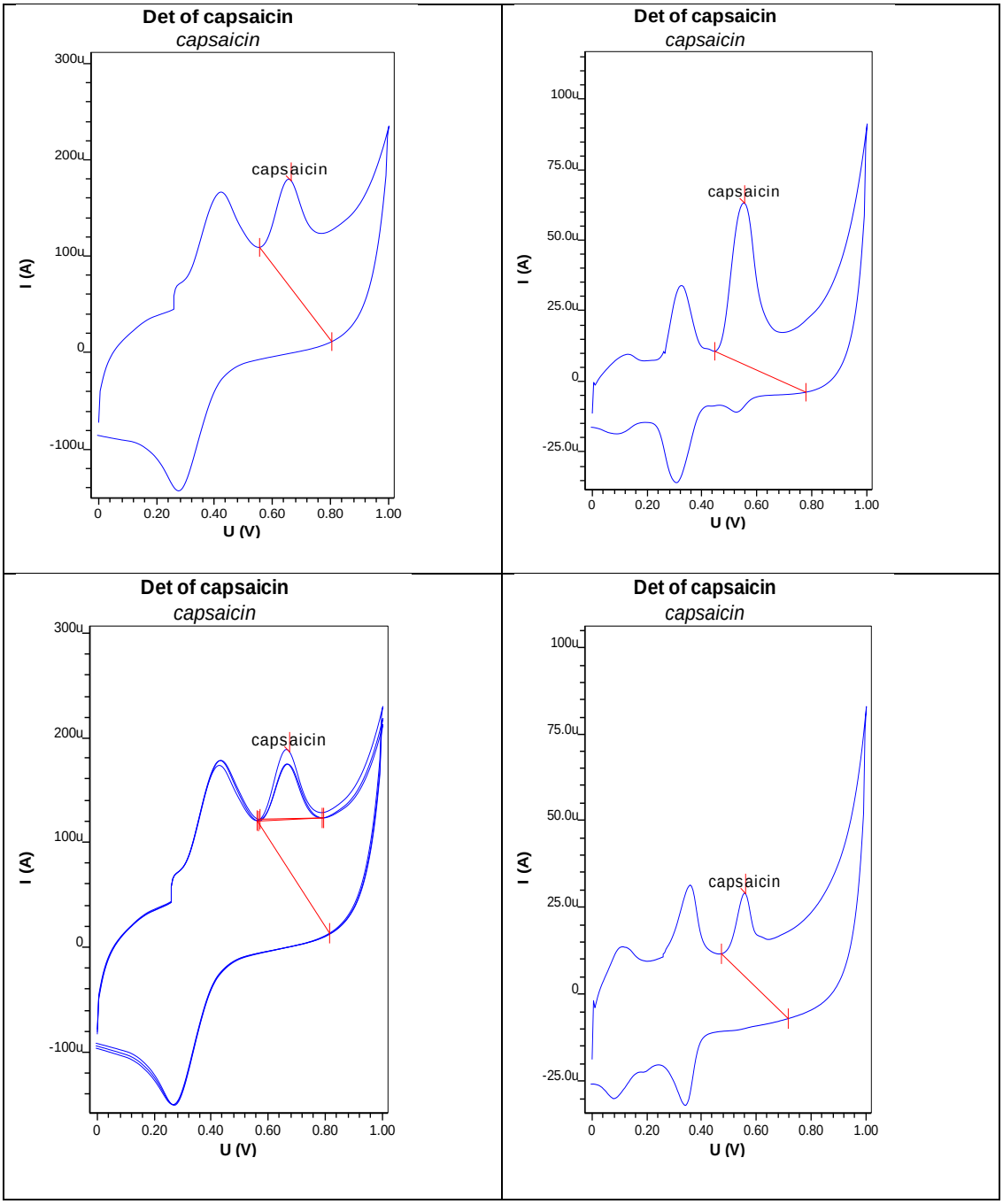

B2: GCE- MWCNT, DPV Voltammograms

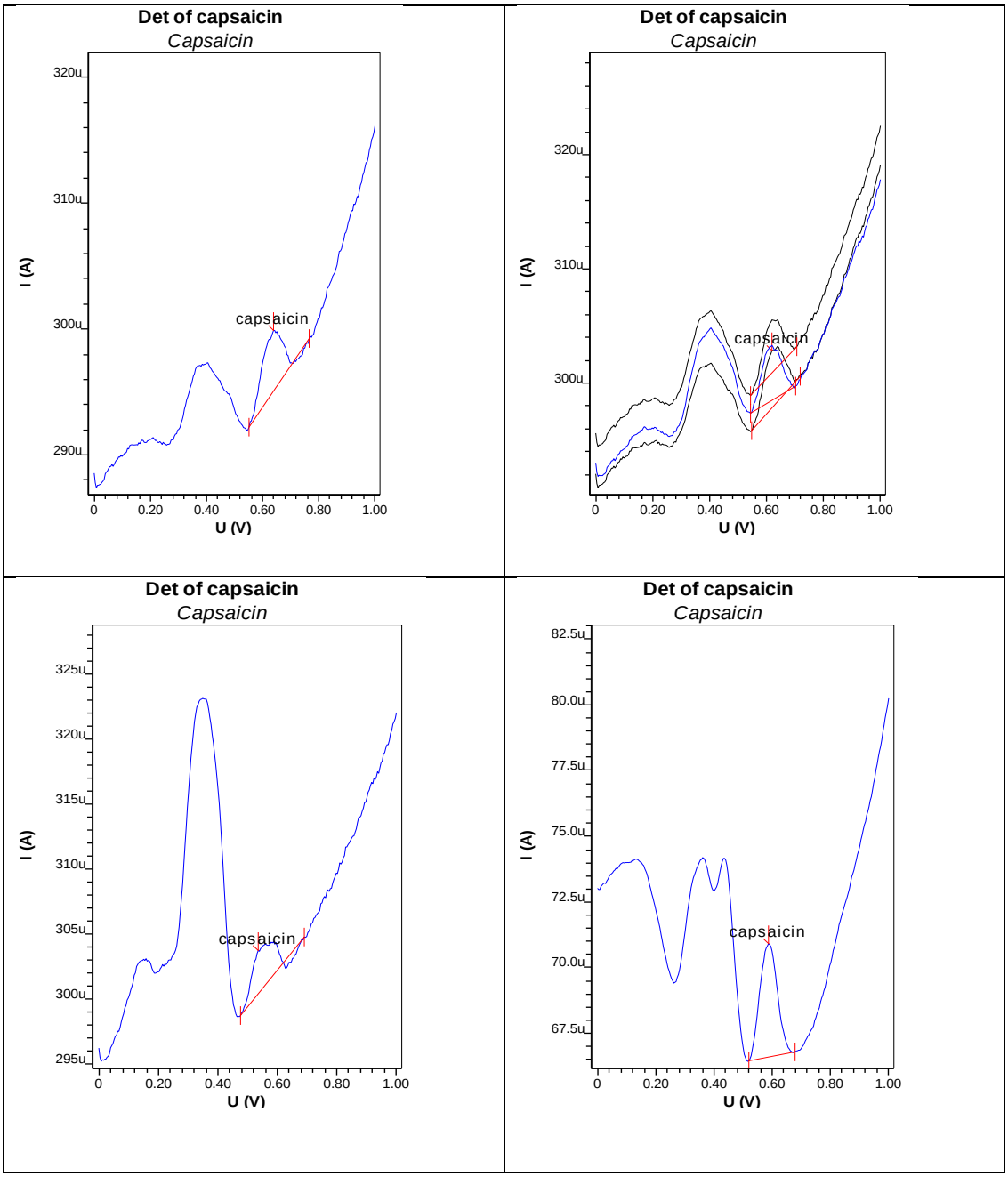

C1: GCE- MWCNT- GOx, CV Voltammograms

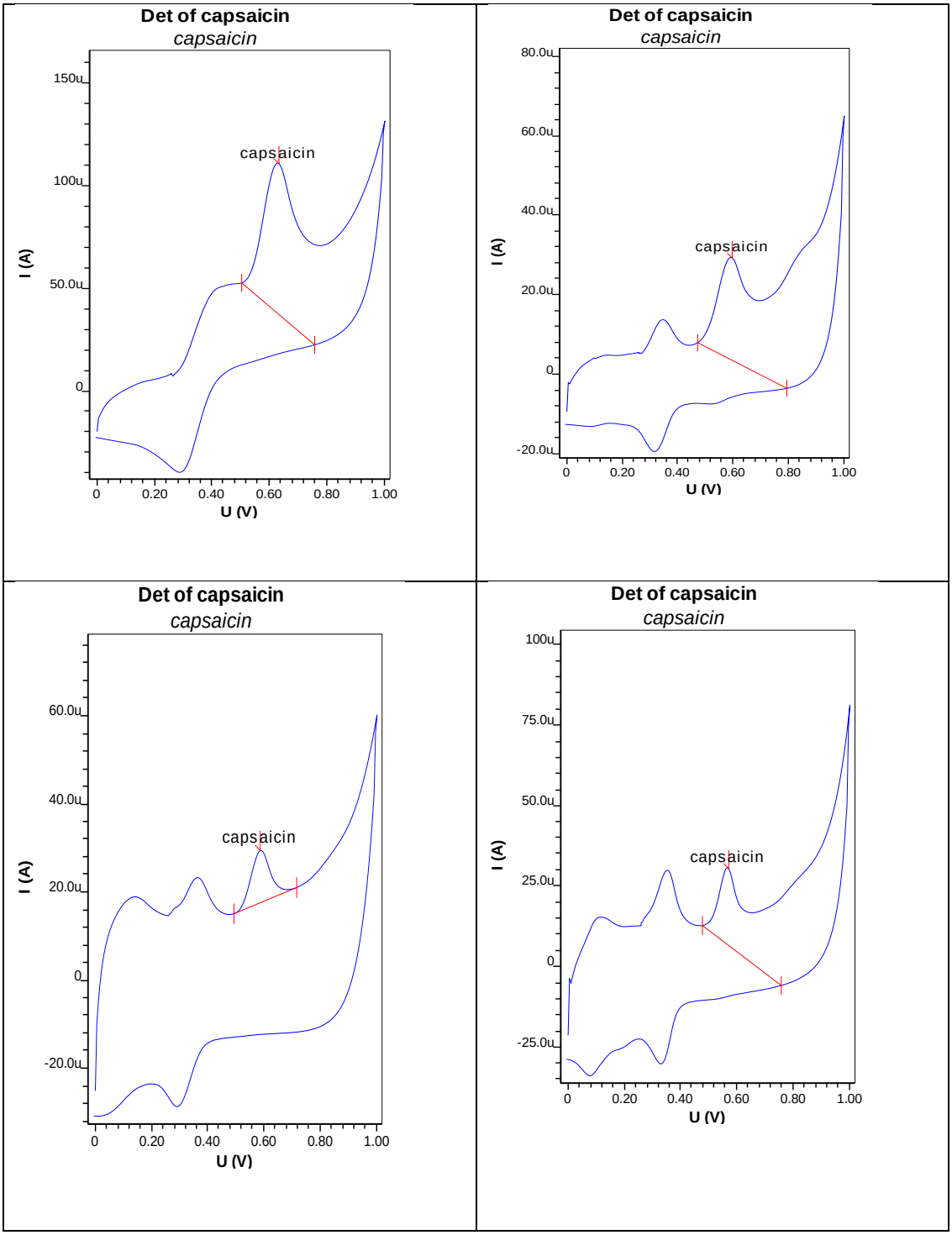

C2: GCE- MWCNT- GOx, DPV Voltammograms

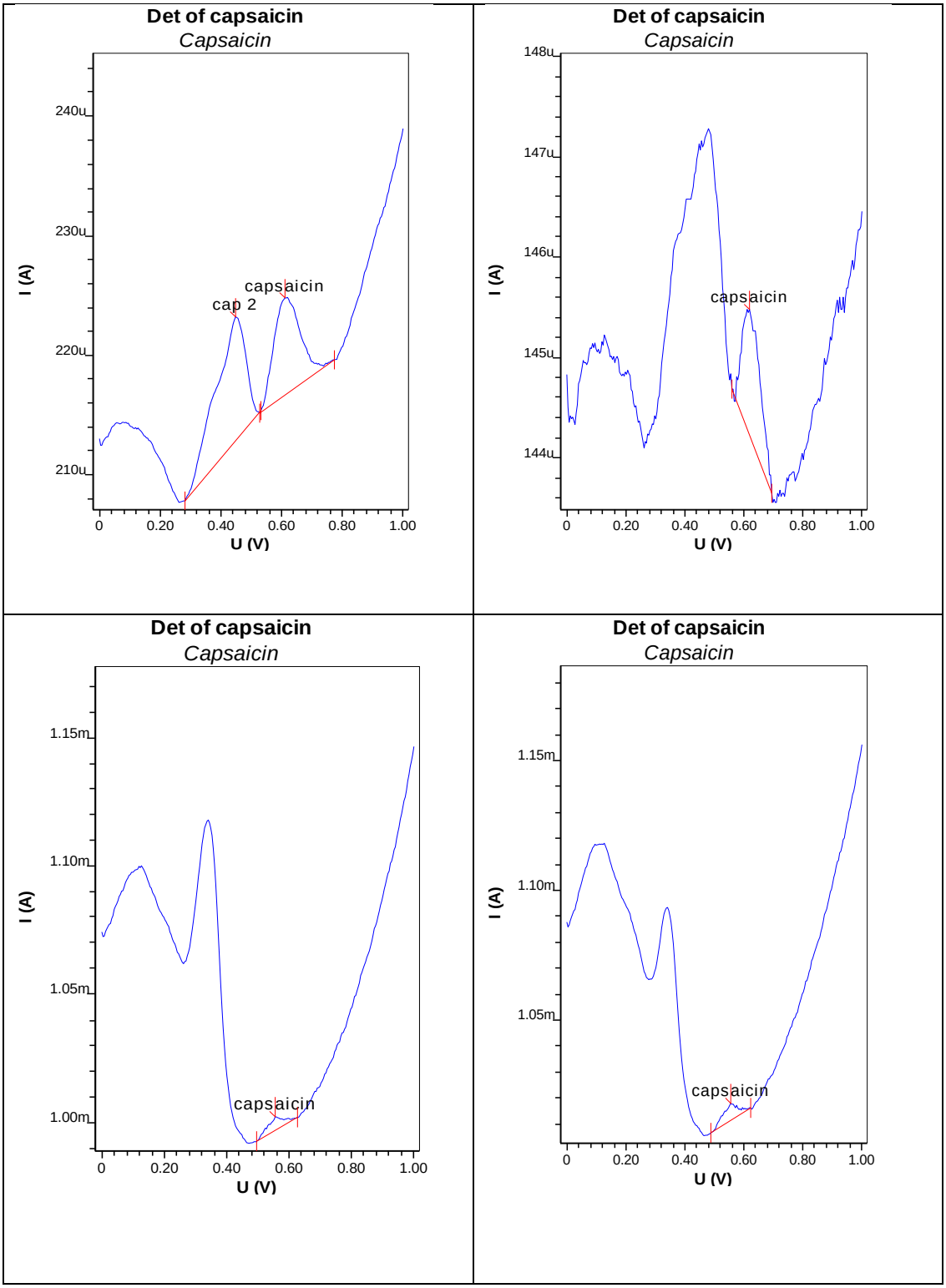

D1: GCE- MWCNT- PAL, CV Voltammograms

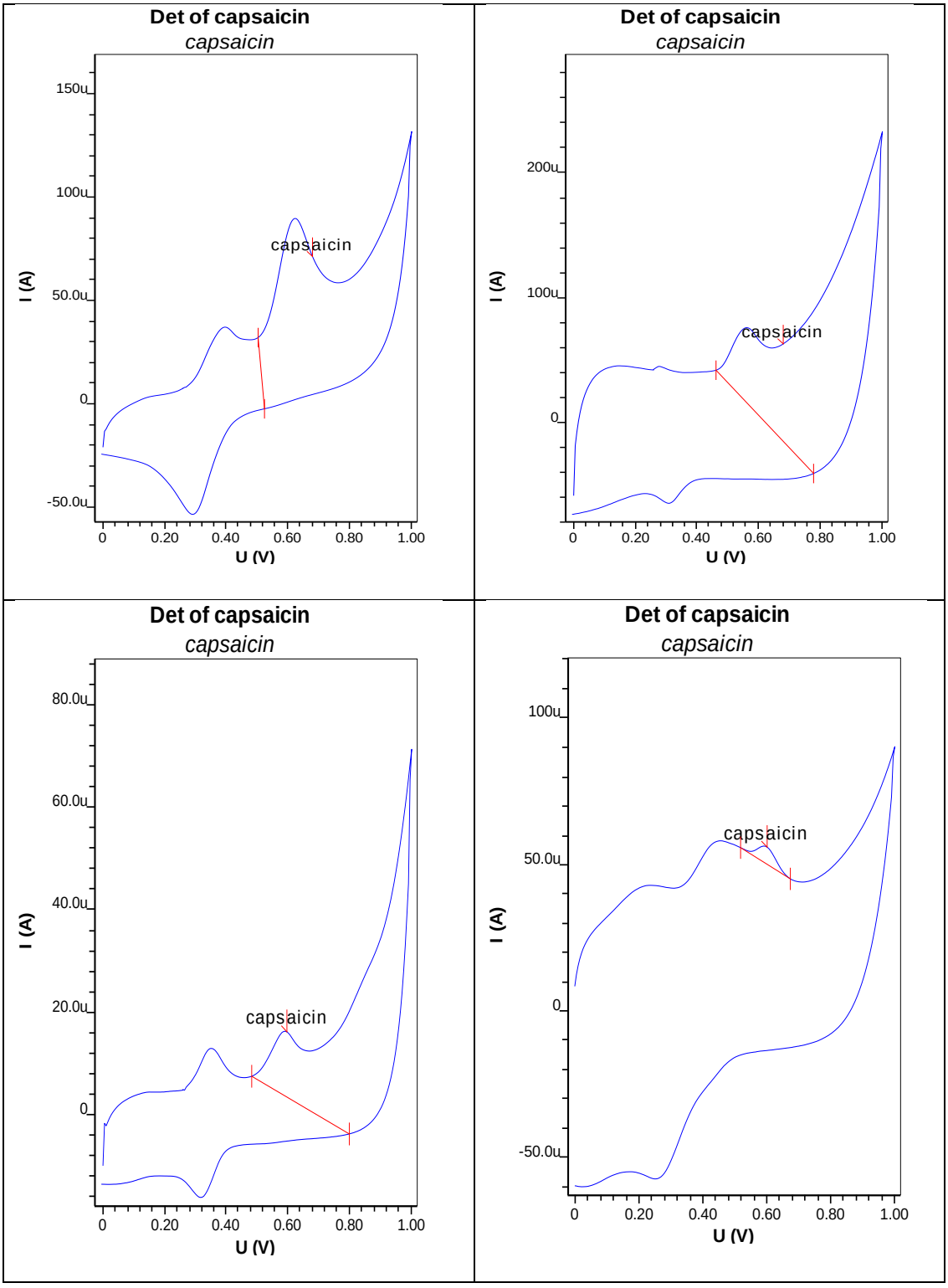

D2: GCE- MWCNT- PAL, DPV Voltammograms

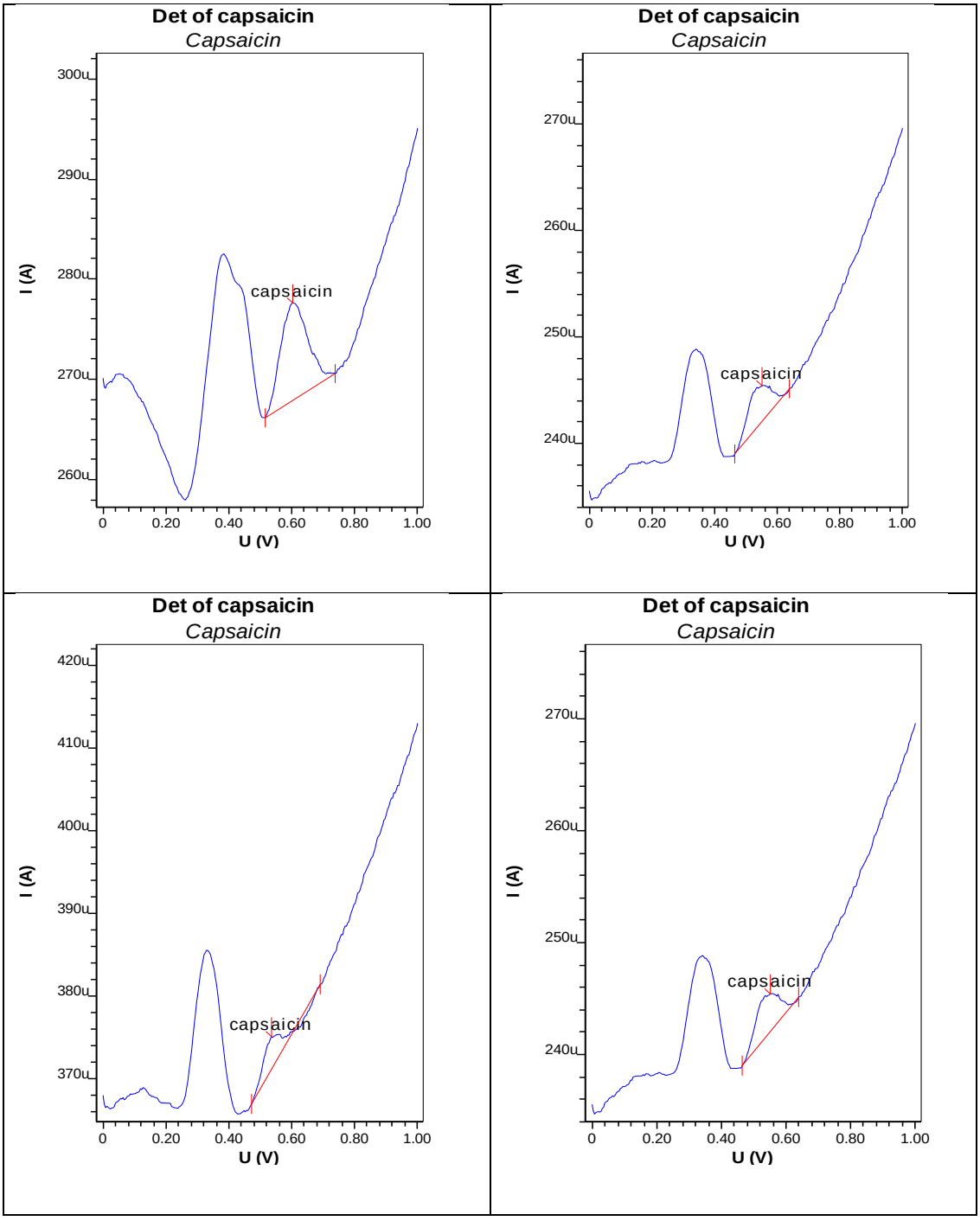

Appendix 3 Platinum Electrode Voltammograms

A1: Bare Pt-E, CV Voltammograms

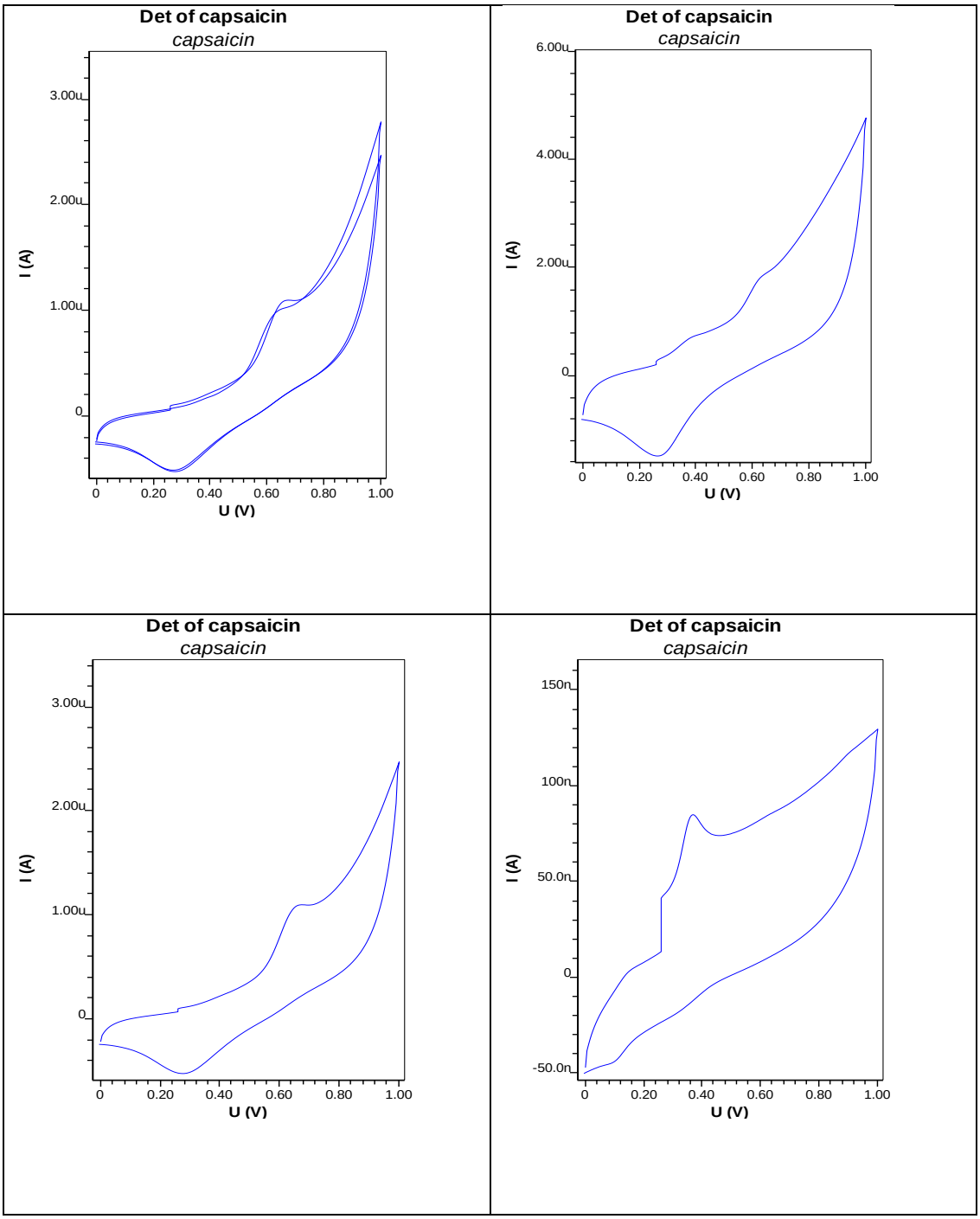

A2: Bare Pt-E, DPV Voltammograms

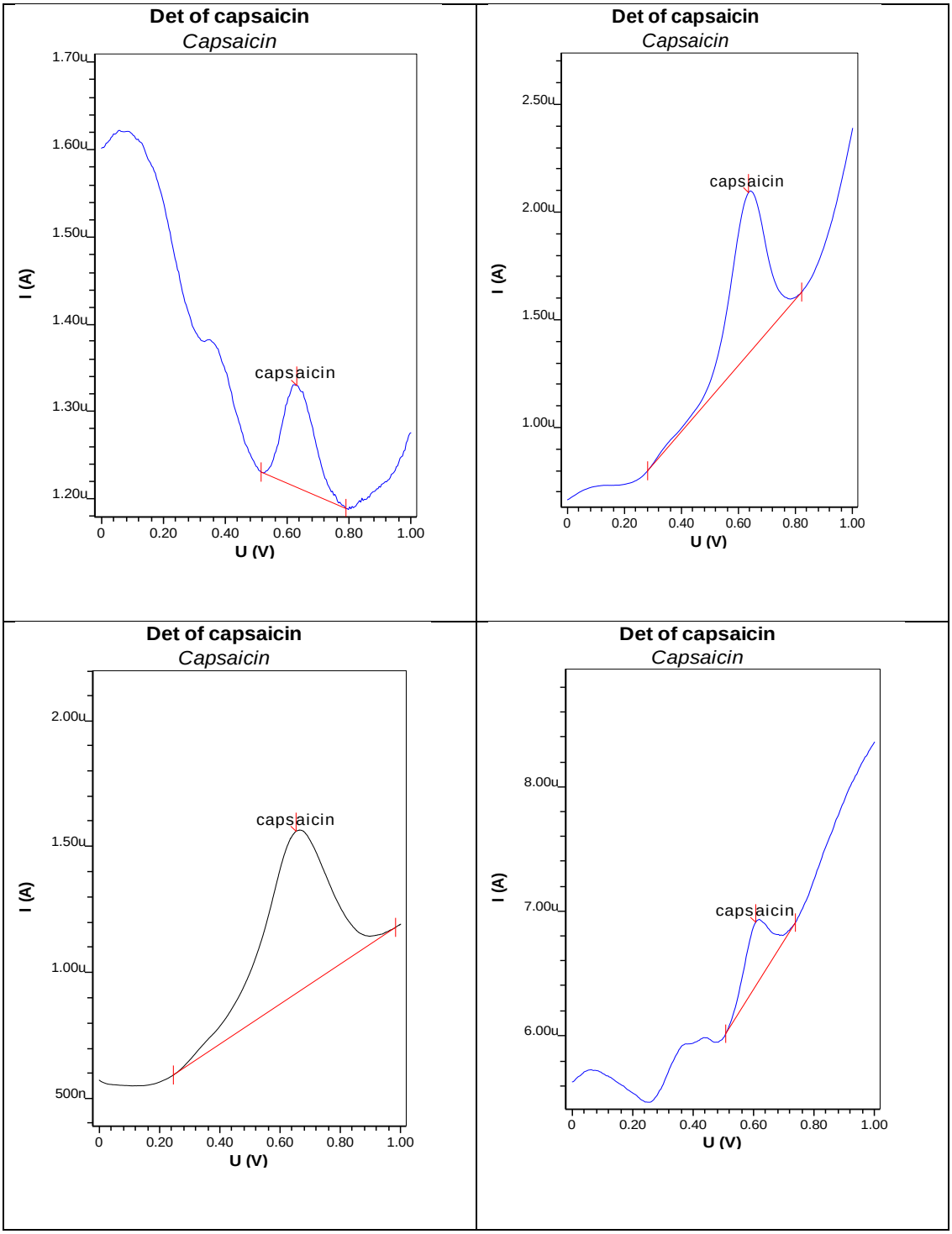

B1: Pt-E- MWCNT, CV Voltammograms

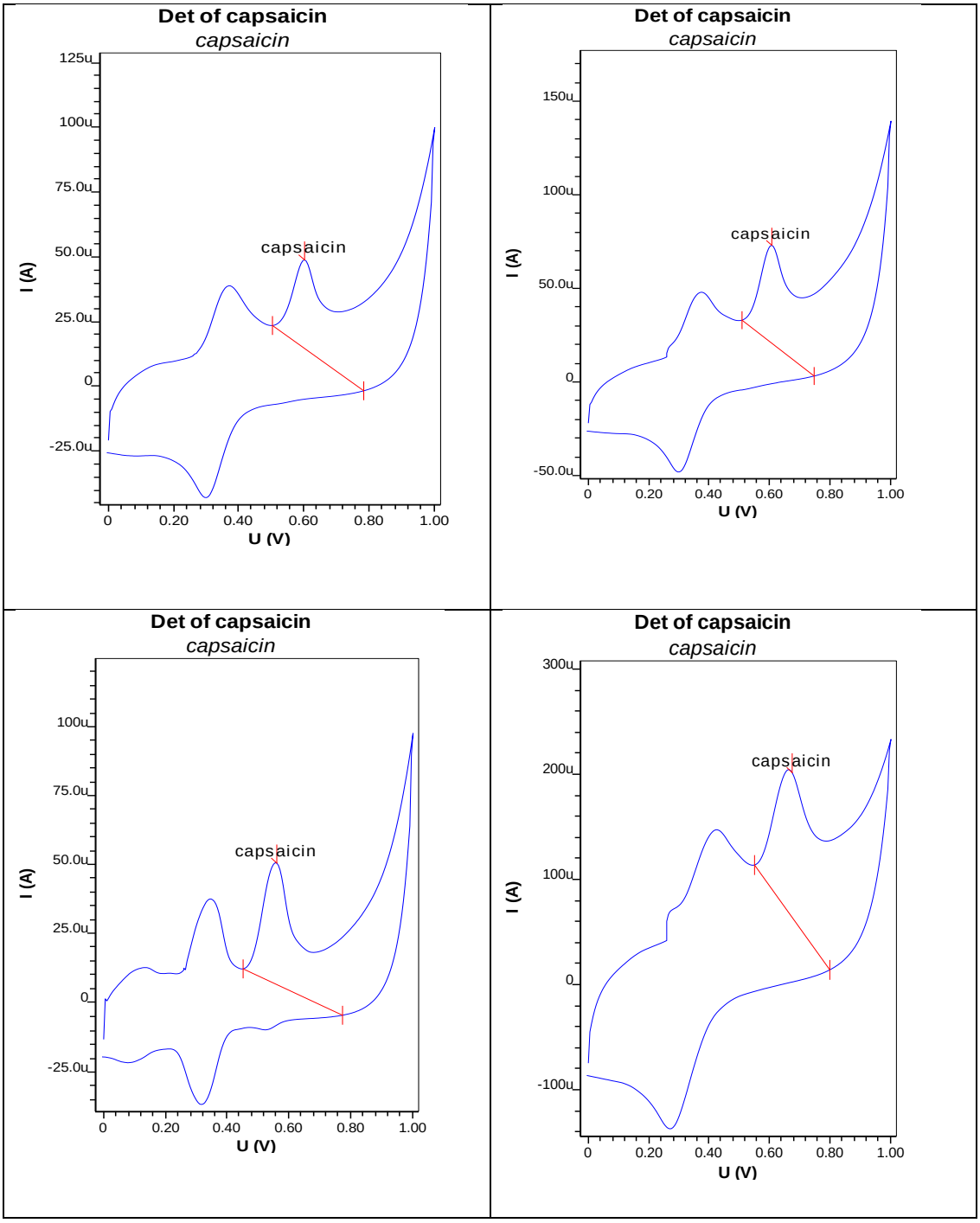

B2: Pt-E – MWCNT, DPV Voltammograms

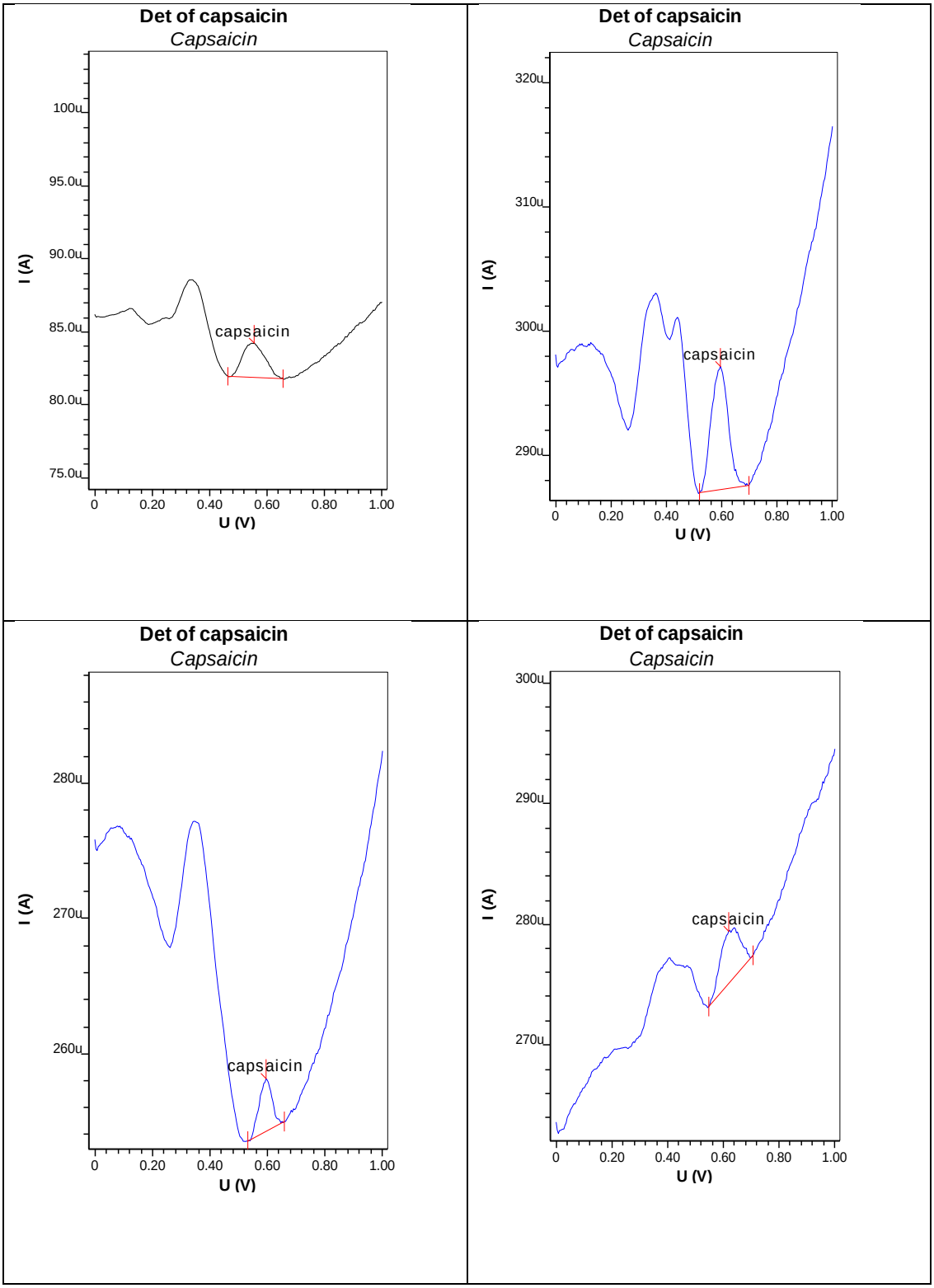

C1: Pt-E – MWCNT- GOx, CV Voltammograms

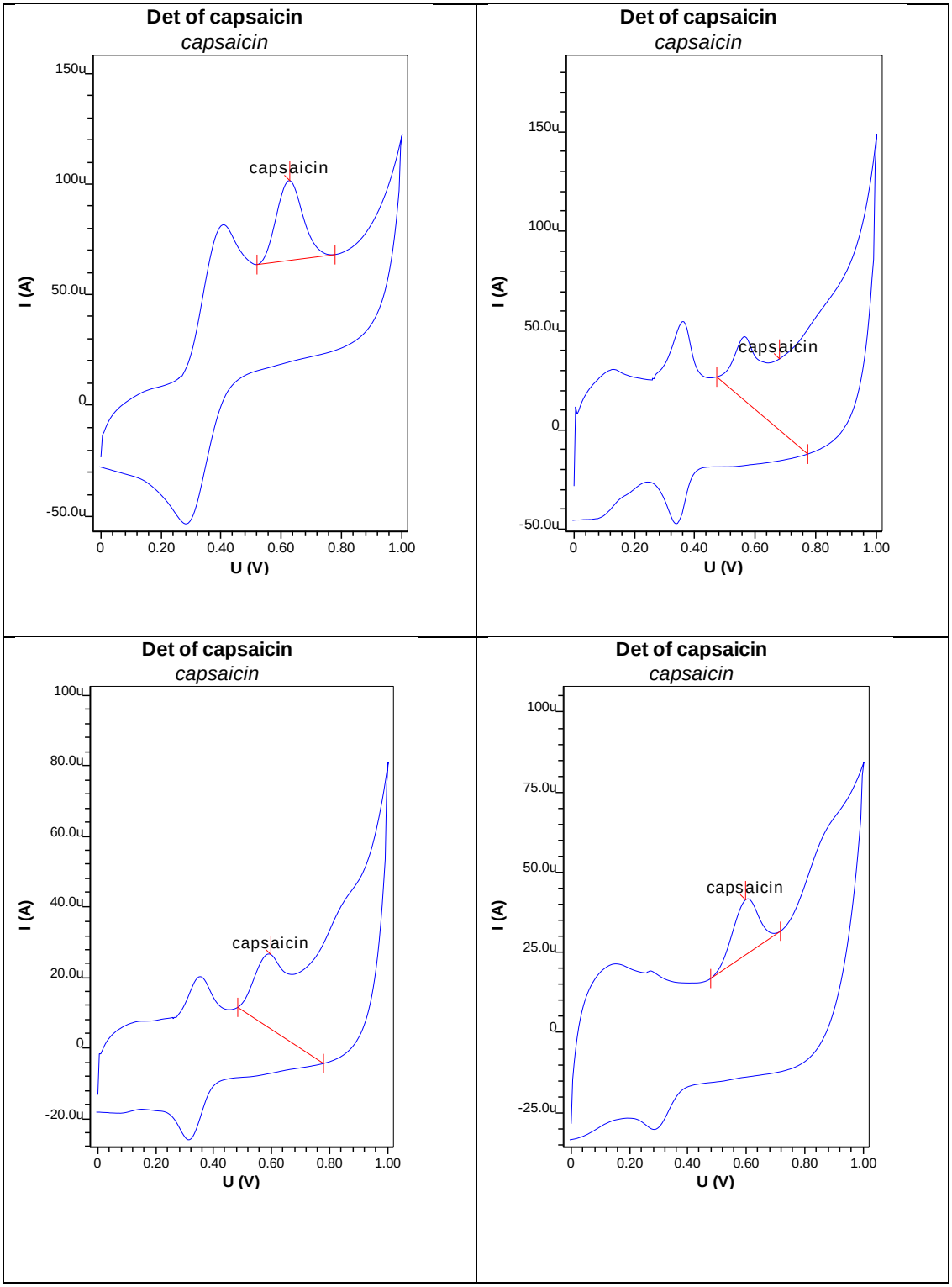

C2: Pt-E – MWCNT- GOx, DPV Voltammograms

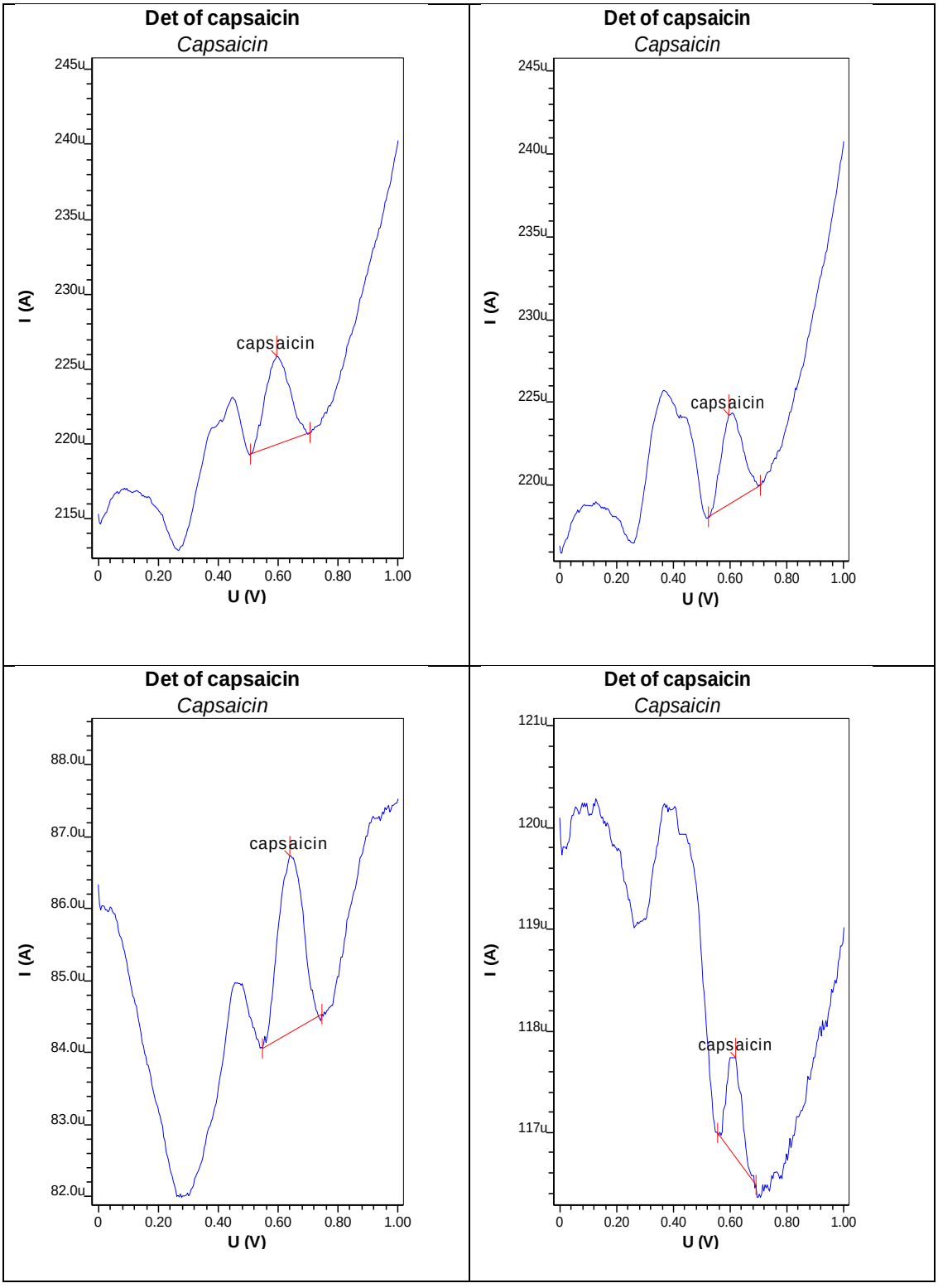

D1: Pt-E – MWCNT – PAL, CV Voltammograms

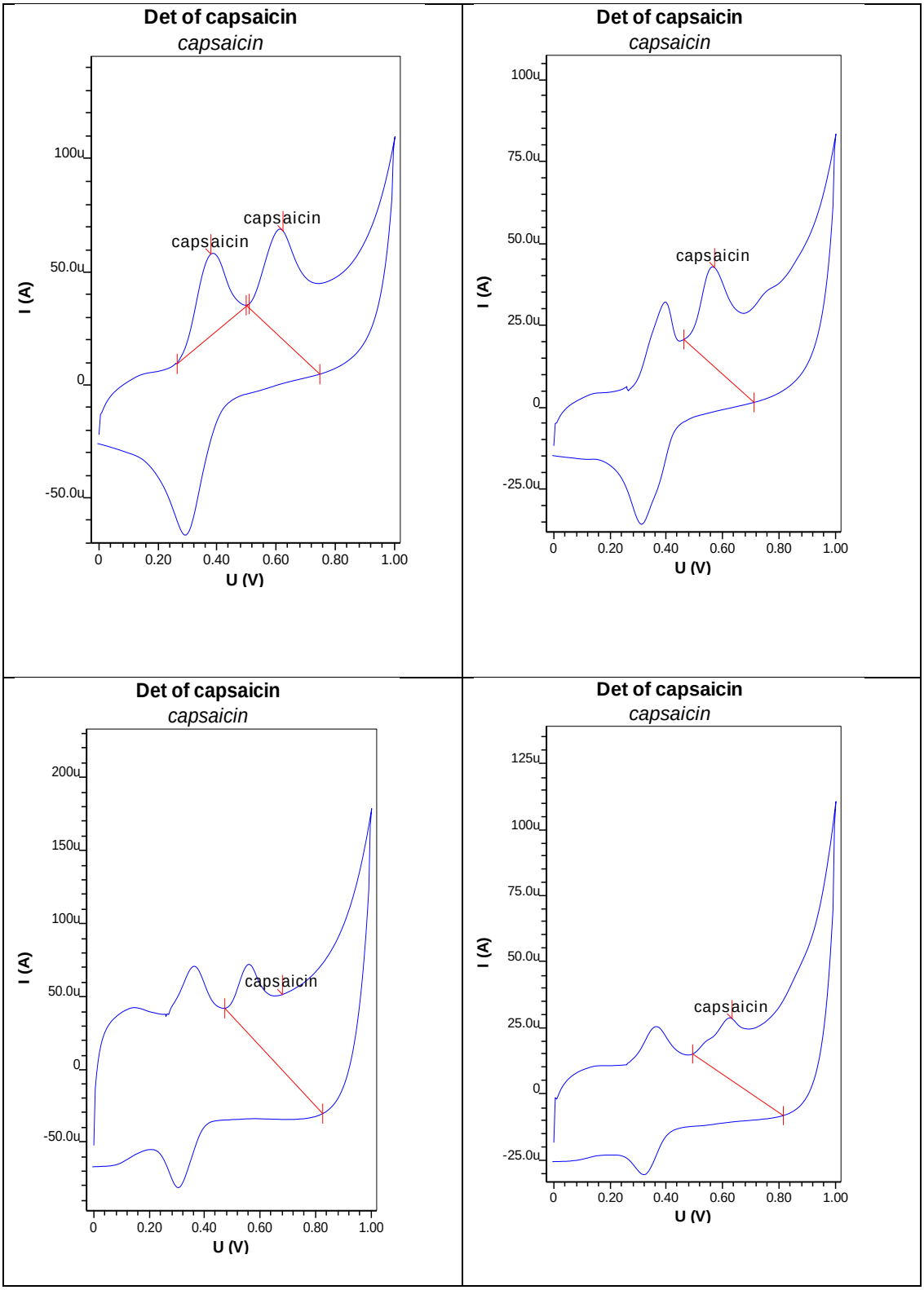

D2: Pt-E – MWCNT – PAL, DPV Voltammograms

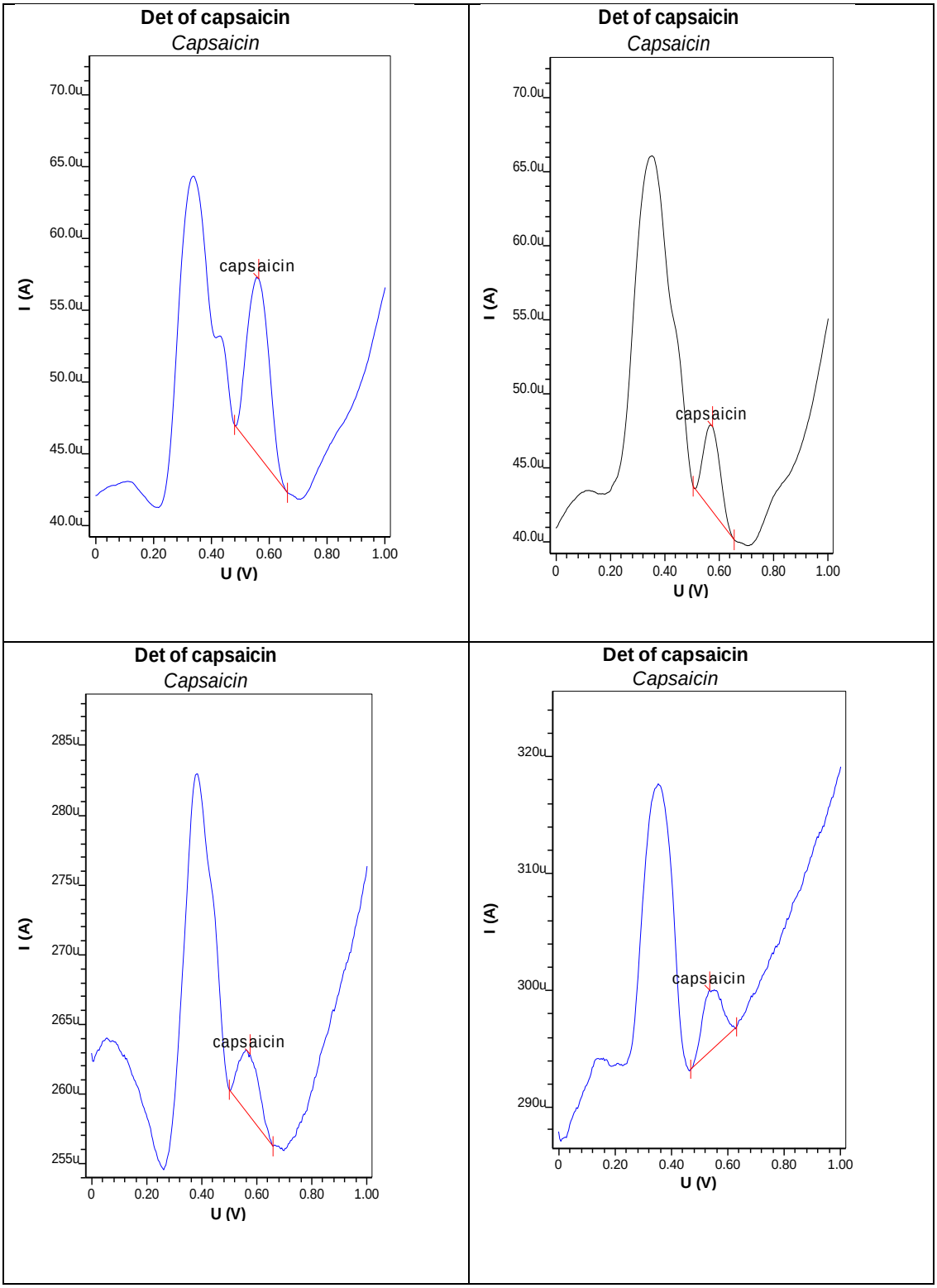

Appendix 4: Gold Electrode Voltammograms

A1: Bare Au-E, CV Voltammograms

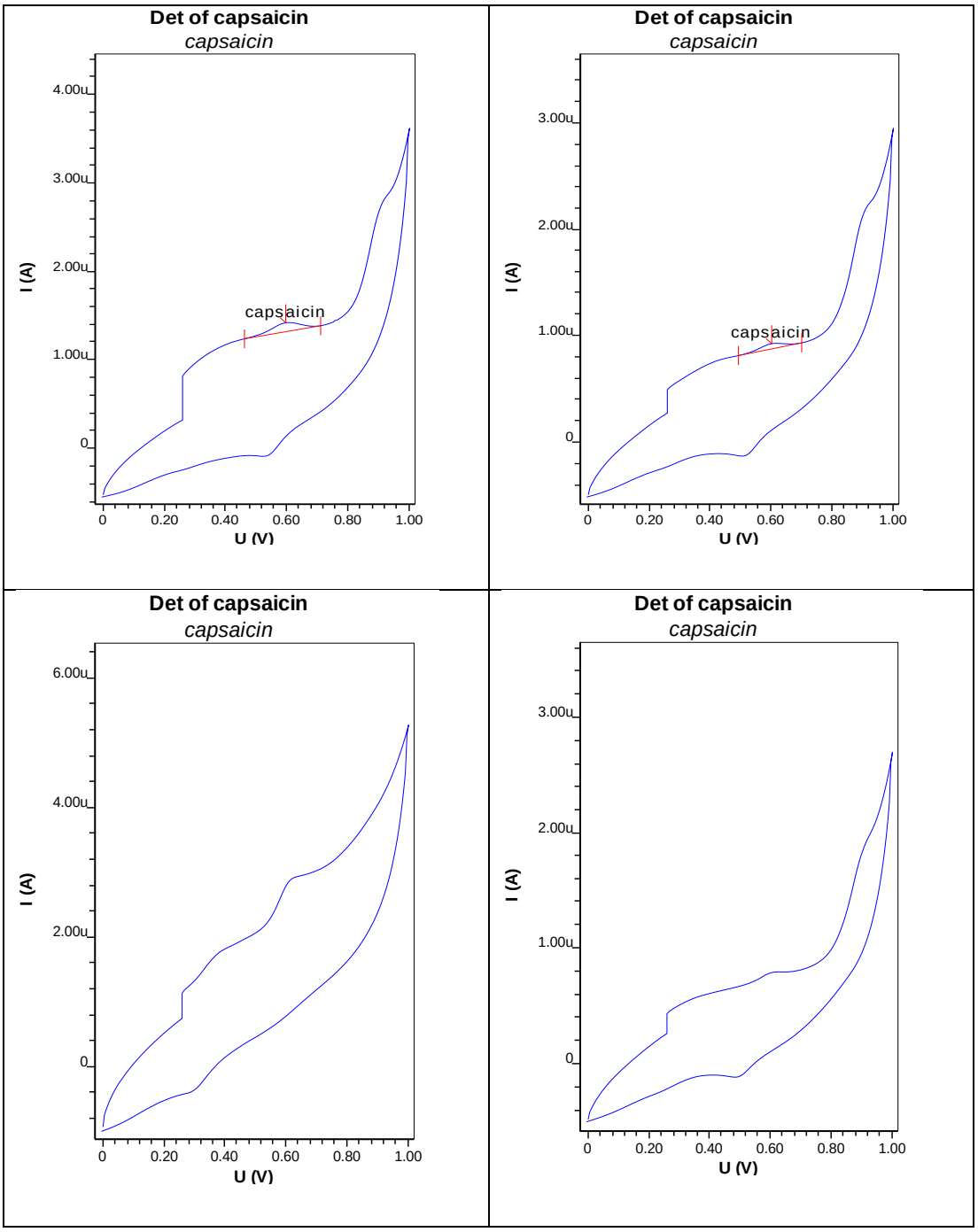

A2: Bare Au-E, DPV Voltammograms

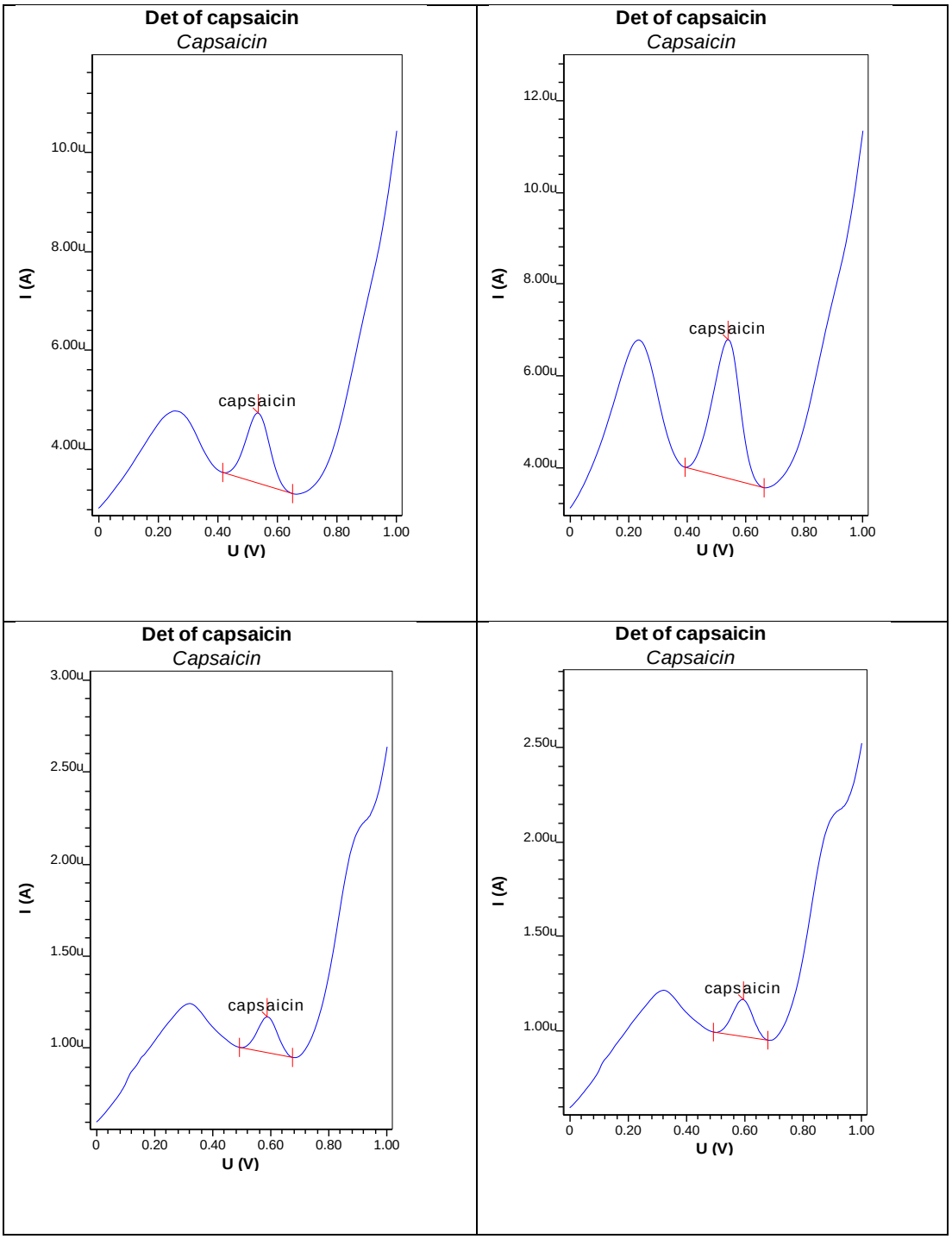

B1: Au- MWCNT, CV Voltammograms

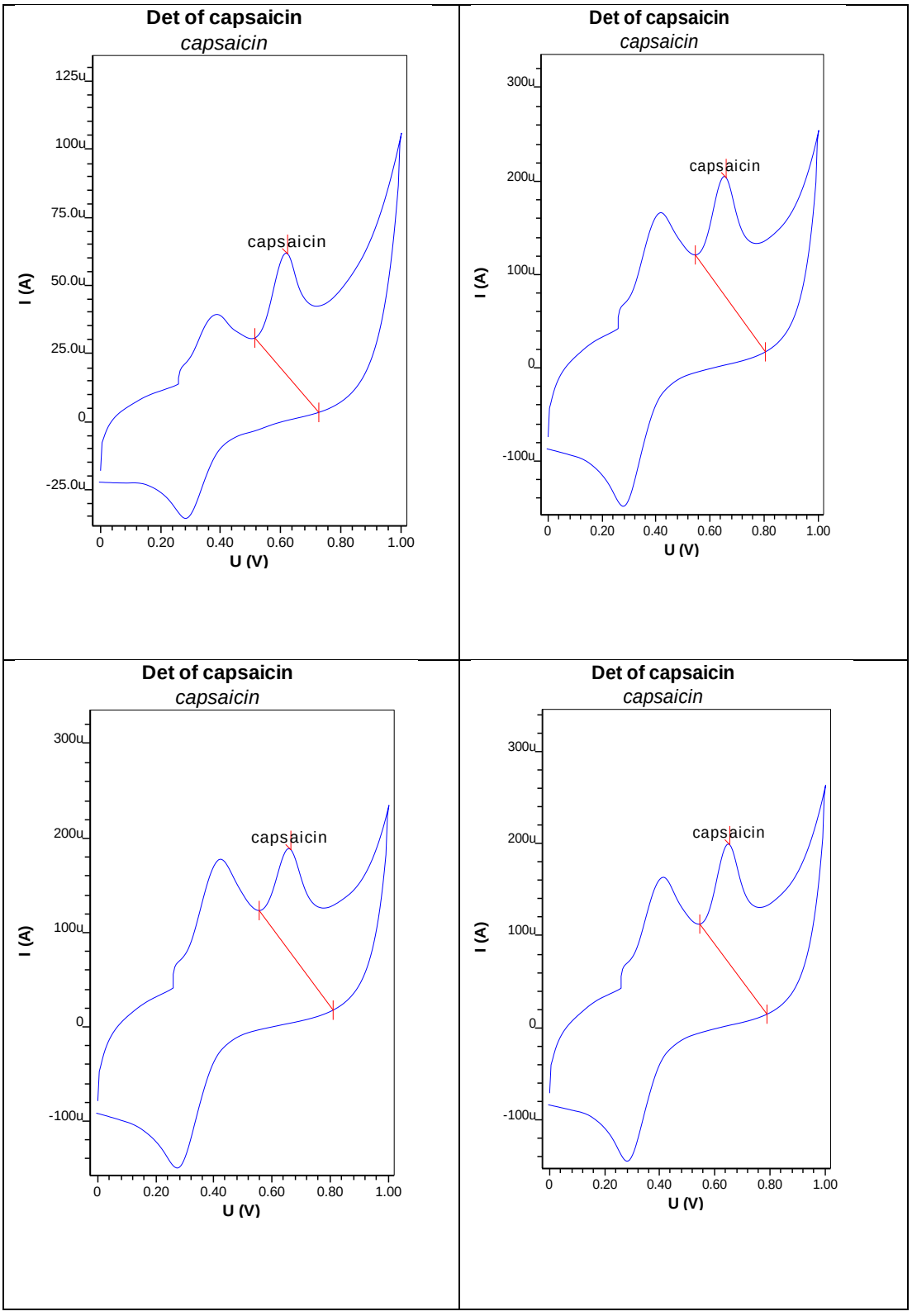

B2: Au- MWCNT, DPV Voltammograms

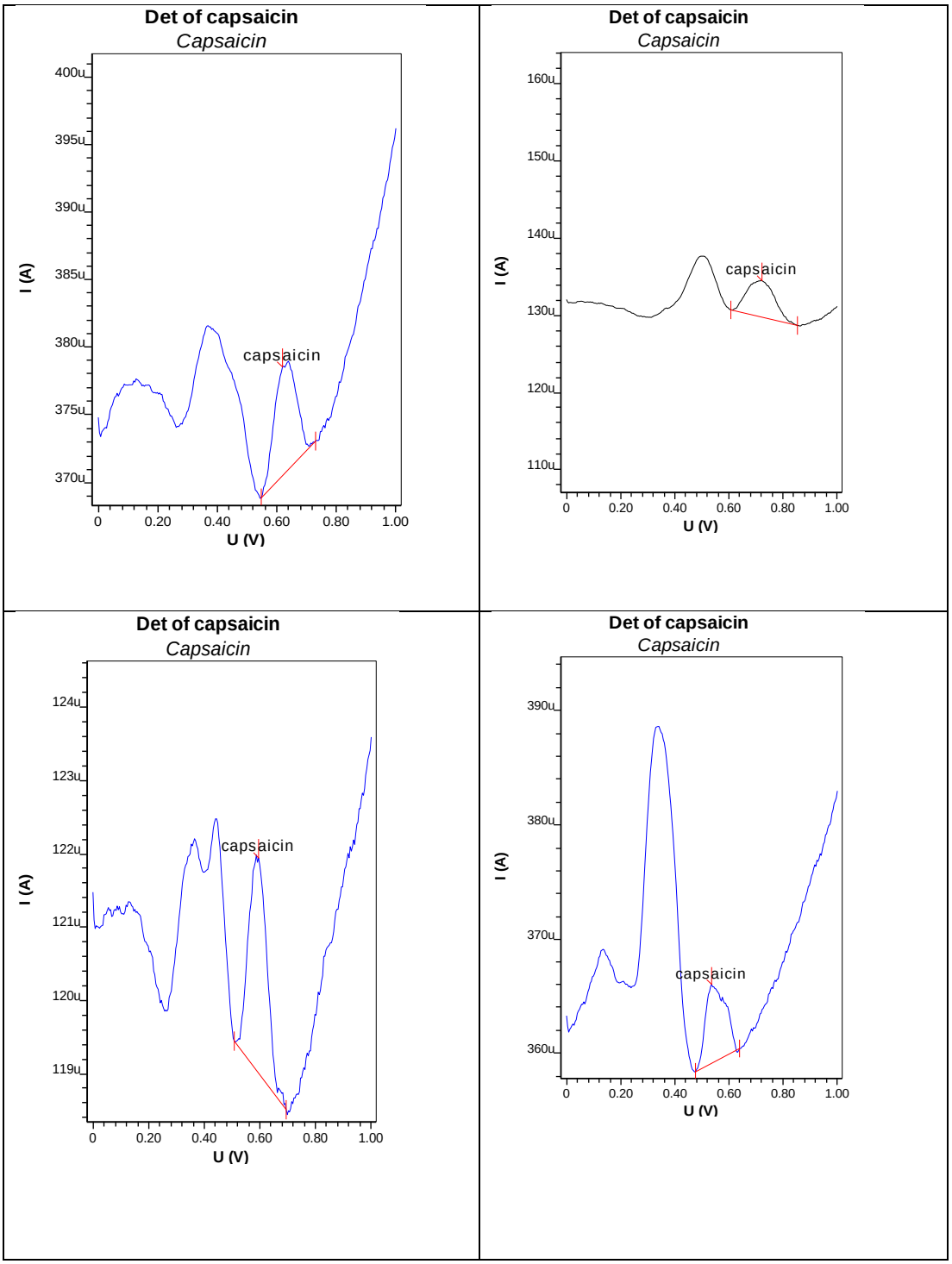

C1: Au-E- MWCNT- GOx, CV Voltammograms

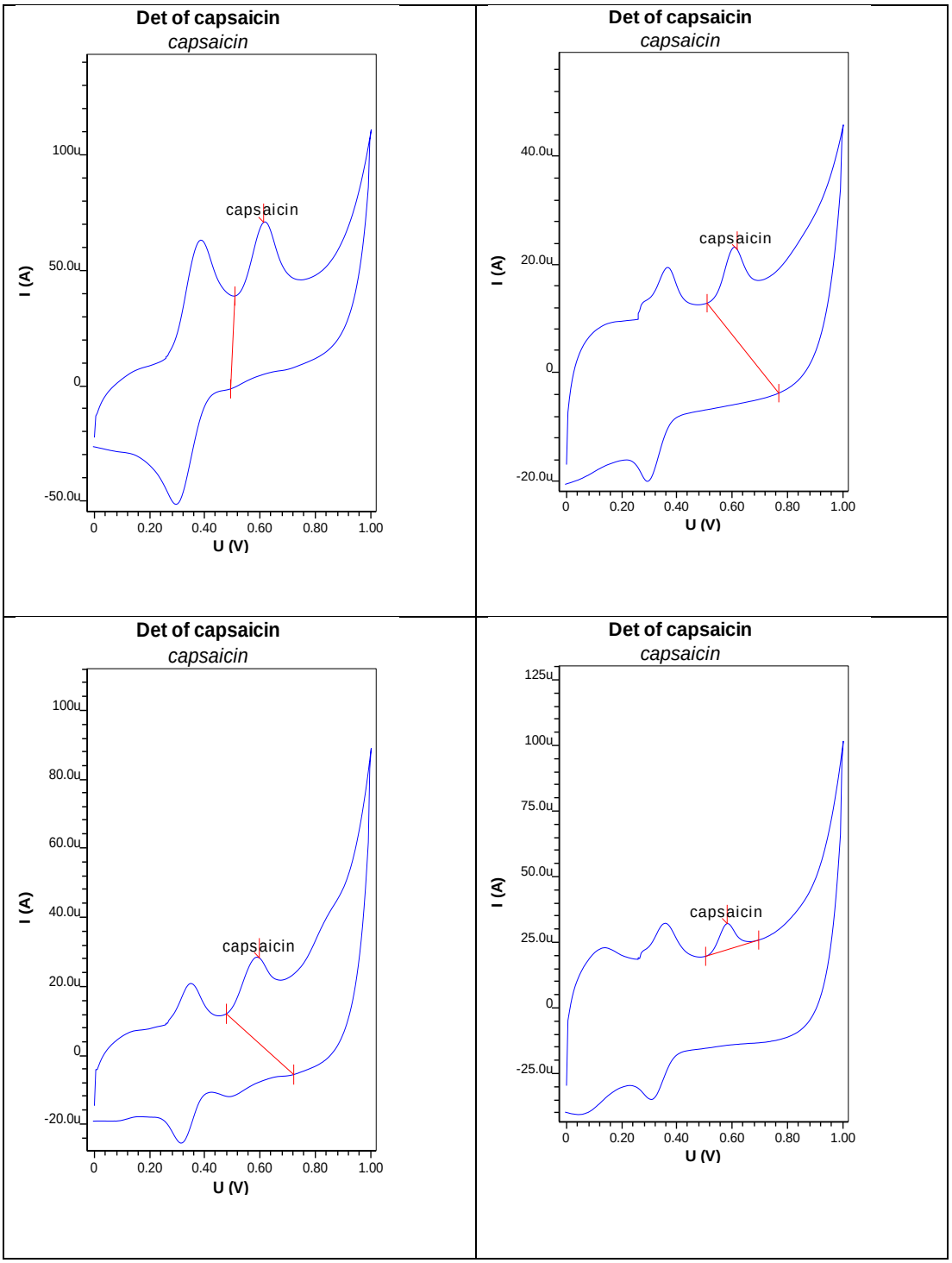

C2: Au-E- MWCNT- GOx, DPV Voltammograms

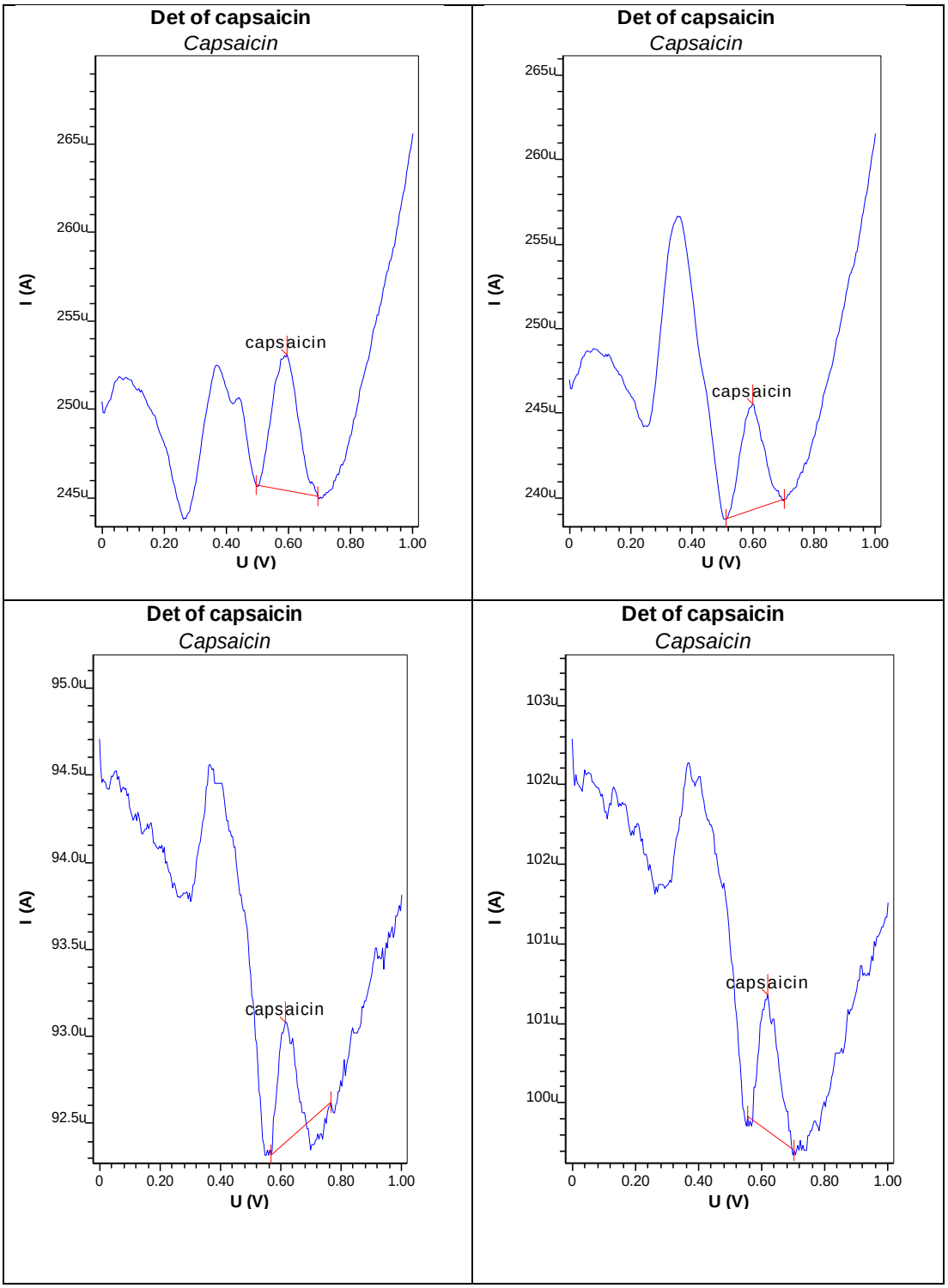

D1: Au-E- MWCNT- PAL, CV Voltammograms

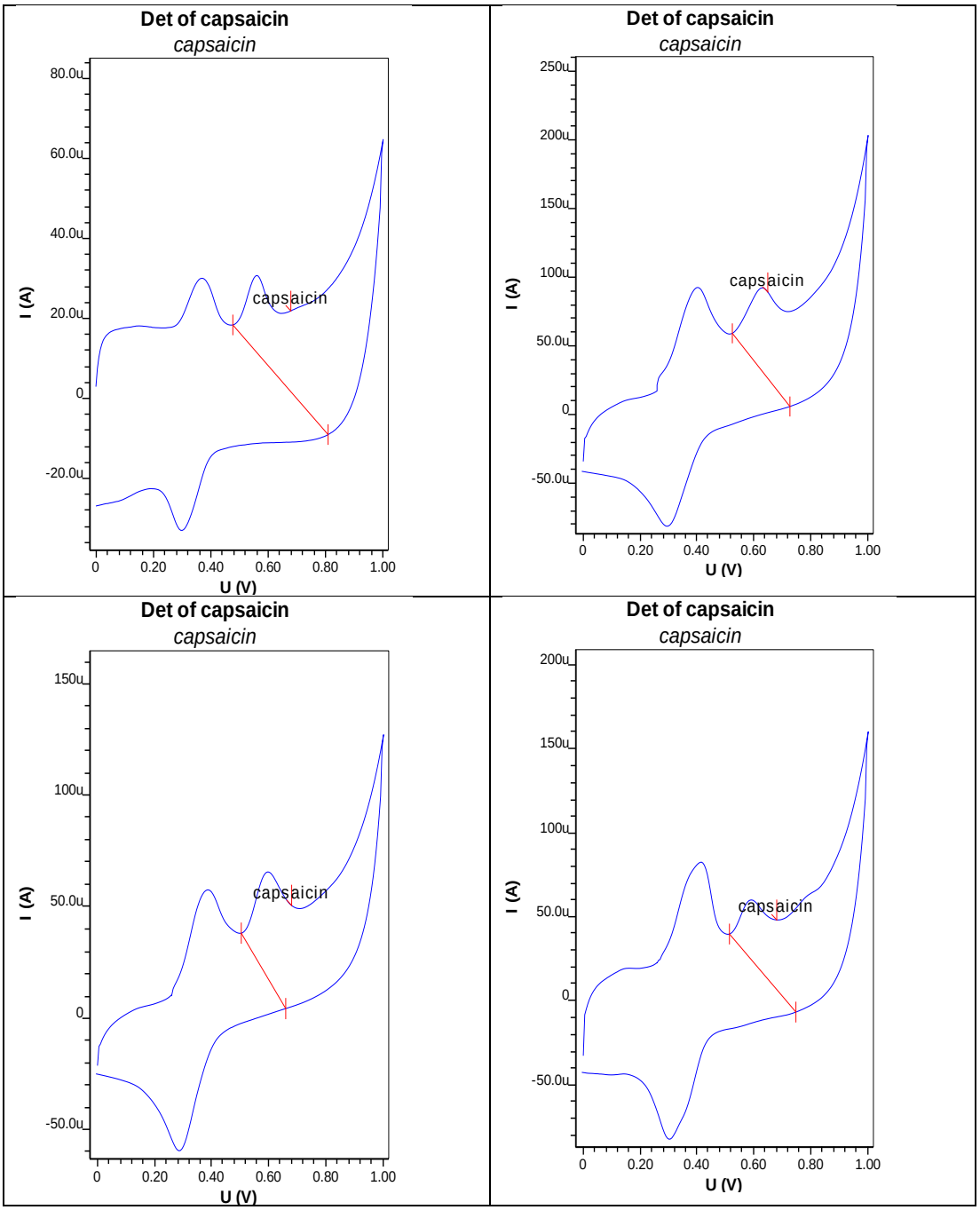

D2: Au-E- MWCNT- PAL, DPV Voltammograms

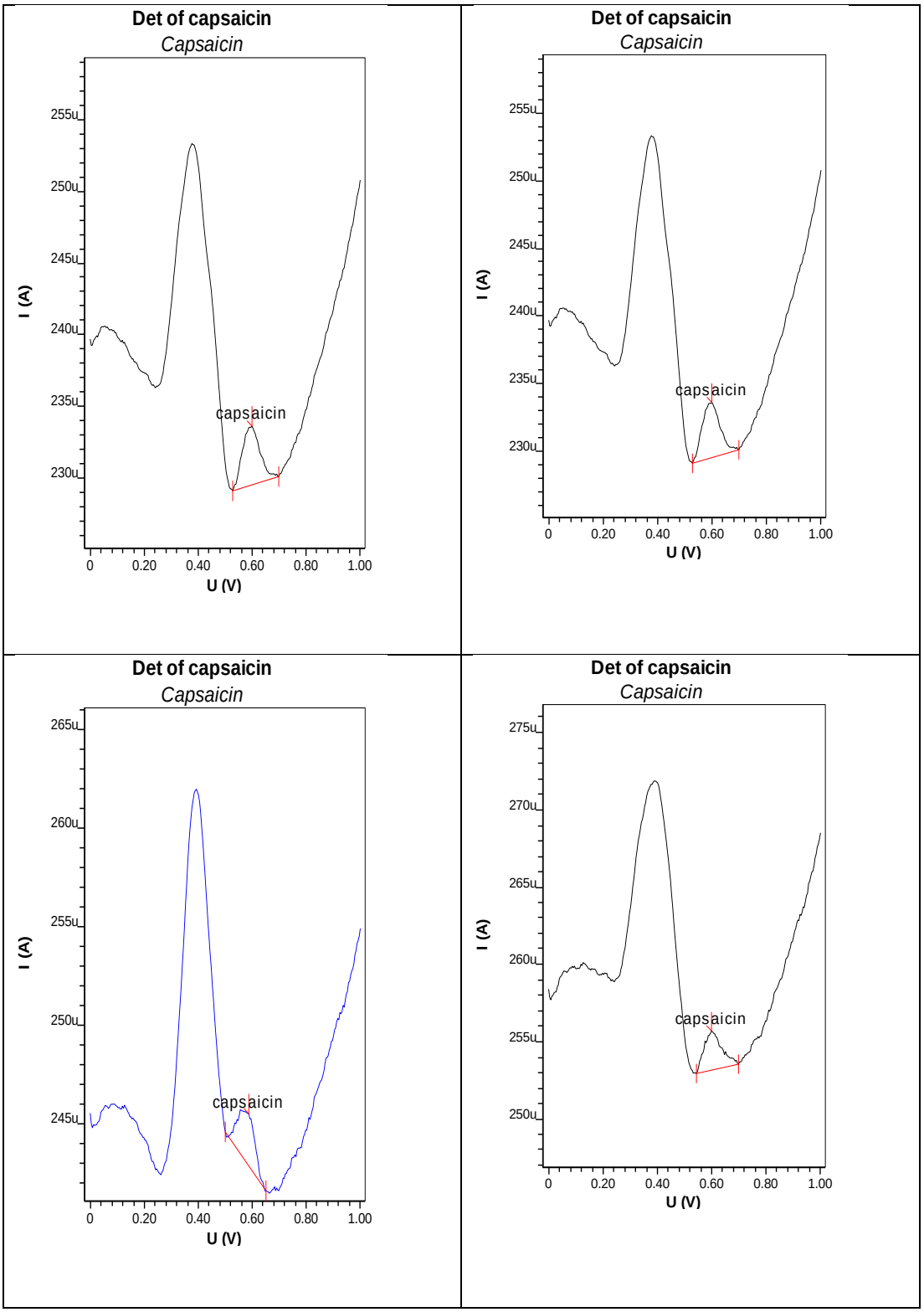

PUBLICATIONS

Analytical Letters
Publication details, including instructions for authors and subscription information:
http://www.tandfonline.com/loi/lanl20

Electrochemical Determination of Capsaicin and Silymarin Using a Glassy Carbon Electrode Modified by Gold Nanoparticle Decorated Multiwalled Carbon Nanotubes

Thabani Mpanza [a b], Myalowenkosi I. Sabela [a], Sanele S. Mathenjwa [a], Suvardhan Kanchi [a] & Krishna Bisetty [a]

[a] Department of Chemistry, Durban University of Technology, Durban, South Africa

[b] Department of Chemistry, Mangosuthu University of Technology, Jacobs, South Africa

Accepted author version posted online: 23 Jun 2014.Published online: 02 Sep 2014.

To cite this article: Thabani Mpanza, Myalowenkosi I. Sabela, Sanele S. Mathenjwa, Suvardhan Kanchi & Krishna Bisetty (2014) Electrochemical Determination of Capsaicin and Silymarin Using a Glassy Carbon Electrode Modified by Gold Nanoparticle Decorated Multiwalled Carbon Nanotubes, Analytical Letters, 47:17, 2813-2828, DOI: 10.1080/00032719.2014.924010

To link to this article: http://dx.doi.org/10.1080/00032719.2014.924010

Analytical Letters, 47: 2813–2828, 2014

ISSN: 0003-2719 print/1532-236X online
DOI: 10.1080/00032719.2014.924010

Taylor & Francis
Taylor & Francis Group

Sensors

ELECTROCHEMICAL DETERMINATION OF CAPSAICIN AND SILYMARIN USING A GLASSY CARBON ELECTRODE MODIFIED BY GOLD NANOPARTICLE DECORATED MULTIWALLED CARBON NANOTUBES

Thabani Mpanza,[1,2] Myalowenkosi I. Sabela,[1] Sanele S. Mathenjwa,[1] Suvardhan Kanchi,[1] and Krishna Bisetty[1]

[1]*Department of Chemistry, Durban University of Technology, Durban, South Africa*

[2]*Department of Chemistry, Mangosuthu University of Technology, Jacobs, South Africa*

The goal of this study was to develop a suitable electroanalytical method for the determination of primary compounds in the extracts of capsicum and silymarin. For this purpose, a glassy carbon electrode immobilized with multiwalled carbon nanotubes decorated with gold nanoparticles was characterized by high resolution transmission electron microscopy and attenuated total reflectance infrared spectroscopy. The developed electrochemical sensor had a linear dynamic range from 0.15 to 35.0 μM. In addition, the limits of quantification for silymarin and capsaicin with the gold nanoparticle decorated multiwalled carbon nanotubes were 0.1564 and 0.2761 μg L^{-1} with relative standard deviations (n = 3) of 1.65% and 2.09% and equivalent mass percentages of 93.33% and 62.02%, respectively. The methodology may be employed for the determination of capsaicin and silymarin in pharmaceutical and food products.

Keywords: Capsaicin; Cyclic voltammetry (CV); Differential pulse voltammetry (DPV); Gold nanoparticles (AuNPs); Multiwalled carbon nanotubes (MWCNTs); Silymarin

INTRODUCTION

In recent years, nanoscience has made considerable progress toward the manufacture and characterization of new materials. Due to unique properties, carbon nanotubes, which have attracted the attention of several researchers (Singh et al. 2010; Dresselhaus and Dresselhaus 2001; Lu et al. 2008) and consist of a series of

Received 20 January 2014; accepted 1 May 2014.

Address correspondence to K. Bisetty and M. Sabela, Department of Chemistry, Durban University of Technology, P.O. Box 1334, Durban 4000, South Africa. E-mail: bisettyk@dut.ac.za and myalosabela@gmail.com

Color versions of one or more of the figures in the article can be found online at www.tandfonline.com/lanl.

cylindrical graphite sheets, are combined in a unique manner to provide high electrical conductivity, stability, and mechanical strength. Numerous novel applications of singlewalled (SW) and multiwalled (MW) carbon nanotubes (CNTs) reported in literature include energy (Ruoff, Qian, and Liu 2003), electronics (Endo at al. 2004), mechanical (Ruoff et al. 2003), biological, and biosensor applications (Ensafi et al. 2011; Karimi-Maleh, Biparva, and Hatami 2013; Liang and Zhuobin 2003; Musameh et al. 2002; Noviandri and Rakhmana 2012; Sanati et al. 2014; Shahmiri et al. 2013; Tashkhourian et al. 2009; Tavana at al. 2012; J. Wang et al. 2002; S. G. Wang et al. 2003; Zhang and Gorski 2005). More recent modifications of electrodes with nanomaterials for electrochemical studies have gained widespread interest for the quantification of biomolecules. Specifically, the unique properties of CNTs render them useful support materials for nanoparticles (Elyasi, Khalilzadeh, and Karimi-Maleh 2013; Singh et al. 2010). Electrodes, especially those modified with heavy metal nanoparticles, usually exhibit higher electrocatalytic activity toward compounds with slower redox processes at the bare electrodes (Tashkhourian et al. 2009). Some of the reported noble metal nanoparticles decorated on single/multiwalled carbon nanotubes (SWCNTs/MWCNTs) include gold (Liang and Zhuobin 2003; J. Wang et al. 2002; S. G. Wang et al. 2003), platinum (Elyasi et al. 2013; Niu et al. 2012), and silver (Shi et al. 2011; T. Wang et al. 2010; Sanghavi et al. 2013). Their capabilities in various applications have drawn a great deal of attention on the evaluation of natural dietary agents including fruits, vegetables, and spices as they show antioxidant properties; hence, the development of suitable analytical techniques remains a challenge. In this work, MWCNTs decorated with gold nanoparticles (AuNPs) immobilized on a glassy carbon electrode were used for the quantification of silymarin and capsaicin. These phytochemical compounds were chosen based on the presence of guaiacol and resorcinol rings. To the best of our knowledge, such work has not been previously reported.

Silymarin consists of four flavonolignan isomers: silybin, isosilybin, silydianin, and silychristin. Among them, silybin is the most active and commonly used flavonolignan. Silymarin has significant biological properties such anti-oxidant, antilipid peroxidative, antifibrotic, anti-inflammatory membrane stabilizing immunomodulatory, and liver regenerating mechanisms (Cacciapuoti et al. 2013; Huseini et al. 2006; Pradhan and Girish 2006; Saller, Meier, and Brignoli 2001). They are orally absorbed and excreted mainly through the bile as sulfates and conjugates, and are used in treating various liver, kidney, heart, pancreas, and lung diseases due to oral efficacy and good safety profiles (Abenavoli et al. 2011; Cacciapuoti et al. 2013; Huseini et al. 2006, Kabir et al. 2014). Capsaicin, on the other hand, belongs to a group of pungent chemical compounds found in hot peppers referred to as capsaicinoids (capsicum annum and capsicum frutescens) (Reilly, Crouch, and Yost 2001). Capsaicin and its derivative dihydrocapsaicin are derived from the phenylalkaylamide alkaloid (capsaicinoids) group and they strongly induce the burning taste of chili (Supalkova et al. 2007). Studies related to the separation and characterization of these two compounds (silymarin and capsaicin) have been reported using thin-layer chromatography (TLC), high-performance liquid chromatography (HPLC), HPLC–electrospray ionization mass spectrometry (HPLC–EIMS), gas chromatography–mass spectrometry (GC–MS), spectrophotometry (Barbero et al. 2008; Cai et al. 2009; Ding et al. 2001; Ha et al. 2010; Kvasnička et al. 2003;

Lee et al. 2006; Lee, Narayan, and Barrett 2007; Liu et al. 2009; Meghreji et al. 2010; Othman et al. 2011; Peña-Alvarez, Ramírez-Maya, and Alvarado-Suárez 2009; Rahman, Khan, and Azmi 2004; Supalkova et al. 2007), capillary zone electrophoresis (CZE) (Kvasnička et al. 2003; Liu et al. 2010), and electrochemical methods (El-Desoky and Ghoneim 2011; Hassan et al. 2008; Kachoosangi, Wildgoose, and Compton 2008). The broader goal of this work was to enhance the performance of a glassy carbon electrode by immobilization of MWCNTs decorated with AuNPs while using silymarin and capsaicin as test compounds. Moreover, the study also included a comparative evaluation of modified and unmodified electrodes to assess the contribution of the AuNPs decorated MWCNTs aimed at improving electrochemical detection. The electrodes were characterized by high resolution transmission electron microscopy (HRTEM) and attenuated total reflectance infrared (ATR-IR) spectroscopy.

EXPERIMENTAL

Apparatus

All electroanalytical measurements were performed using a 797 VA Computrace (Metrohm Herisau, Switzerland). Voltammetric curves were recorded at room temperature using a three electrode system. The working electrode was a 3 mm diameter glassy carbon electrode (GCE), a Ag/AgCl (saturated AgCl, 3 M KCl) was used as a reference electrode, and a platinum wire served as the counter electrode. A pH/ion meter coupled with a stirrer (Metrohm, Herisau, Switzerland) was used to adjust the pH of the buffer solutions. Attenuated total reflectance infrared (ATR-IR) spectra of the AuNPs decorated MWCNTs were obtained using a Varian 800 FT-IR Scimitar Series supplied by SMM Instruments (Durban, South Africa (SA)). Morphology studies were done using a high resolution transmission electron microscope (HRTEM) model JEM 2100 equipped with a LaB_6 emitter (Max Oxford instruments). All working solutions were prepared with deionized water from a purification system, Aqua MaxTM Basic 360 (Trilab, SA). The electrochemical buffers together with the designated samples were refrigerated at 4°C and all analytical measurements were performed at room temperature.

Reagents and Chemicals

Silymarin powder purchased from Sigma Aldrich (Durban, South Africa) was used without any further purification. A 1 M standard stock solution of silymarin was prepared in methanol and stored in at 4°C. The desired solutions were prepared daily by appropriate dilution of the stock with methanol. A 55% (*v*/*v*) nitric acid solution was supplied by Merck (Durban, South Africa). Capsaicin and 20–30% multiwalled carbon nanotubes, O.D × L 7–12 nm × 0.5–10 μm were purchased from Aldrich (Durban, SA). Glacial acetic acid, *N,N*-dimethylformamide, and sodium acetate anhydrous were supplied by Associated Chemical Enterprises (Johannesburg, South Africa). Nitrogen (99.9% pure) was obtained from Afrox (Durban, South Africa). Alumina powder $\leq$3 μm used for cleaning the surface of a glassy carbon electrode was supplied by Metrohm (Durban, South Africa A). Ethanol

and methanol were supplied by Capital Lab Suppliers (Durban, South Africa). The synthesis of ammonium morpholine dithiocarbamate was performed using a previously reported protocol (Kanchi et al. 2013; Kanchi, Singh, and Bisetty 2014).

Sodium acetate buffer pH 4.75 was prepared by dissolving approximately 82.0 g of sodium acetate in a 1 L of distilled water. The desired pH was achieved by quantitatively adding glacial acetic acid and thereafter stored at 4°C.

The gold nanoparticles were prepared by boiling and vigorously stirring approximately 50 mL of 0.01% $HAuCl_4$ solution while adding 50 mM trisodium citrate dropwise until a color change from pale yellow to blue was observed. When the solution turned to red-violet, the solution was allowed to boil while stirring for another 10 min.

Preparation of MWCNTs-GCE and AuNP-MWCNTs-GCE

The 5 mg of MWCNTs were dispersed in 1 mL of *N,N*-dimethylformamide and sonicated (Noviandri and Rakhmana 2012; J. Wang et al. 2002). The glassy carbon electrode was manually cleaned by polishing with alumina and electrochemically by cycling 0.0 to 2.0 V in distilled water containing 3 to 5 drops of 55% nitric acid. This sequential process ensured the removal of any physisorbed or chemisorbed materials from the electrode surface. Subsequently, the glassy carbon electrode was coated with the prepared MWCNTs by manual deposition ensuring a uniform spread on the tip of the electrode. The modified glassy carbon electrode was heated at 80°C to evaporate the *N,N*-dimethylformamide and allowed to cool to room temperature.

The decoration of the MWCNTs with AuNPs involved the functionalization of the thiol groups with approximately 0.2 g ammonium morpholine dithiocarbomate complexed with the MWCNTs followed by heating at 80°C for 2 hours. The thiol group served as a linkage by capping the AuNPs in an exohedral conjugation through the addition of 15 mL of AuNPs to the functionalized MWCNTs. The prepared AuNPs-MWCNTs were attached to the glassy carbon electrode. Transmission electron micrographs for the pure MWCNTs and AuNPs-MWCNTs (Figure 1) confirmed the morphology.

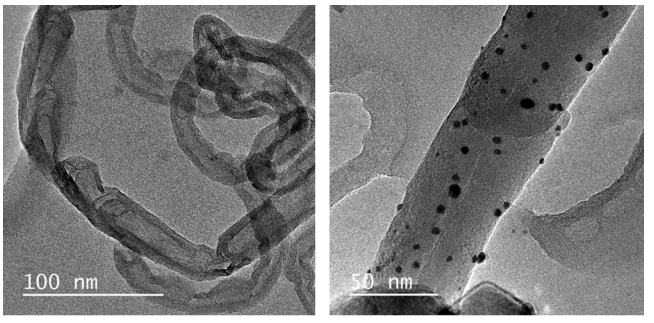

(a) (b)

Figure 1. High-resolution transmission electron micrograph (HRTEM) of (a) multiwalled carbon nanotubes and (b) multiwalled carbon nanotubes decorated with gold nanoparticles obtained at 100 nm and 50 nm.

Sample Preparation

Two tablets of silymarin were accurately weighed, grounded to fine powder, and dissolved in methanol by sonication for 15 min at ambient temperature. The solutions were passed through 0.45-μm filters prior to injection into the electrochemical cell.

Ripe chilies were crushed, blended, and 100 g were added to approximately 350 mL of absolute ethanol and heated to reflux for 120 min. The solids were removed by filtration and discarded. The reddish-brown liquid was distilled to remove excess ethanol. The remaining extracts were cooled to room temperature and stored at 4°C until the electrochemical studies.

Electrochemical Measurements with MWCNTs-GCE and AuNPs-Ammonium Morpholine Dithiocarbamate-MWNCTs-GCE

Approximately 10 mL of the sodium acetate supporting electrolyte (pH 4.75) was introduced into the electrochemical cell in which either a bare glassy carbon electrode or a decorated glassy carbon electrode was immersed prior to electrochemical measurements. Several cyclic sweeps were applied until a low background current was achieved. An aliquot of the analyte solution was then introduced into the electrochemical cell, and a pre-concentration potential was applied to the working electrode while the solution was stirred at 400 rpm. At the end of the pre-concentration time, stirring was stopped and a 5 s equilibration period allowed the solution to be quiescent. The voltammograms were then recorded by scanning the potential towards the positive direction using differential pulse or linear sweep potential at a rate of 0.03 V/s. After each measurement, the working electrode was removed from the instrument and rinsed with deionized water.

RESULTS AND DISCUSSION

Characterization of AuNPs-MWCNTs

HRTEM morphology of the undecorated multiwalled carbon nanotubes (Figure 1a) illustrated hollow cylindrically shaped MWCNTs conjugate formation depicted by the presence of AuNPs (Figure 1b). The covalent bonding of ammonium morpholine dithiocarbamate on the surface of MWCNTs prior to decoration with AuNPs also reduced nanoparticle aggregation, thus enhancing uniform attachment around the surface of the functionalized MWCNTs. The conjugation mechanism is also dependent on the chelation of the gold nanoparticles with the sulfur atom of the ammonium morpholine dithiocarbamate complex.

Infrared Analysis

The MWCNTs exhibited a strong absorbance often indistinguishable from the background noise when using KBr discs for infrared spectroscopy thus making it necessary to use attenuated total reflectance (ATR). The spectra shown in Figure 2 were recorded and collected over the range 4,000–550 cm^{-1} at 3 cm^{-1} resolution, and hence peaks corresponding to ammonium morpholine dithiocarbamate on the surface of MWCNTs were elucidated. As expected, MWCNTs did not produce

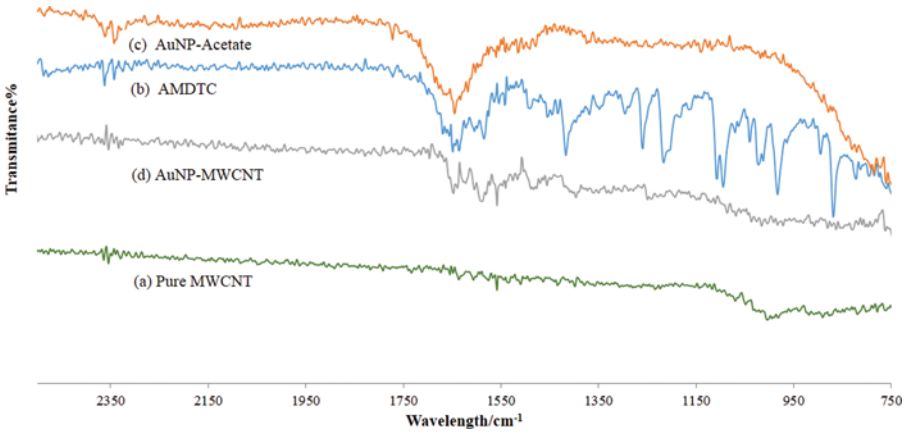

Figure 2. Infrared spectra of (a) pure multiwalled carbon nanotubes, (b) ammonium morpholine dithiocarbamate, (c) gold nanoparticles-acetate, and (d) gold nanoparticles-multiwalled carbon nanotubes.

any spectral absorption while from the gold nanoparticles-acetate, a C=O stretching vibration at 1640 cm^{-1} was observed after conjugation of the AuNPs with the MWCNTs. However, this band was relatively small, probably due to the lower concentration of the prepared AuNPs. Primary amine bands were observed in the 1580 cm^{-1} region, due to the presence of ammonium morpholine dithiocarbamate retained in the final conjugation. This was confirmed by the participation of the sulfur atoms rather than nitrogens and oxygens in the complexation of AuNPs-MWCNTs, resulting in linkage of oxygen atoms of the ammonium morpholine dithiocarbamate complex to the glassy carbon electrode.

Electrochemical Studies

Electrochemical studies were performed using silymarin and capsaicin as the electroactive species. The differences in their electrochemical behavior are due to the presence of the guaiacol and resorcinol rings, respectively. Cyclic voltammograms presented in Figure 3 illustrate well-defined electroactivity with redox reversibility and a charge-transfer controlled process with higher stability. Figures 3a–b illustrated a single reversible peak in the sodium acetate buffer at pH 4.75 for silymarin and capsaicin. This electrochemical reaction involves charge transfer that was enhanced by the surface of the AuNPs-MWCNTs attached to the glassy carbon electrode. According to the results reported in literature and those obtained in this study, particularly for silymarin (Figure 3a), the first oxidation peak E_{p1} at 0.68 V was attributed to the oxidation of *o*-methoxy-phenolic moiety (C-20) of the *E* ring of silymarin molecule (Trouillas et al. 2008). The second oxidation peak, E_{p2}, at 0.43 V was attributed to oxidation of the resorcinol group (C-7) via the transfer of electrons. Moreover, both E_{p1} and E_{p2} values for silymarin shifted towards a less positive potential as the pH increases, indicating the involvement of protons in the electrode processes. In both compounds, E_{p2} appears at a much higher potential. The reaction is reversible with similar redox behavior observed

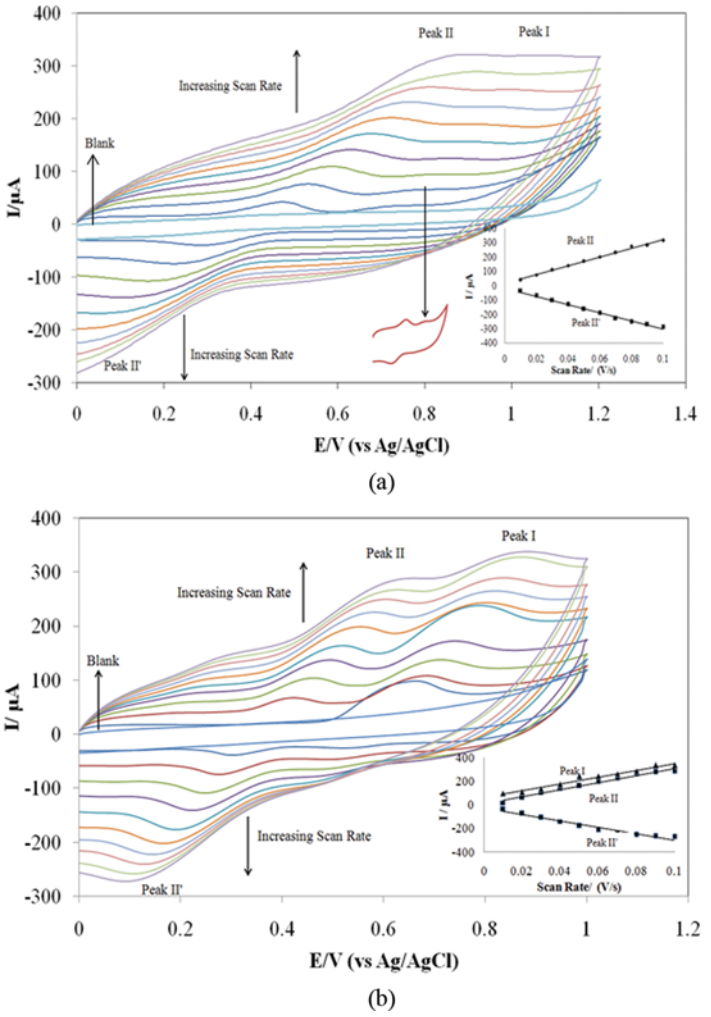

Figure 3. Effect of scan rate from 0.01 to 0.1 V/s on (a) silymarin and (b) capsaicin.

in both compounds having one -OH group (capsaicin) and five -OH groups (silymarin) due to the guaiacol moiety. The characteristic irreversible electrochemical oxidation of the guaiacol unit of the capsaicin molecule produces the redox reaction of capsaicin in the scan involving the loss of two electrons and protons, similar to the well-established systems of *o*-benzoquinone reported in the literature (Sims et al. 2009). The oxidation and reduction peak heights increased significantly when AuNPs-MWCNTs-GCE were used, indicating a much better surface area and electrical conductivity compared to the bare glassy carbon electrode. Hence, the decoration of MWCNTs with AuNPs facilitates electron transfer between the analytes and modified electrode surfaces. The data for cyclic and differential pulse voltammetry are shown in Table 1.

Table 1. Determination of silymarin and capsaicin standards using a bare glassy carbon electrode (GCE), multiwalled carbon nanotubes on GCE (GCE-MWCNTs), and gold nanoparticles (AuNPs) on MWCNTS-GCE (AuNP-MWCNTs-GCE)

			GCE		MWCNT-GCE		AuNP-MWCNTs-GCE	
Technique	Peak	Parameters	CAP	SMR	CAP	SMR	CAP	SMR
CV	I	E_{pa} (mV)	0.72	0.82	0.62	0.79	0.65	0.68
		E_{pc} (mV)	–	–	–	–	–	–
		i_{pa} (μA)	8.58	4.33	9.32	5.46	11.20	5.90
		i_{pc} (μA)	–	–	–	–	–	–
	II	E_{pa} (mV)	0.41	0.49	0.34	0.52	0.45	0.43
		E_{pc} (mV)	0.29	0.28	0.25	0.35	0.21	0.23
		i_{pa} (μA)	11.40	11.09	10.40	15.57	16.20	28.40
		i_{pc} (μA)	7.99	10.22	8.45	13.02	13.50	26.10
	III	E_{pa} (mV)	–	–	0.08	–	0.17	–
		E_{pc} (mV)	–	–	–	–	–	–
		i_{pa} (μA)	–	–	2.91	–	3.10	–
		i_{pc} (μA)	–	–	–	–	–	–
DPV	I	E_p (mV)	0.56	0.96	0.71	1.08	0.53	1.08
		i_p (μA)	0.40	0.77	0.69	1.25	0.80	2.71
	II	E_p (mV)	0.32	0.64	0.44	0.67	0.33	0.67
		i_p (μA)	0.20	0.45	0.70	0.69	1.70	2.74
	III	E_p (mV)	–	–	–	0.28	0.12	0.28
		i_p (μA)	–	–	–	0.37	0.10	0.51

Note: CV: cyclic voltammetry; DPV: differential pulse voltammetry; CAP: capsaicin; SMR: silymarin.

Effect of Scan Rate

In comparing the effect of scan rates on the cyclic voltammograms (Figures 3a–b) for silymarin and capsaicin, it is clear that both anodic peaks of capsaicin were dominant throughout the scanning rate (0.01–0.1 V/s) whereas silymarin showed a reversible peak II, while Peak I was observed at a lower scan rate recorded at 0.03 V/s. However, as the scan rates increased, the peak potentials of the anodic peaks (I and II) shifted toward a more positive potential, whereas peak II' (cathodic peak) shifted toward a negative potential. The relationship between the redox peak currents and the scan rates were correlated at peak II = 0.991 and II' = 0.973 for silymarin and peak I = 0.971, II = 0.983 and II' = 0.965 for capsaicin. Interestingly, as the scanning rates approached 0.1 V/s, the linearity of the graphs was altered thus confirming that adsorption rather than diffusion was the preferred mechanism of detection.

Differential Pulse Voltammetry

Differential pulse voltammetry of 0.35 mM silymarin in sodium acetate buffer at pH 4.75 on the bare GCE, MWCNTs-GCE, and AuNPs-MWCNTs-GCE were recorded following a 60 s pre-deposition against the Ag/AgCl electrode in 3 M KCl. Following preconcentration, a broader oxidation peak was observed at the bare electrode, while a well-resolved peak was observed at the modified glassy

carbon electrode, indicating better adsorption of silymarin and capsaicin on the MWCNTs-GCE and the AuNPs-MWCNTs-GCE (Figure 4). These enhancements of the peak current were expected, due to the stronger adsorptive properties of the AuNPs and MWCNTs, probably increasing the deprotonation of the phenolic moiety in both sylimarin and capsaicin (El-Desoky and Ghoneim 2011). Furthermore, slight shifts in the peak potentials were also observed with a shift more to the left for the AuNPs-MWCNTs-GCE, whereas for the bare glassy carbon electrode it shifted more toward the right. These differences confirm the better sensitivity of the modified electrode than the bare electrode. To emphasize these differences, overlays of the differential pulse voltammograms were prepared to relate potential

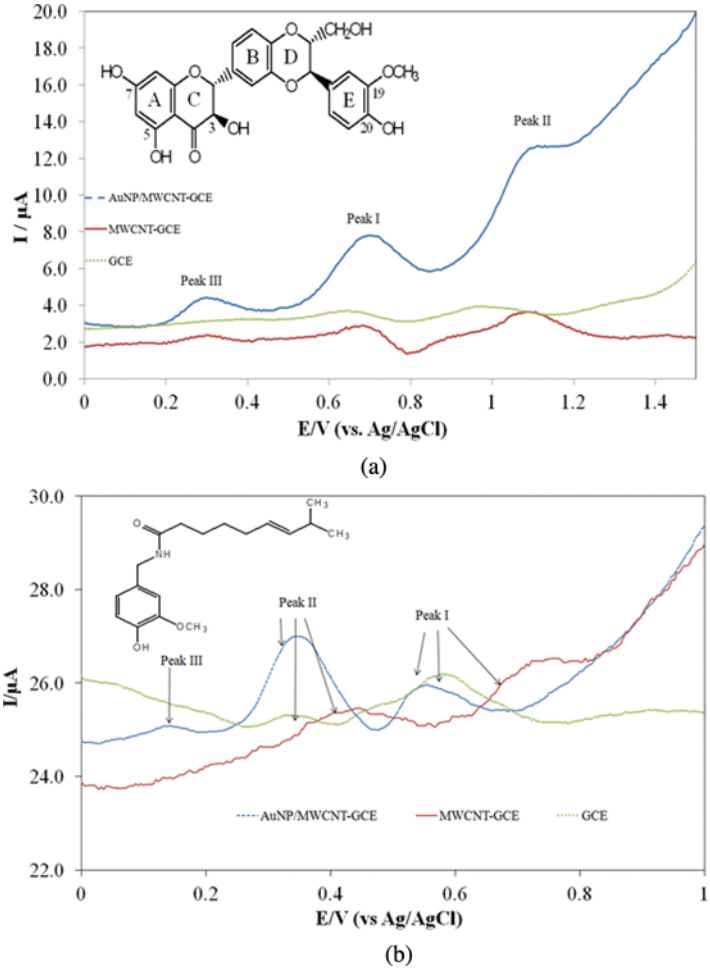

Figure 4. Differential pulse voltammograms of (a) silymarin and (b) capsaicin using bare glassy carbon electrode (GCE); multiwalled carbon nanotubes on a GCE (MWCNTs-CGE), and gold nanoparticles on a MWCNT-GCE (Au-MWCNTs-CGE) with a pulse time of 0.04 s, a sweep rate of 0.010 V/s, and a step of 0.003 V.

Table 2. Comparison of previous studies for the determination of capsacin and silymarin

Experimental			Analytical Parameters				
Methods	Sample	Analyte	Linear dynamic range [Equation]	R^2	Limit of detection	Limit of quantification	Reference
SPME-GC–MS	peppers and pepper sauces	capsaicin dihydrocapsaicin	0.109–1.323 μg/mL 0.107–1.713 μg/mL	>0.9970 >0.9970	0.014 μg/mL 0.022 μg/mL	0.069 μg/mL 0.108 μg/mL	Peña-Alvarez et al. 2009
AdsSV MWCNT-BPPGE	chili peppers	capsaicin	0.5 to 15 μm [$y = 5.31 \times 10^{-7}$ x $- 2.52 \times 10^{-7}$]	0.9900	0.31 μM	NR	Kachoosangi et al. 2008
AdsSV MWCNT-SPE	chili peppers	capsaicin	0.5 to 35 μM [$y = 3.07 \times 10^{-7}$ $x - 1.52 \times 10^{-7}$]	0.9900	0.45 μM	NR	
HPCE	capsicum annuum, pepper sauce and porous capsicum plaster	capsaicin dihydrocapsaicin	1 to 400 μg/mL 1 to 400 μg/mL	0.9994 0.9994	0.66 μg/ml 0.0.73 μg/ml	NR	Liu et al. 2010
HPLC–ED	pepper fruit	capsaicin	31.3 to 125 μg/mL	0.9948	305 ng/mL	NR	Supalkova et al. 2007
HPLC fluorescence	hot peppers	capsaicin dihydrocapsaicin	[$y = 112.901x + 187$] [$y = 151.770x + 4589$]	0.9995 0.9995	0.008 mg/L 0.011 mg/L	0.028 mg/L 0.036 mg/L	Barbero et al. 2008
UPLC	gochujang	capsaicin dihydrocapsaicin	0.2 to 10.0 μg/mL 0.2 to 10.0 μg/mL	0.9995 0.9999	0.05 μg/g 0.05 μg/g	0.16 μg/g 0.16 μg/g	Ha et al. 2010
CZE	solubilized silymarin	silymarin	10–200 mg/ml	0.9974	NR	0.5 mg/ml	Kvasnička et al. 2003
SW-AdsASV Bare-CPE	commercial formulations and human serum	silymarin	1×10^{-7} to 4×10^{-6} M [ip (μA) = 2.45 ± 0.003C (μM) − 0.02 ± 2.45×10^{-2}]	0.996	3×10^{-8} M	1×10^{-7} M	El-Desoky and Ghoneim 2011
SW-AdsASV MMT-Ca-CPE		silymarin	7×10^{-9} to 1.5×10^{-6} M [ip (μA) = 10.50 ± 0.017C (μM) + 1.30 ± 7.35×10^{-3}]	0.998	2.1×10^{-9} M	7×10^{-9} M	
DPV	silymarin tablets, capsules, and packets	silymarin	0.10–4.00 mg/L	0.9999	0.030 mg/L	0.090 mg/L	Hassan et al. 2008
UPLC	silymarin	Silybin A Silybin B Isosilybin A	$y = 66.34x + 1.22$ $y = 189.41x + 2.62$ $y = 14.34x + 11.72$	0.9992 0.9990 0.9997	0.68 ng 0.68 ng 1.25 ng	2.5 ng 2.5 ng 5 ng	Liu et al. 2009

		Isosilybin B	$y = 8.16x + 2.11$	0.9991	2.5 ng	10 ng	
		Silydianin	$y = 28.52x + 4.23$	0.9994	2.5 ng	10 ng	
		Silychristin	$y = 70.06x - 2.71$	0.9995	1.25 ng	5 ng	
		Taxifolin	$y = 79.40x + 2.23$	0.9998	0.68 ng	2.5 ng	
RP–HPLC	silymarin, legalon capsule and yiganling tablet	Silybin	0.1437–1.437 μg/μL [$y = 162551x - 88924$]	0.99960	NR	NR	
			$y = 28.52x + 4.23$	0.9994			Silydianin 2.5 ng
		10 ng					
		Silychristin	$y = 70.06x - 2.71$	0.9995			1.25 ng
5 ng							
Taxifolin	$y = 79.40x + 2.23$		0.68 ng	2.5 ng			
		0.9998					
RP–HPLC	silymarin, legalon capsule and yiganling tablet	Silybin	0.1437–1.437 μg/μL [$y = 162551x - 88924$]	0.99960	NR	NR	Ding et al. 2001
		Isosilybin	0.0885–0.885 [$y = 1228090x + 21931$]	0.99959			
		Silydianin	0.0846–0.846 [$y = 755927x + 8791$]	0.99933			
		Silychristin	0.1398–1.398 [$y = 1397620x - 10198$]	0.99958			
HPLC	silybum marianum seed meal	Silybin	1–400 μg/mL [Area = $31.67 + 2.19 \times 10^4$C]	0.9998	0.1 μg/mL	NR	Cai et al. 2009
HPLC		silymarin	18–50 $\mu g/ml^{-1}$ [$\log \nu = 1.024 \log C + 3.235$]	0.9997	2.823 ng/mL	NR	Rahman et al. 2004
UV/VIS	pharmaceutical capsules and tablets	silymarin	[$y = 0.0388x - 0.0139$]	0.9997	0.29 μg/mL	0.90 μg/mL	Meghreji et al. 2010
AdsSV	chili peppers	Capsaicin	0.15 to 35.0 μM $I_p(\mu A) = 46.24\ C - 12.21$	0.9953	0.083 $\mu g\ L^{-1}$	0.276 $\mu g\ L^{-1}$	Current study
	pharmaceutical capsules	Silymarin	0.15 to 35.0 μM $I_p(\mu A) = 168.2\ C - 16.51$	0.9975	0.047 $\mu g\ L^{-1}$	0.156 $\mu g\ L^{-1}$	

Note: CC: correlation coefficient; LDR: linear dynamic range; LOD: limits of detection; LOQ: limits of quantification; NR: not reported; AdsSV: adsorptive stripping voltammetry; DPV: differential pulse voltammetry; SW-AdsASV: square-wave adsorptive anodic stripping voltammetry; CE: capillary electrophoresis; CZE: capillary zone electrophoresis; HPCE-MEKC: high-performance capillary electrophoresis micellar electrokinetic chromatography; RP-HPLC: reverse phase-high performance liquid chromatography; HPLC–ED: High Performance Liquid Chromatography–Electrochemical Detection; LC–MS: liquid chromatography–mass spectrometry; UPLC: ultra-performance liquid chromatography; SPME–GC–MS: solid phase microextraction–gas chromatography–mass spectrometry; MMT-Ca-CPE: montmorillonite-Ca-carbon paste electrode; MWCNT-SPE: multiwalled carbon nanotube-screen-printed electrode; MWCNT-BPPGE: multiwalled carbon nanotube-basal plane pyrolytic graphite electrode.

against current for the three types of electrodes (Figure 4). Two peaks from the bare electrode had higher potentials and lower peak currents compared to the peaks produced by the coated electrodes, which shifted more toward the left of the peak potential with higher peak currents. The enhancement of the peak currents on the coated electrodes was due to good conductivity and strong adsorptive properties of the MWCNTs. However, the peak potentials of the two peaks shifted towards a lower positive potential with increased pH, suggesting the involvement of protons in the electrode process. The anodic currents were probably related to the oxidation of the hydroxyl groups on the C-5 (ring A) position. These results coincided with the review by Singh and co-workers (2010) in which theoretical studies on carbon nanotubes suggested the introduction of extraneous material into the hollow cavities with interesting effects on the physical and electronic properties of the encapsulated materials.

Linear Dynamic Range, Limits of Detection and Quantification

In order to characterize the developed biosensor, differential pulse voltammetry was selected because of its ability to generate sharper and well resolved peaks at lower concentrations. A series of 0.35 mM capsaicin and silymarin standards were analyzed in triplicate and the averages were recorded. Quantitative evaluation was based on a linear relationship between the peak currents and the volume added (concentration) resulting in a good correlation. The equations for the measurements of silymarin and capsaicin were $I_p(\mu A) = 168.2\ C - 16.51$ and $I_p(\mu A) = 46.24\ C - 12.21$ with correlation coefficients of $R^2 = 0.9975$ and $R^2 = 0.9953$, respectively. Table 1 shows a significant improvement in the performance of the developed sensor, primarily due to the AuNPs-MWCNTs coating. The limits of quantification for silymarin and capsaicin calculated with respect to peak II were found to be $0.1564\ \mu g\ L^{-1}$ and $0.2761\ \mu g\ L^{-1}$, respectively.

Reproducibility and Stability

The lifetime of the developed electrochemical sensor is of particular concern, as the MWCNT coating may wear off during the stirring and cleaning period. This was observed over a range of ten runs for five days using the same electrode coating. The repeatability of the current response of the AuNPs-MWCNTs-GCE was examined at 0.5 mM concentration of silymarin.

As the number of runs increased, the sensitivity also decreased due to a significant drop in the current while the peak potential increased, denoting a deterioration of performance. A similar behavior was observed with capsaicin under similar conditions (results not shown). This also confirmed that the mechanism is largely driven by an irreversible adsorption process, resulting in saturation of the AuNPs-MWCNTs-GCE surface. The excellent reproducibility, sensitivity, and higher exchange current density may be associated with the most stable metal nanoparticles formed by gold. The results obtained by the modified GCE for the electrochemical determination of capsaicin and silymarin is compared with the previously reported methods in Table 2.

Analysis of Real Samples

For the purposes of this study, the silybin and capsaicinoid equivalents were electrochemically measured with the developed biosensor in silymarin tablets and chili peppers, respectively. The biosensor for silymarin and capsaicin showed a good reproducibility with relative standard deviations ($n = 3$) of 1.65 and 2.09 and mass percentages of 93.33% and 62.02%, respectively.

CONCLUSIONS

The decoration of the multiwalled carbon nanotubes with gold nanoparticles provided limits of quantification of 0.1564 and 0.2761 $\mu g\,L^{-1}$ for silymarin and capsaicin, respectively. Interestingly, a significant improvement was observed for immobilization on the glassy carbon electrode as the multiwalled carbon nanotubes decorated with gold nanoparticles did not fall off during the analysis, thereby confirming the predominance of covalent bonding on the surface of glassy carbon electrode. Further investigation should be performed to increase the lifetime of the electrode and to optimize the performance of the electrochemical sensor. Distinct advantages of using both MWCNTs and AuNPs included excellent reproducibility, sensitivity, steady coating, and high exchange current density for both silymarin and capsaicin. Future studies may entail the development of an enzyme coated on the surface of Au-MWCNTs-GCE sensor complemented with computational calculations to elucidate the mechanism between the enzyme and the nanomaterial.

FUNDING

The authors gratefully acknowledge the financial assistance from the National Research Foundation (NRF) of South Africa and Durban University of Technology for the Postgraduate Development and Support (PGDS) award.

REFERENCES

Abenavoli, L., G. Aviello, R. Capasso, N. Milic, and F. Capasso. 2011. Milk thistle for treatment of nonalcoholic fatty liver disease. *Hepat. Mon.* 11: 173–177.

Barbero, G. F., A. Liazid, M. Palma, and C. G. Barroso. 2008. Ultrasound-assisted extraction of capsaicinoids from peppers. *Talanta* 75: 1332–1337.

Cacciapuoti, F., A. Scognamiglio, R. Palumbo, R. Forte, and F. Cacciapuoti. 2013. Silymarin in non alcoholic fatty liver disease. *World J. Hepatol.* 5: 109–113.

Cai, X. L., D. N. Li, J. Q. Qiao, H. Z. Lian, and S. K. Wang. 2009. Determination of silymarin flavonoids by HPLC and LC-MS and investigation of extraction rate of silymarin in *Silybum marianum* fruits by boiling water. *Asian J. Chem.* 21: 63–74.

Ding, T., S. Tian, Z. Zhang, D. Gu, Y. Chen, Y. Shi, and Z. Sun. 2001. Determination of active component in silymarin by RP-LC and LC/MS. *J. Pharm. Biomed. Anal.* 26: 155–161.

Dresselhaus, M. S., and G. Dresselhaus. 2001. Ph. Avouris (Eds.): Carbon nanotubes. *Topics Appl. Phys.* 80: 173–211.

El-Desoky, H. S., and M. M. Ghoneim. 2011. Stripping voltammetric determination of silymarin in formulations and human blood utilizing bare and modified carbon paste electrodes. *Talanta* 84: 223–234.

Elyasi, M., M. A. Khalilzadeh, and H. Karimi-Maleh. 2013. High sensitive voltammetric sensor based on Pt/CNTs nanocomposite modified ionic liquid carbon paste electrode for determination of Sudan I in food samples. *Food Chem.* 141: 4311–4317.

Endo, M., T. Hayashi, Y. A. Kim, M. Terrones, and M. S. Dresselhaus. 2004. Applications of carbon nanotubes in the twenty-first century. *Phil. Trans. R. Soc. Lond. A* 362: 2223–2238.

Ensafi, A. A., H. Karimi-Maleh, S. Mallakpour, and M. Hatami. 2011. Simultaneous determination of N-acetylcysteine and acetaminophen by voltammetric method using N-(3, 4-dihydroxyphenethyl)-3,5-dinitrobenzamide modified multiwall carbon nanotubes paste electrode. *Sensors Actuators B* 155: 464–472.

Ha, J., H. Y. Seo, Y. S. Shim, H. J. Nam, H. Seog, M. Ito, and H. Nakagawa. 2010. Rapid method for the determination of capsaicin and dihydrocapsaicin in Gochujang using ultra-high-performance liquid chromatography. *J. AOAC Int.* 93: 1905–1911.

Hassan, E. M., E. F. Khamis, E. I. El-Kimary, and M. A. Barary. 2008. Development of a differential pulse voltammetric method for the determination of Silymarin/Vitamin E acetate mixture in pharmaceuticals. *Talanta* 74: 773–778.

Huseini, H. F., B. Larijani, R. Heshmat, H. Fakhrzadeh, B. Radjabipour, T. Toliat, and M. Raza. 2006. The efficacy of Silybum marianum (L.) Gaertn. (silymarin) in the treatment of type II diabetes: A randomized, double-blind, placebo-controlled, clinical trial. *Phytother. Res.* 20: 1036–1039.

Kabir, N., H. Ali, M. Ateeq, M. F. Bertino, M. R. Shah, and L. Franzel. 2014. Silymarin coated gold nanoparticles ameliorates CCl_4-induced hepatic injury and cirrhosis through down regulation of hepatic stellate cells and attenuation of Kupffer cells. *RSC Adv.* 4: 9012–9020.

Kachoosangi, R. T., G. G. Wildgoose, and R. G. Compton. 2008. Carbon nanotube-based electrochemical sensors for quantifying the 'heat' of chili peppers: the adsorptive stripping voltammetric determination of capsaicin. *Analyst* 133: 888–895.

Kanchi, S., P. Singh, and K. Bisetty. 2014. Dithiocarbamates as a hazardous remediation agents: A critical review on progress in environmental chemistry for inorganic species: Study of 20th century. *Arabian J. Chem.* 7: 11–25.

Kanchi, S., P. Singh, M. I. Sabela, K. Bisetty, and V. N. Nuthalapati. 2013. Polarographic catalytic hydrogen wave technique for the determination of copper(II) in leafy vegetables and biological samples. *Int. J. Electrochem. Sci.* 8: 4260–4282.

Karimi-Maleh, H., P. Biparva, and M. Hatami. 2013. A novel modified carbon paste electrode based on NiO/CNTs nanocomposite and (9,10-dihydro-9,10-ethanoanthracene-11,12-dicarboximido)-4-ethylbenzene-1,2-diol as a mediator for simultaneous determination of cysteamine, nicotinamide adenine dinucleotide and folic acid. *Biosensor. Bioelectron.* 48: 270–275.

Kvasnička, F., B. Biba, R. Ševčika, M. Voldřicha, and J. Krátká. 2003. Analysis of the active components of silymarin. *J. Chromatogr. A* 990: 239–245.

Lee, J. I., B. H. Hsu, D. Wu, and J. S. Barrett. 2006. Separation and characterization of silybin, isosilybin, silydianin and silychristin in milk thistle extract by liquid chromatography-electrospray tandem mass spectrometry. *J. Chromatogr. A* 1116: 57–68.

Lee, J. I., M. Narayan, and J. S. Barrett. 2007. Analysis and comparison of active constituents in commercial standardized silymarin extracts by liquid chromatography–electrospray ionization mass spectrometry. *J. Chromatogr. B* 845: 95–103.

Liang, W., and Y. Zhuobin. 2003. Direct electrochemistry of glucose oxidase at a gold electrode modified with single-wall carbon nanotubes. *Sensors* 3: 544–554.

Liu, H., Z. Du, and Q. Yuan. 2009. A novel rapid method for simultaneous determination of eight active compounds in silymarin using a reversed-phase UPLC-UV detector. *J. Chromatogr. B* 877: 4159–4163.

Liu, L., X. Chen, J. Liu, X. Deng, W. Duan, and S. Tan. 2010. Determination of capsaicin and dihydrocapsaicin in Capsicum annuum and related products by capillary electrophoresis with a mixed surfactant system. *Food Chem.* 119: 1228–1232.

Lu, X., J. Zhou, W. Lu, Q. Liu, and J. Li. 2008. Carbon nanofiber-based composites for the construction of mediator-free biosensors. *Biosensors and Bioelectronics* 23: 1236–1243.

Meghreji, M. A., C. N. Patel, J. B. Dave, R. Badmanaban, and J. A. Patel. 2010. Validated method for silymarin by spectrophotometry in bulk drug and pharmaceutical formulations. *J. Chem. Pharm. Res.* 2: 396–400.

Musameh, M., J. Wang, A. Merkoci, and Y. Lin. 2002. Low-potential stable NADH detection at carbon-nanotube-modified glassy carbon electrodes. *Electrochem. Commun.* 4: 743–746.

Niu, X., H. Zhao, C. Chen, and M. Lan. 2012. Platinum nanoparticle-decorated carbon nanotube clusters on screen-printed gold nanofilm electrode for enhanced electrocatalytic reduction of hydrogenperoxide. *Electrochimica Acta* 65: 97–103.

Noviandri, I., and R. Rakhmana. 2012. Carbon paste electrode modified with carbon nanotubes and Poly(3-Aminophenol) for voltammetric determination of paracetamol. *Int. J. Electrochem. Sci.* 7: 4479–4487.

Othman, Z. A. A., Y. B. H. Ahmed, M. A. Habila, and A. A. Ghafar. 2011. Determination of capsaicin and dihydrocapsaicin in *Capsicum* fruit samples using high performance liquid chromatography. *Molecules* 16: 8919–8929.

Peña-Alvarez, A., E. Ramírez-Maya, and L. Á. Alvarado-Suárez. 2009. Analysis of capsaicin and dihydrocapsaicin in peppers and pepper sauces by solid phase microextraction–gas chromatography–mass spectrometry. *J. Chromatogr. A* 1216: 2843–2847.

Pradhan, S. C., and C. Girish. 2006. Hepatoprotective herbal drug, silymarin from experimental pharmacology to clinical medicine. *Indian J. Med. Res.* 124: 491–504.

Rahman, N., N. A. Khan, and S. N. H. Azmi. 2004. Kinetic spectrophotometric method for the determination of silymarin in pharmaceutical formulations using potassium permanganate as oxidant. *Pharmazie* 59: 112–116.

Reilly, C. A., D. J. Crouch, and G. S. Yost. 2001. Quantitative analysis of capsaicinoids in fresh peppers, Oleoresin capsicum and pepper spray products. *J. Forensic Sci.* 46: 502–509.

Ruoff, R. S., D. Qian, and W. K. Liu. 2003. Mechanical properties of carbon nanotubes: Theoretical predictions and experimental measurements. *C. R. Physique.* 4: 993–1008.

Saller, R., R. Meier, and R. Brignoli. 2001. The use of silymarin in the treatment of liver diseases. *Drugs* 61: 2035–2063.

Sanati, A. L., H. Karimi-Maleh, A. Badiei, P. Biparva, and A. A. Ensafi. 2014. A voltammetric sensor based on NiO/CNTs ionic liquid carbon paste electrode for determination of morphine in the presence of diclofenac. *Mater. Sci. Eng. C* 35: 379–385.

Sanghavi, B. J., S. M. Mobin, P. Mathur, G. K. Lahiri, and A. K. Srivastava. 2013. Biomimetic sensor for certain catecholamines employing copper(II) complex and silver nanoparticle modified glassy carbon paste electrode. *Biosensors and Bioelectronics* 39: 124–132.

Shahmiri, M. R., A. Bahari, H. Karimi-Maleh, R. Hosseinzadeh, and N. Mirnia. 2013. Ethynylferrocene–NiO/MWCNT nanocomposite modified carbon paste electrode as a novel voltammetric sensor for simultaneous determination of glutathione and acetaminophen. *Sensor. Actuator. B* 177: 70–77.

Shi, Y., Z. Liu, B. Zhao, Y. Sun, F. Xu, Y. Zhang, Z. Wen, H. Yang, and Z. Li. 2011. Carbon nanotube decorated with silver nanoparticles via noncovalent interaction for a novel nonenzymatic sensor towards hydrogen peroxide reduction. *J. Electroanal. Chem.* 656: 29–33.

Sims, M. J., Q. Li, R. T. Kachoosangi, G. G. Wildgoose, and R. G. Compton. 2009. Using multiwalled carbon nanotube modified electrodes for the adsorptive striping voltammetric determination of hesperidin. *Electrochim. Acta* 54: 5030–5034.

Singh, R., T. Premkumar, J. Shin, and K. E. Geckeler. 2010. Carbon nanotube and gold-based materials: A symbiosis. *Chem. Eur. J.* 16: 1728–1743.

Supalkova, V., H. Stavelikova, S. Krizkova, V. Adam, A. Horna, L. Havel, P. Ryant, P. Babula, and R. Kizek. 2007. Study of capsaicin content in various parts of pepper fruit by Liquid Chromatography with electrochemical detection. *Acta Chim. Slov.* 54: 55–59.

Tashkhourian, J., M. R. Hormozi Nezhad, J. Khodavesi, and S. Javadi. 2009. Silver nanoparticles modified carbon nanotube paste electrode for simultaneous determination of dopamine and ascorbic acid. *J. Electroanal. Chem.* 633: 85–91.

Tavana, T., M. A. Khalilzadeh, H. Karimi-Maleh, A. A. Ensafi, H. Beitollahi, and D. Zareyee. 2012. Sensitive voltammetric determination of epinephrine in the presence of acetaminophen at a novel ionic liquid modified carbon nanotubes paste electrode. *J. Mol. Liq.* 168: 69–74.

Trouillas, P., P. Marsal, A. Svobodová, J. Vostálová, R. Gažák, J. Hrbáć, P. Sedmera, et al. 2008. Mechanism of the antioxidant action of silybin and 2,3-dehydrosilybin flavonolignans: A joint experimental and theoretical study. *J. Phys. Chem. A* 112: 1054–1063.

Wang, J., M. Li, Z. Shi, N. Li, and Z. Gu. 2002. Investigation of the electrocatalytic behavior of single-wall carbon nanotube films on an Au electrode. *Microchem. J.* 73: 325–333.

Wang, S. G., Q. Zhang, R. Wang, S. F. Yoon, J. Ahn, D. J. Yang, J. Z. Tian, J. Q. Li, and Q. Zhou. 2003. Multi-walled carbon nanotubes for the immobilization of enzyme in glucose biosensors. *Electrochem. Commun.* 5: 800–803.

Wang, T., M. Kaempgen, P. Nopphawan, G. Wee, S. Mhaisalkar, and M. Srinivasan. 2010. Silver nanoparticle-decorated carbon nanotubes as bifunctional gas-diffusion electrodes for zinc–air batteries. *J. Power Sources* 195: 4350–4355.

Zhang, M., and W. Gorski. 2005. Electrochemical sensing based on redox mediation at carbon nanotubes. *Anal. Chem.* 77: 3960–3965.

Biosensors and Bioelectronics 83 (2016) 45–53

Contents lists available at ScienceDirect

Biosensors and Bioelectronics

journal homepage: www.elsevier.com/locate/bios

Electrochemical sensing platform amplified with a nanobiocomposite of L-phenylalanine ammonia-lyase enzyme for the detection of capsaicin

Myalowenkosi I. Sabela [a,*], Thabani Mpanza [a,b], Suvardhan Kanchi [a,*], Deepali Sharma [a], Krishna Bisetty [a,*]

[a] Department of Chemistry, Durban University of Technology, P.O Box 1334, Durban 4000, South Africa
[b] Department of Chemistry, Mangosuthu University of Technology, P.O. Box 12363, Jacobs 4026, South Africa

ARTICLE INFO

Article history:
Received 11 January 2016
Received in revised form
12 April 2016
Accepted 13 April 2016
Available online 14 April 2016

Keywords:
Capsaicin
Phenylalanine ammonia lyase
Differential pulse voltammetry
Electrochemical biosensor
Food samples
Molecular docking

ABSTRACT

The present study involves the development of a sensitive electrochemical biosensor for the determination of capsaicin extracted from chilli fruits, based on a novel signal amplification strategy using enzyme technology. For the first time, platinum electrode modified with multiwalled carbon nanotubes where phenylalanine ammonia-lyase enzyme was immobilized using nafion was characterized by attenuated total reflectance infrared spectroscopy, transmittance electron microscopy and thermo-gravimetric analysis supported by computational methods. Cyclic and differential pulse voltammetry measurements were performed to better understand the redox mechanism of capsaicin. The performance of the developed electrochemical biosensor was tested using spiked samples with recoveries ranging from 98.9 to 99.6%. The comparison of the results obtained from bare and modified platinum electrodes revealed the sensitivity of the developed biosensor, having a detection limit (S/N=3) of 0.1863 μg mL^{-1} and electron transfer rate constant (*ks*) of 3.02 s^{-1}. Furthermore, adsorption and ligand-enzyme docking studies were carried out to better understand the redox mechanisms supported by density functional theory calculations. These results revealed that capsaicin forms hydrogen bonds with GLU355, GLU541, GLU586, ARG and other amino acids of the hydrophobic channel of the binding sites thereby facilitating the redox reaction for the detection of capsaicin.

1. Introduction

Capsaicin (8-methyl-*N*-vanillyl-trans-6-nonenamide), is an alkaloid compound found mainly in hot chilli peppers and fruits (capsicum annum and capsicum frutescence) (Reilly et al., 2001; Srinivasan, 2015). Together with its derivative, dihydrocapsaicin, they have a strongest burning effects that is believed to be evolved as a plant protection against herbivores (Supalkova et al., 2007). Capsaicinoids have been reported to have high antioxidant activity (Henderson et al., 1999), anti-tumoral (Sanchez et al., 2006), anti-bacterial (Satyanarayana, 2006) and anti-carcinogenic properties (Huynh and Teel, 2005). Capsaicin has been used for different applications in the past; for example: manufacturing of spices, chilli sauces, pain-inducing defensive pepper sprays (Pershing et al., 2006) and creams for the treatment of painful conditions such as psoriasis, rheumatoid arthritis, diabetic neuropathy, cluster headache and reflex sympathetic dystrophy (Hautkappe et al., 1998). Sanchez and co-workers have reported capsaicin as a promising anti-tumor agent in hormone^{-}refractory prostate cancer (Sanchez et al., 2006). It has also been reported that the metabolism of capsaicinoids by enzymes such as P450 can produce reactive electrophiles capable of modifying biological macromolecules (Reilly and Yost, 2006).

Literature studies revealed that carbon nanotubes (CNTs), due to their unique sensing properties have received considerable attention in the field of electrochemical sensing. Some of their unique properties includes excellent conductivity, large surface area and good biocompatibility (Bathinapatla et al., 2015, 2016; Dresselhaus et al., 1988; Hu and Hu, 2009; Wang and Dai, 2015). For this purpose, they are widely used in electronic, biomedical, pharmaceutical, catalytic, analytical and material fields. Additionally, their special nanostructural properties are attributed to their overwhelming advantages in fabricating electrochemical sensors.

* Corresponding authors.
E-mail addresses: myalosabela@gmail.com (M.I. Sabela), ksuvardhan@gmail.com (S. Kanchi), bisettyk@dut.ac.za (K. Bisetty).

http://dx.doi.org/10.1016/j.bios.2016.04.037
0956-5663/

The CNT-based electrochemical transducers offer substantial improvements in the performance of amperometric enzyme electrodes, immunosensors and biosensors (Kachoosangi et al., 2008; Lyons and Keeley, 2008; Wang, 2005). Specifically, phenylalanine ammonia-lyase received much attention for studies involving the regulation of phenolic biosynthesis. The phenolic portion of capsaicinoids is formed from phenylalanine as a product in the phenylpropanoid pathway (Reyes-Escogido et al., 2011; Sutoh et al., 2006). This enzyme possesses primary features of an electron mediator, because of its stability and good catalytic activity. Electron transfer in biological systems is one of the key reasons for considerable interest in the direct electron transfer between redox enzyme and electrode surfaces (Kuznetsov and Ulstrup, 1999).

In the past, several methods have been reported for the determination of capsaicin, namely: Scoville organoleptic test (Kachoosangi et al., 2008), high performance liquid chromatography (Othman et al., 2011; Supalkova et al., 2007), thin layer chromatography (Spanyar and Blazovich, 1969), UV–vis spectroscopy (Othman et al., 2011), optical biosensor (Mohammad et al., 2014) and electrochemistry (Kachoosangi et al., 2008; Manaia et al., 2012; Mohammad et al., 2013; Randviir et al., 2013; Ya et al., 2012; Yardım and Şentürk, 2013).

However the classical method, 'Scoville Organoleptic Test' suffers from few drawbacks such as cost factor, lack of proximity and poor sensitivity. On the other hand, HPLC methods have some limitations like elaborate sample preparation, high cost of instrument, and sample preparation for the detection of capsaicinoids. Recently, Xue and co-workers reported an electrochemical sensor for the detection of capsaicin using mesoporous cellular foams (Xue et al., 2015). To the best of our knowledge, this is the first electrochemical biosensor using PAL/Nafion/MWCNTs/Pt-E reported for the detection of capsaicin. The developed biosensor offers advantages such as reproducibility, repeatability, precision, accuracy and objectivity over the classical Scoville and HPLC methods. The PAL/Nafion/MWCNTs/Pt-E biosensor is simple, cost effective and sensitive compared to existing chromatographic methods.

Capsaicin is a hydrophobic molecule, characterized into 3 functional groups; the aromatic head group with hydrogen bond potentiality, the dipolar amide bond region and the hydrophobic tail (see supplementary data, Fig. S1). The approach used in this work took advantage of the characteristic feature of this molecule probing its ability to undergo redox process through enzymatic reactions. Accordingly, this work reports on the performance of a platinum electrode (Pt-E) modified with multiwalled carbon nanotubes (MWCNTs) coated with phenylalanine ammonia-lyase (PAL) enzyme infused with nafion. The PAL enzyme was chosen for the electrochemical redox reaction of capsaicin and its related compounds due to its good catalytic activity. In addition, adsorption of the enzyme on the MWCNTs along with the interaction between the enzyme and capsaicin molecule were performed using molecular docking studies. Moreover, the electrochemical methods employed in this study demonstrated the proof-of-concept that this approach can easily be incorporated into a biosensing device that is relatively simple and less expensive, in contrast to the existing Scoville test and HPLC methods used in the food industry.

2. Experimental

2.1. Instrumentation

Voltammetric measurements were carried out using a three electrode system in an electrochemical cell (Metrohm, Herisau, Switzerland) consisting of a 3 mm diameter disc-working electrode (Pt-E); Ag/AgCl as a reference (saturated AgCl, 3 M KCl) electrode, and the platinum wire as a counter electrode using a 797 VA Computrace instrument. A 781 pH/ion meter coupled with an 801 stirrer (Metrohm, Herisau, Switzerland) was used to adjust the pH of the buffer solutions at room temperature. All working solutions including the buffer were prepared with deionized water from a water purification system, Aqua MaxTM Basic 360 (Trilab, South Africa (SA)). Since MWCNTs are insoluble in most solvents, sonication in DMF was employed using an Ultra-sonic 50,194 (Labcon, SA) for effective dispersion, prior to immobilization on Pt-E. The Scientific oven Series 2000 was used to evaporate DMF. The attenuated total reflectance (ATR) spectra were obtained using Perkin-Elmer FTIR, Midrand, South Africa. Thermal analysis studies were carried out on the TGA/DSC, 1 SF/1346 model operating on a STAR^e Software version 9.20 supplied by Mettler Toledo (Johannesburg, SA). The samples were placed in a 10 μL alumina sample holder for thermal analysis at a heating rate of 10 °C min^{-1}.

2.2. Reagents and chemicals

All chemicals were of analytical grade and used as received without any further purification. Capsaicin-360376-IG (cas no. 404–86–4) and 20–30% MWCNT basis, O.D. × L 7–12 nm × 0.5–10 μm (cas number 308,068–56–6) were purchased from Sigma Aldrich (Durban, SA). *N,N*-dimethylformamide (DMF) (cas no. 68–12–2), glacial acetic acid (cas no. 64–19–7) and sodium acetate anhydrous were supplied by Associated Chemical Enterprises (Johannesburg, SA). Nitrogen gas (99.9% purity) was obtained from AFROX (Durban, SA). Ethanol (absolute, 99.9%) used for extraction of samples and nafion (cas no. 31,175–20–9), were supplied by Capital Lab Supplies (Durban, SA). Phenylalanine ammonia lyase-*Rhodotorula glutanis* (PAL) (101M8617) was purchased from Sigma-Aldrich, USA.

2.3. Preparation of working solutions

Sodium acetate buffer solution of pH 4.0 was prepared by mixing sodium acetate and acetic acid (0.1 M each) in a ratio of 15:85 respectively. This solution was then stored at 4 °C until used. The solution of PAL enzyme was prepared by adding approximately 3.0 mg into 1 mL of 67 mM phosphate buffer solution (pH 7.4). The standard solution of capsaicin was prepared by dissolving approximately 10 mg capsaicin standard powder in 100 mL of absolute ethanol (99.9% purity) to produce 100 mg L^{-1} standard solution and refrigerated at 4 °C.

2.4. Preparation of PAL/Nafion/MWCNTs/Pt-E

The bare Pt-E was prepared manually by polishing on a mirror like surface with an alumina slurry (≤ 3 μm) and then rinsed with distilled water. Then, the MWCNTs previously dispersed in DMF (5 mg in 1 mL) and sonicated for 5 min were immobilized onto the surface of the Pt-E by dropping 10 μL aliquot and oven-dried at 50 °C. Later, ~ 10 μL of 5% nafion solution was casted to form a film on MWCNTs/Pt-E. The PAL enzyme was physically adsorbed on the Nafion/MWCNTs/Pt-E surface by dropping 10 μL and allowing the solvent to dry at room temperature for 2 h. The modified PAL/Nafion/MWCNTs/Pt-E electrode was then rinsed with the buffer solution prior to the electrochemical determinations. The optimized electrochemical detection conditions were as follows: 10 mL of 0.1 M acetate buffer solution pH 4.0 used as an electrolyte, 0.2 mL chilli extract and scan rate of 0.01 V s^{-1}.

2.5. Sample preparation

Capsaicin was extracted from chilli fruits as reported in the Methods section (Mpanza et al., 2014; Othman et al., 2011). Briefly, 100 g of the crushed chilli pepper fruits were transferred into a 500 mL round bottom flask containing 350 mL of absolute ethanol. The mixture was refluxed for 2 h and the solid residue was removed by filtration through a Whatman filter paper of 0.45 μm pore size and discarded. Furthermore, the reddish-brown filtrate was distilled to remove the excess ethanol from the extract. The remaining chilli extracts were refrigerated at 4 °C for subsequent electrochemical studies.

2.6. Computational methodology

2.6.1. Procedure for interaction of PAL with capsaicin using molecular docking

The crystal structure of the PAL enzyme was obtained from the RCSB Protein Data Bank (ID1T6J) (Calabrese et al., 2004) in a complex form. The whole enzyme was selected and hydrogen atoms were added. Then the water and the residue molecules present in the enzyme structure were removed. Furthermore, the structure was cleaned to have a desirable confirmation. The CHARMm forcefield was applied to enzyme while the protonation occurred at pH 7.4, corresponding to an ionic strength of 0.145. The ionization and residue *pKa* demonstrated that the enzyme possessed a zero charge at pH 7.7 and electrostatic energy of -36.00 kJ mol^{-1}.

Capsaicin ligand obtained from pubchem (CID: 1,548943) database was optimized with Gaussian 09 (Frisch et al., 2009) and thereafter the conformation with the lowest energy was used for the docking simulation using Discovery Studio 4.0 (Wu et al., 2003). Docking studies were performed using the CDOCKER module in Discovery studio 4.0, whereby the PAL enzyme was held rigid while the capsaicin ligands were flexible. The CHARMm forcefield was used as an energy grid forcefield for docking and scoring function calculations. The conformation with the highest docking score obtained by CDOCKER energy was used for the binding energy calculations.

3. Results and discussion

3.1. Characterization of PAL/Nafion/MWCNTs/Pt-E

The TEM image obtained for PAL/Nafion/MWCNTs nanobiocomposite was shown in Fig. 1A. There was no sputtering done onto samples prior to microscopic studies as the resolution of the nanotubes was adequate. The PAL/Nafion/MWCNTs nanobiocomposite exhibited a more dense structural morphology with a hollow wired structure of the regular pure MWCNTs. The enzyme immobilization, on the surface was not attached in a unique fashion. The ATR-IR spectrum in Fig. 1B was recorded in the range 4000–500 cm^{-1}. The spectrum of pure MWCNTs showed a peak at 1740 cm^{-1}, assigned to the stretching mode of C=C bonds that formed the carbon nanotubes side wall framework. The peak observed at 2962 cm^{-1} corresponds to C-H asymmetric and symmetric stretching modes. However, a less intense and broader peak observed at 3312 cm^{-1} corresponds to the O-H group of the carboxylic acid. In the case of PAL/Nafion/MWCNTs spectrum, a broader peak at 3312 cm^{-1} is attributed to the O-H stretching, whereas peaks observed at 2962 cm^{-1} corresponds to C-H stretching bands. The peak observed at 1638 cm^{-1} is assigned to the C=C bond stretch while the 1037 cm^{-1} peak attributed to an

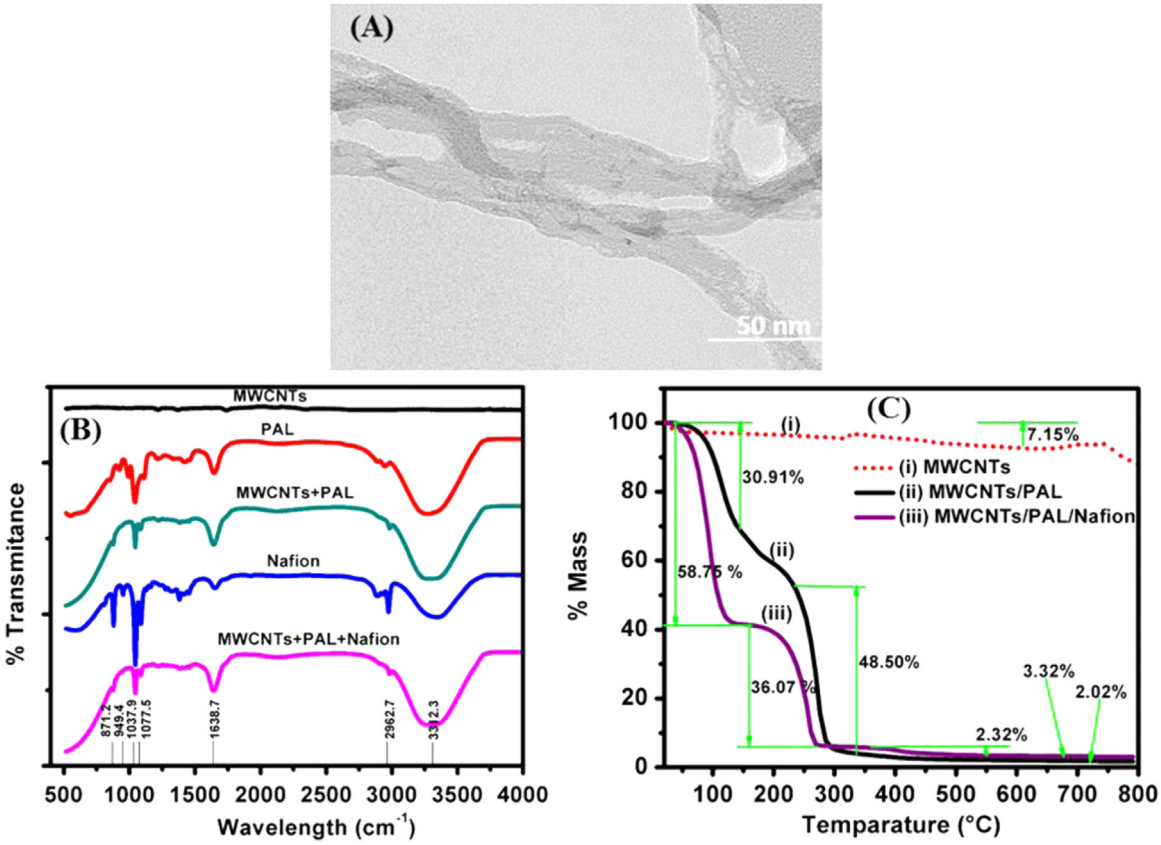

Fig. 1. TEM image of (**A**) PAL/Nafion/MWCNTs nanobiocomposite (**B**) ATR-IR spectra of MWCNTs, PAL enzyme, PAL/MWCNTs, Nafion and PAL/Nafion/MWCNTs (**C**) TGA curves of (i) MWCNTs, (ii) PAL/MWCNTs and (iii) PAL/Nafion/MWCNTs.

aromatic C-H bend. The pure nafion spectrum showed C-O-C, S-O and CF_2 stretching vibrations at 871 cm^{-1}, 1045 cm^{-1} and 1077 cm^{-1} respectively. The spectrum also showed a broader O-H stretching at 3312 cm^{-1} and C-H alkyl group stretching at 2963 cm^{-1}. The PAL enzyme spectrum has an amide bond peak observed at 1639 cm^{-1} that remains prominent in the final composite used for Pt-E modification.

The electrode composite was further studied for thermal stability and quantification of the composition by thermal gravimetric analysis (TGA) as illustrated in Fig. 1C. This approach was very informative for understanding the thickness of the Pt-E surface corresponding to the modification of each layer. The MWCNTs curve showed a change in mass (decomposition temperature) at 350 °C, another typical gradient drop in mass is noticed at about 750 °C, due to the oxidation of carbon (Bom et al., 2002). The MWCNTs modified with PAL enzyme showed a TGA profile with two shoulders observed at 56 °C and 248 °C, with a mass loss of 30.91% and 48.50%, respectively. The first mass loss phase in PAL/MWCNTs curve can be attributed to the irreversible thermal denaturation of the enzyme, normal dehydration process of PAL and the loss of DMF which was used as a dispersion medium. Beyond 248 °C a further drop in mass percentage is observed due to the melting and decomposition processes of PAL around 300 °C. The PAL/Nafion/MWCNTs curve showed similar trends to that of PAL/MWCNTs, but with a higher loss of 58.75% in the first step followed by a 36.07% loss. Interestingly, there is an additional mass loss step of 2.32% between 390 °C and 400 °C, beyond that 3.32% is left behind with a slightly greater than 2.02% that is retained from PAL/Nafion/MWCNTs. This conforms that the addition of PAL/Nafion does improve the thermal stability of the nanobiocomposite and most likely the ionic polymer, nafion, improve the interfacial adhesion of PAL on the MWCNTs.

3.2. Electrochemical characterization of PAL/Nafion/MWCNTs/Pt-E

Electrochemical determination of capsaicin was explored by cyclic voltammetry (CV) and differential pulse voltammetry (DPV) signals. The analyses were conducted using bare and modified Pt-E with PAL/Nafion/MWCNTs as depicted in Scheme, 1. The Pt-E has been widely used for several decades because of its excellent corrosion resistance and good electrical conductivity.

The bare Pt-E was mechanically polished as described in previous studies (Bathinapatla et al., 2015, 2016; Mpanza et al., 2014) and thereafter modified to obtain the CV and DPV scans are illustrated in Fig. 2A and B. In both the scans it is evident that a biosensor exhibited higher capsaicin peak currents than the bare and PAL/Nafion/MWCNTs/Pt-E respectively.

In Fig. 2A, the CV scans of a bare Pt-E showed only prominent oxidation peak (*pa1*) at 0.58 V with 9.55 μA and reduction peak (*pc2*) at 0.32 V. The non-existence of the second peak (*pa2*) around 0.35 ± 0.03 V is noticed which raises concern about the sensitivity of the bare Pt-E. When MWCNTs were introduced, the second oxidation peak (*pa2*) was detected at 0.38 V. This is a good reflection of the improvement in the sensitivity of the electrode upon addition of MWCNTs to the bare Pt-E. Moreover, the presence of MWCNTs changed the detection capability of the electrode completely as the current of *pa1* increased to 51.75 μA and therefore, there is a significant difference in the current signal of both CV and DPV in contrast to the bare Pt-E. The PAL enzyme further enhanced sensitivity of the modified electrode to 59.37 μA; this is attributed to a better surface area and electrical conductivity of the nanobiocomposite, resulting in an additional reduction peak (*pc1*) observed at 0.57 V. The DPV scans in Fig. 2B also followed the same pattern as CV scans (Fig. 2A), where the introduction of MWCNTs drastically increased the sensitivity of the Pt-E. This confirmed that the electrochemical oxidation of capsaicin at the PAL/Nafion/MWCNTs electrode was a diffusion-controlled process described by the following equation for *pa1* and *pa2*:

$$E_p - E_{p/2} = \frac{1.857RT}{\alpha F} = \frac{47.7}{\alpha} mV \quad (1)$$

Where, E_p and $E_{p/2}$ represent the peak potential and the half-height, α is the electron transfer coefficient, *R* and *F* represent the usual significance (Li et al., 2015). The charge transfer coefficient (α) was calculated to be 0.25 and of 0.17 for *pa2* and *pa1*, respectively. Thereafter, the electron transfer rate constant (*ks*) was calculated using Laviron"s equation at modified electrode for a

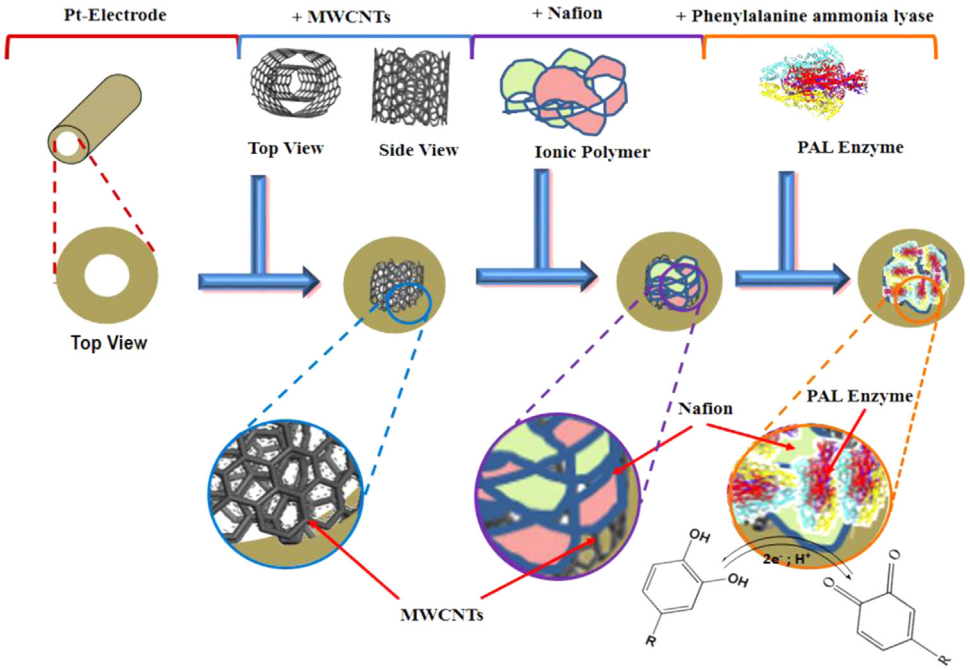

Scheme 1. Pt-E modification with PAL/Nafion/MWCNTs for the detection of capsaicin.

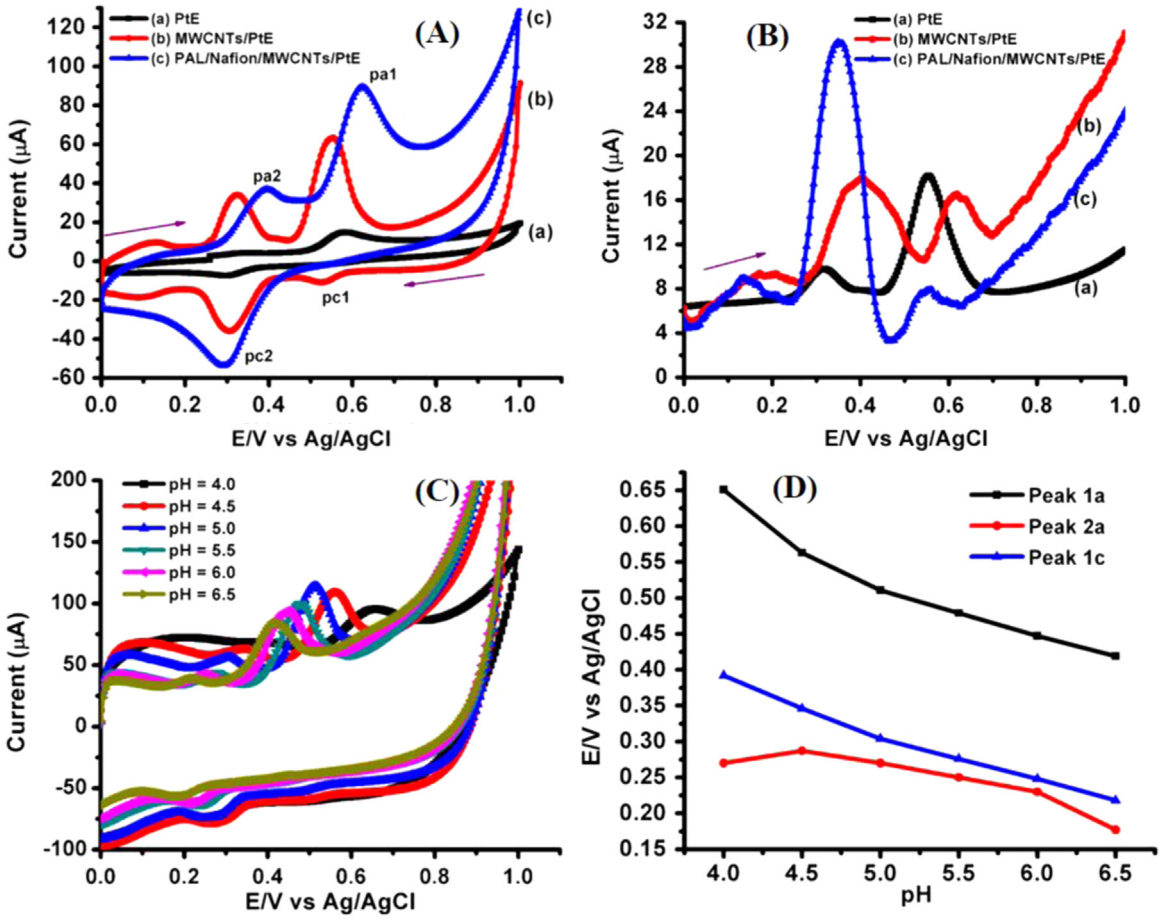

Fig. 2. Voltammograms for (**A**) Cyclic and (**B**) Differential pulse voltammetric responses of capsaicin at 0.1 V (vs Ag/AgCl) with the bare Pt-E (curve a), MWCNTs/Pt-E (curve b) and PAL/Nafion/MWCNTs/Pt-E (curve c). (**C-D**) Effect of pH on peak potential (V) and peak current (I_p) for electrochemical detection of capsaicin between 4.0 and 6.5. Optimized conditions: Deposition potential =0.5 V; Deposition time =60 s; Scan rate =0.1 V s^{-1} for 5 cycles.

charge transfer coefficient (α) of 0.42 at 100 mV s^{-1} on a quasi-reversible reduction peak at 0.1 V (versus Ag/AgCl) (Laviron, 1979a, 1979a, 1979b).

$$logks = \alpha\log(1-\alpha) + (1-\alpha)\log\alpha - \log\frac{RT}{nFv} - \frac{(1-\alpha)\alpha nF\Delta E_p}{2.3RT} \quad (2)$$

Where, R is the gas constant (8.314 J K^{-1} mol^{-1}), T is the temperature (298 K), F is the Faraday constant (96,485 C mol^{-1}), ΔEp represents the peak-to-peak separation ($\Delta Ep = (E_{pa}+E_{pc})/2$), v is the scan rate in V s^{-1}; n is the number of electrons transferred. The *ks* value of the PAL/Nafion/MWCNTs/Pt-E was calculated to be 3.02 s^{-1}. One can deduce that this is probably due to larger surface area of the Nafion/MWCNTs/Pt-E in comparison to the bare Pt-E, and due to the catalytic activity of PAL enzyme on the modified Pt-E. Furthermore, higher the peak current for PAL/Nafion/MWCNTs/Pt-E and MWCNTs/Pt-E signals compared to bare Pt-E, stronger the adsorption effect on modified Pt-E than on the bare Pt-E. It was interesting to notice that the oxidation and reduction peak heights are significantly increased in the order of bare Pt-E < MWCNTs/Pt-E < PAL/Nafion/MWCNTs/Pt-E. The PAL/Nafion/MWCNTs/Pt-E superiority over bare Pt-E is based on it catalytic activity, surface area and significant diffusion process of capsaicin on a modified Pt-E based electrochemical biosensor.

3.3. Optimization of pH and scan rate based on peak currents

Using the nanobiocomposite PAL/Nafion/MWCNTs/Pt-E, the influence of the pH ranging from 4.0 to 6.5 on the detection of capsaicin was evaluated. Fig. 2C shows almost all the peaks shifted linearly towards a lower potential with an increase in pH. However, the corresponding current density dropped significantly in the case of *pa2* and *pc2*, indicating that the redox mechanisms corresponding to the catechol and 1, 2 benzoquinone rings were not favoured at higher pHs.

The effect of pH on both the current and potential of *pa1* and *pa2* are illustrated in Fig. 2D similar behaviour were observed for the scan rates between 0.1 and 1.0 V s^{-1} for capsaicin in 0.1 M acetate buffer of pH 4.0. The relationship between E_{pa} and ln v (see supplementary data, Fig. S2) of the scan rates followed the equations: $E_{pa2}=0.102$ ln $v+0.5252$ ($R^2=0.9888$) and $E_{pa1}=0.0937$ ln $v+0.7843$ ($R^2=0.9608$). The redox reaction in the last step (III) of the mechanism (Scheme, 2) was displayed in CV as *pc2* and *pa1*. At an optimum scan rate of 100 mV s^{-1}, PAL/Nafion/MWCNTs/Pt-E showed 79.37 μA of the peak current which was 8-fold compared to peak current measured at bare Pt-E (9.55 μA) indicated a fair catalytic activity of the nanobiocomposite materials.

3.4. Redox mechanism of capsaicin

From the mechanism for the electrochemical oxidation/reduction of capsaicin (Kachoosangi et al., 2008) shown in Scheme, 2, illustrates that the chemical structure in "I" has a guaiacol ring, a benzene with –OH and OCH_3 substituents. It losses H^+ from the alcohol group forming the intermediate structure "II" which further breaks the ethyl group through hydrolysis in acidic medium to become benzoquinone. The benzoquinone is much more stable than the guaiacol ring and therefore, one reversible peak is observed in the CV due to the formation of the catechol with the gain

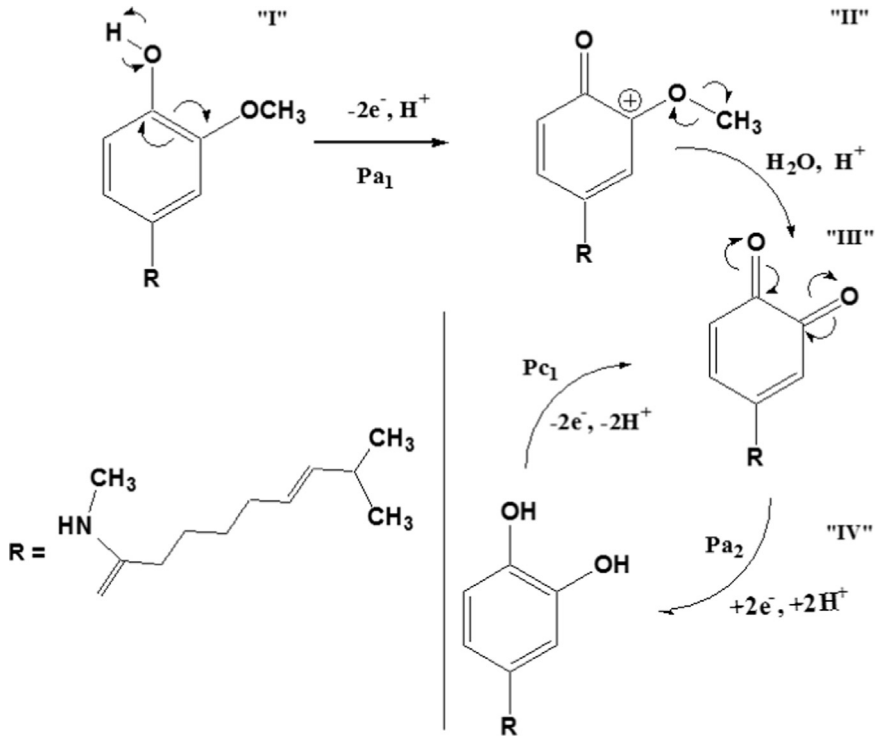

Scheme 2. Mechanism for the electrochemical oxidation/reduction of capsaicin. Pa and Pc refers to the anodic and cathodic peaks respectively.

of $2e^-$ and $2\ h^+$ ions. Overall, it is significant that the conversion of capsaicin by losing H^+ions (guaiacol to benzophenone) is a forward reaction attributed to *pa1* in Fig. 2A. The reaction between benzoquinone and catechol is reversible as represented by *pc1* and *pc2*, respectively in Fig. 2A (Kachoosangi et al., 2008; Xue et al., 2015).

3.5. Reproducibility, repeatability and stability of PAL/Nafion/MWCNTs/Pt-E

The reproducibility and repeatability of the developed electrochemical biosensor were evaluated at 0.25 μg mL^{-1} of capsaicin. The obtained current variation measurements using the PAL/Nafion/MWCNTs/Pt-E suggests acceptable repeatability with RSD values ranging from 4.56% to 7.31% (n=6). The reproducibility measurements were obtained using the different electrodes for same capsaicin concentration resulting in promising RSD values of 2.10–4.93% (n=6). The obtained RSD values indicates that the results were reproducible using PAL/Nafion/MWCNTs/Pt-E. The stability of the developed electrochemical biosensor was studied by determining the current response in 0.25 μg mL^{-1} of capsaicin for six replicate measurements (n=6) over three successive days using the same coating. The electrochemical biosensor maintained 91% of its original response by the third day, hence its activity was retained to a large extent. The data obtained by PAL/Nafion/MWCNTs/Pt-E for the detection of capsaicin was compared with the already reported methods in the literature as shown in Table, 1.

3.6. Effect of interferences on detection of capsaicin

The selectivity of the present electrochemical biosensor towards capsaicin was evaluated by the simultaneous addition of some common organic and inorganic compounds. The interferents such as catechol (25 μg mL^{-1}) and their derivatives (urushiol, catecholamine, catechin) (25 μg mL^{-1}), 4-chlorophenol (25 μg mL^{-1}), dichlorophenol (25 μg mL^{-1}), trichlorophenol (25 μg mL^{-1}), pentachlorophenol (25 μg mL^{-1}), Na^+ (25 μg mL^{-1}), Mg^{2+}(25 μg mL^{-1}), and K^+(25 μg mL^{-1}) were added to 0. 45 μg mL^{-1} of standard capsaicin solution and then current responses were measured. The obtained results revealed that there were no changes in the current response. The applied tolerance limit for the interference species at the maximum concentration resulted in a relative error of ±5%. However, 50-fold catechol and their derivatives and 10-fold 4-cholorophenol, dichlorophenol, trichlorophenol, pentachlorophenol, Na^+, $Mg^{2+}$and K^+had no effect on the detection of capsaicin. Therefore, our results indicates that the developed electrochemical biosensor, PAL/Nafion/MWCNTs/Pt-E has an excellent selectivity for the detection of capsaicin.

3.7. Real sample analysis

In order to convert an electrochemical sensor into a biosensor, the PAL enzyme was immobilized on the Nafion/MWCNTs/Pt-E. The developed electrochemical biosensor contributed to a better performance and higher sensitivity for the detection of capsaicin in real samples. The capsaicin peaks observed in Fig. 3A, with a correlation coefficient of R^2=0.9987, slope of 0.189 ± 0.003 and the intercept of 10.781 ± 0.213 μA.

The PAL enzyme improved the interfacial adhesion through carboxylation with MWCNTs under acidic conditions and anchored onto the MWCNTs exhibiting catalytic activity and promoting the direct electron transfer for the detection of capsaicin which enhances the sensitivity of electrochemical biosensor. In 0.1 M acetate buffer solution (pH 4.0), the DPV response of the PAL/Nafion/MWCNTs/Pt-E sensor to capsaicin increased about 8-fold as compared with the Nafion/MWCNTs/Pt-E sensor, with a detection limit of (S/N=3) 0.1863 μg mL^{-1}. The capsaicinoid equivalent extracted from the chilli pepper fruits showed a mass percentage of 67.08% and 68.30% (m/m) with a relative standard deviations of 2.32 (n=6) and 1.92 (n=6) using electrochemical biosensor and HPLC, respectively. Clearly, the poor standard deviation is attributed to inconsistencies with the regeneration of exactly the same

Table 1
Comparison of present electrochemical biosensor with the reported analytical methods for the detection of capsaicin.

Analytical method	Electrode modification	Analytical parameters		Merits/Demerits	Citation
		R^2	LOD's		
LSV/SWV/DPV/Amperometry	MCFs/CPE	0.9990	0.08 μM	Good Linearity, low detection limits, excellent performance, but less stable	(Xue et al., 2015)
Amperometry	HRP/Ferrocene	0.998	1.94 μM	Biosensor is simple but less stable and sensitive	(Mohammad et al., 2013)
AdsSV	Boron-Doped Diamond Electrode	0.986	0.034 μM	The detection limits were satisfactory, but the electrode is highly expensive	(Yardım, 2011)
SPME-GC–MS	–	0.9970	0.014 μg mL^{-1}	Low detection limits were achieved, but very expensive instrumentation	(Peña-Alvarez et al., 2009)
AdsSV	MWCNT/SPE	0.996	0.31 μM	Fair performance, but the detection limits were high and life time of the electrode is less	(Kachoosangi et al., 2008)
UV-Visible	MBTH/Sol-gel/Butyl acrylate/HRP/Chitosan	0.986	51.92 ppm	The technique is cost effective, but LOD's were very high. The electrode modification is complicated involves too many components with poor performance	(Mohammad et al., 2014)
CE	–	0.9994	0.66 μg mL^{-1}	High detection limits	(Liu et al., 2010)
HPLC	–	0.998	0.09 μg g^{-1}	Expensive technique and elaborate sampling procedure is required	(Othman et al., 2011)
AdsSV	Pencil Graphite Electrode	0.997	1.12 ng mL^{-1}	Cost Effective electrode modification with excellent detection limit	(Yardım and Şentürk, 2013)
EIS-CV	MWCNT-SPE	0.99	0.45 μM	The electrode modification is cost effective, but achieved high detection limits	(Randviir et al., 2013)
LSV	MS-NH_2-FMS-CPE	0.9965	0.020 μmol L^{-1}	Good Recoveries with low detection limit	(Ya et al., 2012)
DPV	PAL/Nafion/MWCNTs/Pt-E	0.9987	0.1863 μg mL^{-1}	Good reproducibility, repeatability, stability of the electrode material. Fair recoveries were achieved. PAL/Nafion/MWCNTs/Pt-E is an anti-interferent material for capsaicin detection	This work

SPME: Solid Phase Micro Extraction, GC–MS: Gas Chromatography-Mass Spectroscopy, HPLC: High Performance Liquid Chromatography, CE: Capillary Electrophoresis, EIS: Electrochemical Impedance Spectroscopy, LSV: Linear Sweep Voltammetry, SWV: Squarewave Voltammetry, DPV: Differential Pulse Voltammetry, AdsSV: Adsorptive Stripping Voltammetry, CV: Cyclic Voltammetry, CPE: Carbon Paste Electrode, SPE: Screen Printing Electrode, MCFs: Mesoporous Cellular Foams, HRP: Horseradish Peroxidase, MWCNTs: Multiwalled Carbon Nanotubes, MBTH: 3-methyl-2-benzothiazolinone hydrazine, MS: Mesoporous Silica, NH_2-FMS: Amino-functionalized mesoporous silica, PAL: Phenylalanine Ammonia Lyase

size of the nanobiocomposite onto the electrode surface. However, the percentage recoveries ranging from 98.9% to 99.6% (n=6) obtained from this study, suggests that the PAL/Nafion/MWCNTs/Pt-E biosensor is a superior electrochemical biosensor for the detection of capsaicin.

3.8. HOMO-LUMO calculations and molecular docking analysis

The electrons transferred from the highest occupied molecular orbitals (HOMO) in a molecule are related to its ability to undergo redox reactions. During the reduction process, the electrons move to the lowest unoccupied molecular orbital (LUMO). Therefore, using the density functional theory (DFT) calculations, the density of the electrons in the molecule can be located thereby predicting the active site of the ligand/molecule based on the electron density maps. The ability of the molecule to undergo redox reactions is dependent on the functional groups or atoms identified through DFT calculations. This should be in agreement with the redox mechanisms and the extent of HOMO-LUMO band gaps of the molecule (Bathinapatla et al., 2016). In this study, the geometry of the molecule was fully optimized at the DFT level using the 6–31+G(d) basis set. The loosely bound electrons in the HOMO shown in Fig. 3B are located in the carbonyl group of the guaiacol ring, in contrast to those displayed in the LOMO.

The redox mechanism (see Scheme, 2) for capsaicin is a quasi-reversible reduction reaction between the -OH and R-O-R groups of the guaiacol ring and the residues of the enzyme resulting in the reversible catechol ring. Therefore, the electron density is in agreement with redox mechanism as shown in Scheme, 2. Docking studies were used to assess the chemical interaction between the capsaicin and the PAL enzyme.

In order to ensure that the prepared ligand mimicked the experimental conditions used, it was allowed to ionize over a pH ranging from 6.5 to 8.5, whilst the tautomers were enumerated. Thereafter, full minimization was performed using a smart minimizer algorithm coupled with the CHARMm forcefield (Wu et al., 2003) using Discovery Studio 4.0. From the same ligand, a total of ten poses were generated with Monte-Carlo ligand conformation generation, and docked using a LigandFit shape filter into an active site of the PAL enzyme with 573.15 $Å^3$ that was derived based on the PDB site record (Venkatachalam et al., 2003). All ten poses were included in the calculation of the binding energies during which the ligand flexible receptor atom properties were created by In Situ Ligand Minimization that enabled the ligand optimization in the binding pocket of the PAL enzyme (Tirado-Rives and Jorgensen, 2006). The energy minimization involved 1000 steps of steepest descent with a RMS gradient tolerance of three followed by conjugate gradient minimization performed with a smart minimizer algorithm. Further analysis revealed that the three π-alkyl interactions with average distances of 4.75, 4.67, 5.03, and 4.51 Å were involved between PAL enzyme and capsaicin. Interestingly these interactions occurred on the hydrophobic end of capsaicin (Fig. 3C).

The hydrophobic map of the PAL enzyme revealed no hydrophobicity in the site and this led to the penetration with hydrogen bonds and hydrophilic interactions. The analysis of ten ligand poses (see supplementary data Table S1) revealed that ARG 596 residue was most favourable because of a stronger hydrogen bonding followed by ARG 450 with the highest hydrophobic counts. However, the conformation with the highest Docking Score (see supplementary data, Table S2 and Figs S3–5) had a seven hydrogen bonds (O-H) with the shortest distance of 1.61 Å between LYS545 and O1 of the carbonyl. Among these bonds, four of them involved oxygen atoms of the GLU residues as an acceptor for protons from the capsaicin molecule. Among the surrounding residues, GLU355 formed three hydrogen bonds, as the most

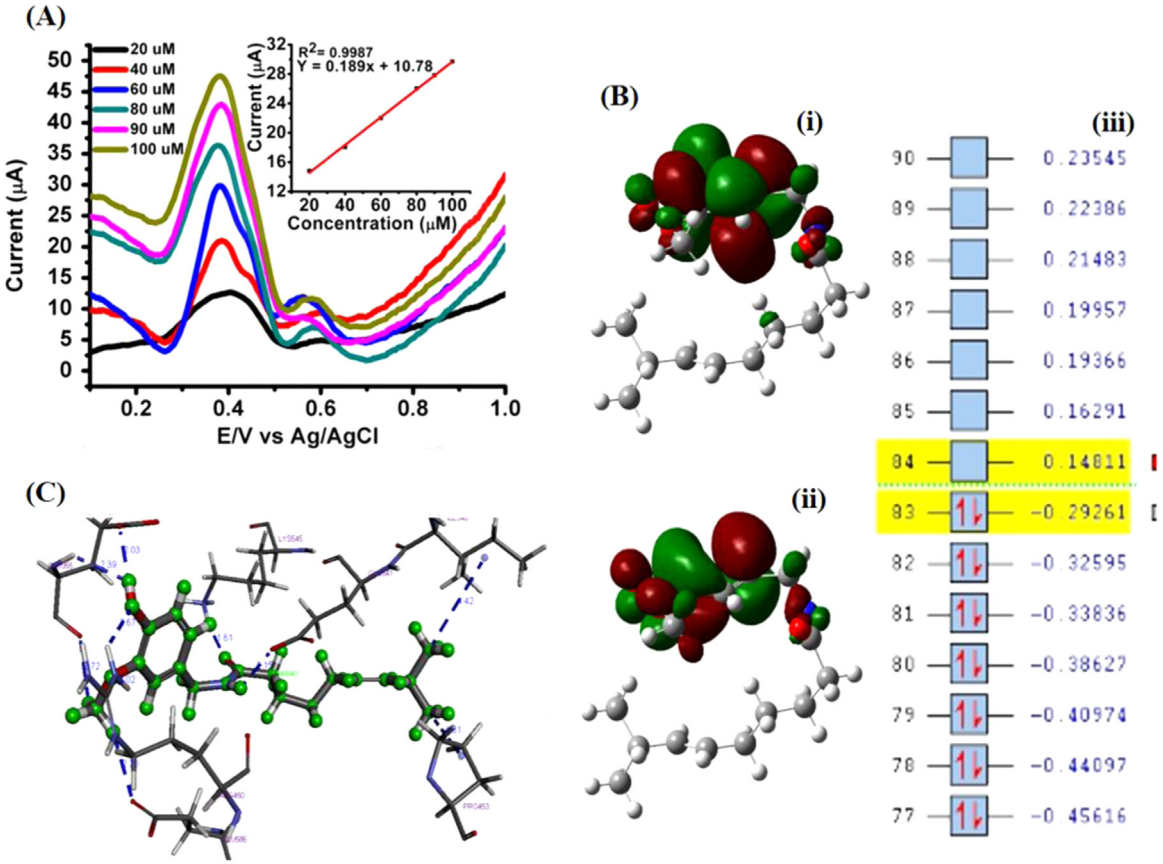

Fig. 3. (A) Differential pulse voltammogram of capsaicin sample (0.2 mL) from chilli pepper fruit extract in 0.1 M acetate buffer solution of pH 4.0; scan rate of 0.013 V s^{-1}; deposition time of 60 s using PAL/Nafion/MWCNTs/Pt-E. **(B)** (i) Highest occupied molecular orbitals (HOMO) and [ii] lowest occupied molecular orbitals (LUMO) of capsaicin and [iii] is the Alpha molecular orbitals of capsaicin obtained with DFT level 6–31+G(d) basis set **(C)** Molecular docking complex of the capsaicin into PAL enzyme binding site.

interactive residue. Further analysis suggested only two hydrophobic-alkyl bonds for residues PRO 453 and ILE 450 with 4.61 Å and 4.42 Å. The carbonyls of the capsaicin molecule appeared to be the focal point of interaction, due to the participation of three hydrogen bonds. These results confirm that the PAL enzyme facilitated the electron transfer from the capsaicin ligand, hence improving the biosensing response.

4. Conclusions

In this paper, a nanocomposite based electrochemical biosensor was developed for the detection of capsaicin, characterized by TEM, TGA, CV and DPV techniques and supported by computational studies. The results revealed that the present electrochemical biosensor showed excellent reproducibility, high sensitivity, steady coating and higher exchange current density for the detection of capsaicin from chilli extracts. Additionally, their magnitudes of the voltammetric signals ranged in the order of PAL/Nafion/MWCNTs/Pt-E > MWCNTs/Pt-E > bare Pt-E, suggesting the role of the PAL enzyme in the signal amplification. Interestingly, our studies confirm that the interaction of the PAL enzyme with the phenolic component of capsaicin is key to the improvement in terms of sensitivity of the electrochemical biosensors. Moreover, HOMO-LUMO calculations obtained at the DFT level, were helpful in the prediction of the most appropriate functional groups or atoms undergoing oxidation or reduction reactions. Molecular docking analysis on the other hand, further revealed that capsaicin showed a stronger tendency to bind with the PAL enzyme *via* hydrogen bonding and hydrophobic interactions. These results confirmed that phenylalanine ammonia enzyme facilitated the electron transfer from the capsaicin ligand, in accordance with the 8-fold signal amplification observed by differential pulse voltammetry. The superior performance of the PAL/Nafion/MWCNTs/Pt-E provided a promising alternative in routine sensing applications of capsaicin in the food industry.

Acknowledgements

The authors gratefully acknowledge the financial assistance from the National Research Foundation (NRF) of South Africa and Durban University of Technology. The authors would like to express their acknowledgment to the Centre for High Performance Computing, an initiative supported by the Department of Science and Technology of South Africa.

Appendix A. Supplementary material

Supplementary data associated with this article can be found in the online version at http://dx.doi.org/10.1016/j.bios.2016.04.037.

References

Bathinapatla, A., Kanchi, S., Singh, P., Sabela, M.I., Bisetty, K., 2015. Biosens. Bioelectron. 67, 200–207.
Bathinapatla, A., Kanchi, S., Singh, P., Sabela, M.I., Bisetty, K., 2016. Biosens. Bioelectron. 77, 116–123.

Bom, D., Andrews, R., Jacques, D., Anthony, J., Chen, B., Meier, M.S., Selegue, J.P., 2002. Nano Lett. 2, 615–619.
Calabrese, J.C., Jordan, D.B., Boodhoo, A., Sariaslani, S., Vannelli, T., 2004. Biochemistry 43, 11403–11416.
Dresselhaus, M.S., Dresselhaus, G., Sugihara, K., Spain, I.L., Goldberg, H.A., 1988. Graphite Fibers and Filaments, 1 ed. Springer-Verlag, Berlin Heidelberg.
Frisch, M.J., Trucks, G.W., Schlegel, H.B., Scuseria, G.E., Robb, M.A., Cheeseman, J.R., Scalmani, G., Barone, V., Mennucci, B., Petersson, G.A., Nakatsuji, H., Caricato, M., Li, X., Hratchian, H.P., Izmaylov, A.F., Bloino, J., Zheng, G., Sonnenberg, J.L., Hada, M., Ehara, M., Toyota, K., Fukuda, R., Hasegawa, J., Ishida, M., Nakajima, T., Honda, Y., Kitao, O., Nakai, H., Vreven, T., Montgomery Jr., J.A., Peralta, J.E., Ogliaro, F., Bearpark, M.J., Heyd, J., Brothers, E.N., Kudin, K.N., Staroverov, V.N., Kobayashi, R., Normand, J., Raghavachari, K., Rendell, A.P., Burant, J.C., Iyengar, S. S., Tomasi, J., Cossi, M., Rega, N., Millam, N.J., Klene, M., Knox, J.E., Cross, J.B., Bakken, V., Adamo, C., Jaramillo, J., Gomperts, R., Stratmann, R.E., Yazyev, O., Austin, A.J., Cammi, R., Pomelli, C., Ochterski, J.W., Martin, R.L., Morokuma, K., Zakrzewski, V.G., Voth, G.A., Salvador, P., Dannenberg, J.J., Dapprich, S., Daniels, A.D., Farkas, Ö., Foresman, J.B., Ortiz, J.V., Cioslowski, J., Fox, D.J., 2009. Gaussian 09. Gaussian, Inc., Wallingford,, CT, USA.
Hautkappe, M., Roizen, M.F., Toledano, A., Roth, S., Jeffries, J.A., Ostermeier, A.M., 1998. Clin. J. Pain. 14, 97–106.
Henderson, D.E., Slickman, A.M., Henderson, S.K., 1999. J. Agric. Food Chem. 47, 2563–2570.
Hu, C., Hu, S., 2009. J. Sens. 2009, 1–40.
Huynh, H.T., Teel, R.W., 2005. Anticancer Res. 25, 117–120.
Kachoosangi, R.T., Wildgoose, G.G., Compton, R.G., 2008. Analyst 133, 888–895.
Kuznetsov, A.M., Ulstrup, J., 1999. Phys. Chem. Chem. Phys. 1, 5587–5592.
Laviron, E., 1979a. J. Electroanal. Chem. Interfacial Electrochem. 97, 135–149.
Laviron, E., 1979a. J. Electroanal. Chem. Interfacial Electrochem. 101, 19–28.
Laviron, E., 1979b. J. Electroanal. Chem. Interfacial Electrochem 100, 263–270.
Li, J., Feng, H., Li, J., Jiang, J., Feng, Y., He, L., Qian, D., 2015. Electrochim. Acta 176, 827–835.
Liu, L., Chen, X., Liu, J., Deng, X., Duan, W., Tan, S., 2010. Food Chem. 119, 1228–1232.
Lyons, M.E.G., Keeley, G.P., 2008. Int. J. Electrochem. Sci. 3, 819–853.
Manaia, M.A.N., Diculescu, V.C., Gil, E.D.S., Oliveira-Brett, A.M., 2012. J. Electroanal. Chem. 682, 83–89.
Mohammad, R., Ahmad, M., Heng, L., 2013. Sensors 13, 10014–10026.
Mohammad, R., Ahmad, M., Heng, L.Y., 2014. Sens. Actuator B-Chem. 190, 593–600.
Mpanza, T., Sabela, M.I., Mathenjwa, S.S., Kanchi, S., Bisetty, K., 2014. Anal. Lett. 47, 2813–2828.
Othman, Z.A.A., Ahmed, Y.B.H., Habila, M.A., Ghafar, A.A., 2011. Molecules 16, 8919–8929.
Peña-Alvarez, A., Ramírez-Maya, E., Alvarado-Suárez, L.Á., 2009. J. Chromatogr. A 1216, 2843–2847.
Pershing, L.K., Reilly, C.A., Corlett, J.L., Crouch, D.J., 2006. J. Appl. Toxicol. 26, 88–97.
Randviir, E.P., Metters, J.P., Stainton, J., Banks, C.E., 2013. Analyst 138, 2970–2981.
Reilly, C.A., Crouch, D.J., Yost, G.S., 2001. J. Forensic Sci. 46, 502–509.
Reilly, C.A., Yost, G.S., 2006. Drug. Metab. Rev. 38, 685–706.
Reyes-Escogido, M., Gonzalez-Mondragon, E.G., Vazquez-Tzompantzi, E., 2011. Molecules 16, 1253–1270.
Sanchez, A.M., Sanchez, M.G., Malagarie-Cazenave, S., Olea, N., Diaz-Laviada, I., 2006. Apoptosis 11, 89–99.
Satyanarayana, M.N., 2006. Crit. Rev. Food Sci. Nutr. 46, 275–328.
Spanyar, P., Blazovich, M., 1969. Analyst 94, 1084–1089.
Srinivasan, K., 2015. Crit. Rev. Food Sci. Nutr. . http://dx.doi.org/10.1080/10408398.10402013.10772090
Supalkova, V., Stavelikova, H., Krizkova, S., Adam, V., Horna, A., Havel, L., Ryant, P., Babula, P., Kizek, R., 2007. Acta Chim. Slov. 54, 55–59.
Sutoh, K., Kobata, K., Yazawa, S., Watanabe, T., 2006. Biosci. Biotechnol. Biochem. 70, 1513–1516.
Tirado-Rives, J., Jorgensen, W.L., 2006. J. Med. Chem. 49, 5880–5884.
Venkatachalam, C.M., Jiang, X., Oldfield, T., Waldman, M., 2003. J. Mol. Graph. Modell. 21, 289–307.
Wang, J., 2005. Electroanalysis 17, 7–14.
Wang, Z., Dai, Z., 2015. Nanoscale 7, 6420–6431.
Wu, G., Robertson, D.H., Brooks, C.L., Vieth, M., 2003. J. Comput. Chem. 24, 1549–1562.
Xue, Z., Hu, C., Rao, H., Wang, X., Zhou, X., Liu, X., Lu, X., 2015. Anal. Methods 7, 1167–1174.
Ya, Y., Mo, L., Wang, T., Fan, Y., Liao, J., Chen, Z., Manoj, K.S., Fang, F., Li, C., Liang, J., 2012. Colloids Surf. B 95, 90–95.
Yardım, Y., 2011. Electroanalysis 23, 2491–2497.
Yardım, Y., Şentürk, Z., 2013. Talanta 112, 11–19.